Université de Montréal

Microbiome cutané et maladie fongique émergente du syndrome du museau blanc chez les chauves-souris d'Amérique du Nord

par

Virginie Lemieux-Labonté

Département de sciences biologiques
Faculté des arts et des sciences

Thèse présentée en vue de l'obtention du grade de
Philosophiæ Doctor (Ph.D.)
en Sciences biologiques

30 Septembre 2020

Université de Montréal

Faculté des arts et des sciences

Cette thèse intitulée

Microbiome cutané et maladie fongique émergente du syndrome du museau blanc chez les chauves-souris d'Amérique du Nord

présentée par

Virginie Lemieux-Labonté

a été évaluée par un jury composé des personnes suivantes :

Éric Harvey
(président-rapporteur)

François-Joseph Lapointe
(directeur de recherche)

B. Jesse Shapiro
(membre du jury)

Sébastien Puechmaille
(examinateur externe)

Christian Gates St-Pierre
(représentant du doyen de la FESP)

Résumé

Le syndrome du museau blanc (SMB), causé par le champignon *Pseudogymnoascus destructans* (Pd), a mis en péril les populations de chauves-souris hibernantes en Amérique du Nord. Certaines espèces sont hautement vulnérables à la maladie alors que d'autres espèces semblent être résistantes ou tolérantes à l'infection. Plusieurs facteurs physiologiques et environnementaux peuvent expliquer ces différences. Or avant 2015, peu d'études avaient porté sur le microbiome de la peau en relation avec cette maladie. La présente thèse vise à caractériser le microbiome cutané de chiroptères affectés par le SMB afin d'identifier les facteurs de vulnérabilité ou de résistance à la maladie. L'objectif principal est de déterminer comment le microbiome est affecté par la maladie ainsi que de déterminer si celui-ci à un rôle dans la protection face à l'infection fongique.

Au **Chapitre 1**, nous avons tout d'abord exploré et comparé le microbiote cutané de petites chauves-souris brunes (*Myotis lucifugus*) non affectées par le SMB avec celui de chauves-souris survivantes au SMB pour tester l'hypothèse selon laquelle le microbiote cutané est modifié par la maladie. Nos résultats montrent que le site d'hibernation influence fortement la composition et la diversité du microbiote cutané. Les sites d'hibernations Pd positifs et négatifs diffèrent significativement en termes de diversité, ainsi qu'en termes de composition du microbiote. La diversité est réduite au sein du microbiote des chauves-souris survivantes au SMB et enrichi en taxons tels que *Janthinobacterium*, Micrococcaceae, *Pseudomonas*, *Ralstonia* et *Rhodococcus*. Certains de ces taxons sont reconnus pour leur potentiel antifongique et des souches spécifiques de *Rhodococcus* et de *Pseudomonas* peuvent inhiber la croissance de Pd. Nos résultats sont cohérents avec l'hypothèse selon laquelle l'infection par Pd modifie le microbiote cutané des chauves-souris survivantes et suggèrent que le microbiote peut jouer un rôle de protection face au SMB.

Au **Chapitre 2**, nous avons étudié le microbiote d'une espèce résistante au champignon Pd en milieu contrôlé avant et après infection afin d'établir la réponse potentielle à la maladie. L'espèce étudiée est la grande chauve-souris brune (*Eptesicus fuscus*) dont le microbiote cutané pourrait jouer un rôle de protection contre l'infection. Nos résultats montrent que la

diversité du microbiote de la grande chauve-souris brune inoculée avec Pd est plus variable dans le temps, tandis que la diversité du microbiote des chauves-souris du groupe contrôle demeure stable. Parmi les taxons les plus abondants, *Pseudomonas* et *Rhodococcus*, deux taxons connus pour leur potentiel antifongique contre Pd et d'autres champignons, sont restés stables durant l'expérience. Ainsi, bien que l'inoculation par le champignon Pd ait déstabilisé le microbiote cutané, les bactéries aux propriétés antifongiques n'ont pas été affectées. Cette étude est la première à démontrer le potentiel du microbiote cutané d'une espèce de chauves-souris pour la résistance au SMB.

Au **Chapitre 3**, le microbiome cutané de la petite chauve-souris brune a été évalué en milieu naturel dans le contexte du SMB, à l'aide de la métagénomique, une approche haute résolution pour observer le potentiel fonctionnel du microbiome (métagénome fonctionnel). Nos résultats ont permis d'établir que le temps depuis l'infection a un effet significatif sur le métagénome fonctionnel. En effet, les chauves-souris dans la première année suivant l'infection ont un métagénome fonctionnel perturbé qui subit une perte de diversité fonctionnelle importante. Toutefois, le métagénome fonctionnel revient à une structure et composition similaire d'avant infection après 10 ans. Certaines fonctions détectées suite à l'infection sont associées à des gènes reliés au transport et à l'assimilation de métaux, des facteurs limitants pour la croissance du champignon. Ces gènes pourraient donc avoir un rôle à jouer dans la résistance ou la vulnérabilité à la maladie. Globalement, l'étude du métagénome chez la petite chauve-souris brune indique une vulnérabilité du métagénome fonctionnel au champignon, mais que celui-ci semble se rétablir après 10 ans. Une telle réponse pourrait avoir un impact sur la résilience de *M. lucifugus*.

Cette thèse a permis d'acquérir des connaissances fondamentales sur le microbiome cutané des chauves-souris en hibernation pour mieux comprendre les communautés microbiennes de la peau dans le contexte du SMB. Le microbiome pourrait en effet jouer un rôle dans la vulnérabilité et la résistance des chauves-souris à la maladie, et il est essentiel d'adapter notre façon d'aborder la protection de ces espèces et de leur microbiome. Nous souhaitons que les travaux de cette thèse permettent de sensibiliser les acteurs de la conservation à l'existence et à l'importance potentielle du microbiome pour la santé de son hôte. Cette thèse fait également état de l'avancement des méthodes d'analyses qui permettront d'être de plus en plus précis et d'appliquer les connaissances du microbiome en biologie de la conservation. **Mots clés** : syndrome du museau blanc, *Pseudogymnoascus destructans*,

résistance, microbiote cutané, microbiome cutané, métagénome fonctionnel, *Eptesicus fuscus*, grande chauves-souris brune, *Myotis lucifugus*, conservation.

Abstract

White-nose syndrome (WNS) caused by the fungus *Pseudogymnoascus destructans* (Pd) has put hibernating bat populations at risk in North America. Some species are highly vulnerable to the disease while other species appear to be resistant or tolerant. Several physiological and environmental factors can explain these differences. However, before 2015, few studies have focused on the skin microbiome in relation to this disease. The present thesis aims to characterize the cutaneous microbiome of bats affected by WNS in order to identify the factors of vulnerability or resistance to the disease. The main objective is to determine how the microbiome can protect against the Pd fungus, or conversely how the microbiome is altered by the fungal infection.

In **Chapter 1**, we first explored and compared the skin microbiota of little brown bats (*Myotis lucifugus*) unaffected by WNS with that of WNS survivors to test the hypothesis that the skin microbiota is modified by the disease. Our results show that the hibernation site strongly influences the composition and diversity of the skin microbiota. The Pd positive and negative sites differ significantly in terms of diversity, as well as in terms of the composition of the microbiota. Diversity is reduced within the microbiota of bats surviving WNS and enriched in taxa such as *Janthinobacterium*, Micrococcaceae, *Pseudomonas*, *Ralstonia*, and *Rhodococcus*. Some of these taxa are recognized for their antifungal potential and specific strains of *Rhodococcus* and *Pseudomonas* may inhibit the growth of Pd. Our results are consistent with the hypothesis that Pd infection modifies the skin microbiota of surviving bats and suggest that the microbiota may play a protective role against WNS.

In **Chapter 2**, we studied in a controlled environment the microbiota of a species that exhibits evidence of resistance with mild WNS symptoms, before and after infection, to establish the potential response to the disease. The species studied is the big brown bat (*Eptesicus fuscus*), whose skin microbiota could play a protective role against infection. Our results show that the diversity of the microbiota of big brown bats inoculated with Pd is more variable over time, while the diversity of the microbiota of the control bats remains stable. Among the most abundant taxa, *Pseudomonas* and *Rhodococcus*, two taxa

known for their antifungal potential against Pd and other fungi, remained stable during the experiment. Thus, although inoculation with the Pd fungus destabilized the skin microbiota, bacteria with antifungal properties were not affected. This study is the first to demonstrate the potential of the skin microbiota of a bat species for resistance to WNS.

In **Chapter 3**, the skin microbiome of the little brown bat was evaluated in the natural environment in the context of WNS, using metagenomics, a higher-resolution approach to observe the functional potential of the microbiome (functional metagenome). Our results established that the time since infection has a significant effect on the functional metagenome. Indeed, bats in the first year after infection have a disrupted functional metagenome that undergoes a significant loss of functional diversity. However, the functional metagenome returns to a similar structure and composition to that observed before infection after 10 years. Certain functions detected following infection are associated with genes linked to the transport and assimilation of metals, known limiting factors for the growth of the fungus. These genes could therefore have a role to play in resistance or vulnerability to the disease. Overall, this metagenomics study indicates functional metagenome vulnerability to the fungus, although the original functional metagenome is reestablished after 10 years. Such diversified response could impact *M. lucifugus* resilence.

This thesis provides fundamental knowledge on the skin microbiome of hibernating bats to better understand the microbial communities of the skin in the context of WNS. The microbiome could indeed play a role in the vulnerability and resistance of bats to disease and it is essential to adapt our way of approaching the protection of these species and their microbiomes. We hope that the results of this thesis will raise awareness among conservation stakeholders about the existence and potential importance of the microbiome for the health of its host. This thesis also reports on the advancement of analytical methods that will make it possible to be more and more precise and to apply knowledge of the microbiome in conservation biology. **Key words**: white nose syndrome, *Pseudogymnoascus destructans*, resistance, skin microbiota, skin microbiome, functional metagenome, *Eptesicus fuscus*, big brown bat, *Myotis lucifugus*, little brown bat, conservation.

Table des matières

Liste des tableaux

Liste des figures

Liste des sigles et des abréviations

ANCOM   *analysis of composition of microbiomes*

AIC   *Akaike information criterion*

ANOVA   *analysis of variance*

ARNr   acide ribonucléique ribosomique

ASV   *amplicon sequence variants*

BLAST   *basic local alignment search tool*

clr   *centred log-ratio*

COG   *clusters of orthologous groups*

COSEPAC   le comité sur la situation des espèces en péril au Canada

db-RDA   *distance base redundancy analysis*

DNTP   *deoxyribonucleotide triphosphate*

Fe2+   ion ferreux ; *ferrous ion*

IndVal   *indicator value tests*

ITS   *internal transcribed spacer*

HF   *high-fidelity*

Mn2+   manganèse ; *manganese*

NaCl   chlorure de sodium; *sodium chloride*

OTU   *operational taxonomic unit*

PBST   *phosphate-buffered saline with Tween® detergent*

PCoA   *principal coordinates analysis*

PCA   *principal component analysis*

PCR   *polymerase chain reaction*

Pd   *Pseudogymnoascus destructans*

QIIME	*quantitative insights into microbial ecology*
qPCR	*quantitative polymerase chain reaction*
RDA	*redundancy analysis*
rRNA	*ribosomal ribonucleic acid*
SD	*standard deviation*
SMB	syndrome du museau blanc
UV	rayonnement ultraviolet ; *ultraviolet radiation*
USDA	*United States Department of Agriculture*
WNS	*white nose syndrome*

Remerciements

François-Joseph Lapointe, merci de m'avoir offert une expérience d'apprentissage exceptionnelle au cours des 5 dernières années. Tu as été un directeur à l'écoute et je te serai toujours reconnaissante de m'avoir apporté ton soutien dans les mauvais moments. Tu as su trouver les bons mots pour m'aider dans mes dilemmes et me faire retrouver ma motivation. Merci de m'avoir fait grandir en tant que chercheuse.

Je remercie mes collègues de laboratoire présents et passés pour leur soutien. Merci Cindy Bouchard, Marianne Cloutier, Nathalie Tessier, Geneviève Dubois et Étienne Lord d'avoir apporté votre énergie au LEMEE et d'avoir contribué à rendre cette expérience mémorable pour moi. Merci à ma fantastique collègue et coup de foudre amical Maïté Ribère. Tu es une « coach » de vie et une complice de crime fantastique.

Un ÉNORME merci au laboratoire de génomique microbienne de Jesse Shapiro qui m'a accordé un soutien inestimable. Un merci particulier à Nicolas Tromas qui m'a aidé à initier mon projet. Merci à Julie Marleau pour son soutien en laboratoire et les moments agréables passés en sa compagnie. Merci à Yves Terrat pour son aide de bioinformaticien aguerri et les discussions sur la réalité universitaire.

Je remercie le Bat lab de Craig K. R. Willis et ses membres. Merci de m'avoir accueilli à bras ouverts dans votre équipe et merci de votre collaboration incroyable tout au long de mon doctorat. Merci au Ministère de la Faune et des Parcs pour leur soutien plus particulièrement Anouk Simard, Ariane Massé, Valérie Simard, Olivier Cameron-Trudel, Jocelyn Caron, Daniele Morin et Aimé Benoist-Chénier. Merci pour votre aide à la récolte d'échantillons et de m'avoir permis de découvrir les chauves-souris du Québec. Merci à Pascal Samson pour sa présence inspirante et les aventures incroyables dans les mines. Je remercie également François Fabianek et Antoine Leblet du Groupe Chiroptères du Québec qui m'ont donné des opportunités de projets au Québec.

Sur une note plus personnelle, merci Louise et Jean-Pierre d'avoir encouragé ma curiosité pour la nature et de m'avoir fait savoir que votre amour était inconditionnel à ma réussite. Je remercie ma sœur Caroline Giguère pour les discussions réconfortantes et son aide inestimable. Merci à Sasha qui du haut de ses trois ans s'intéressait déjà à ma recherche. Merci à mon amoureux Richard LaBrie qui me fait rire et voir la vie du bon côté au quotidien. Je t'aime et merci d'avoir été là pour cette incroyable aventure qu'est la fin d'un doctorat en temps de pandémie.

Avant-propos

© Kaleigh Norquay

Créature de bons ou de mauvais présages selon les cultures, les chauves-souris frappent l'imaginaire depuis des siècles. En Amérique du Nord, les préjugés négatifs persistent et mettent en péril ces animaux déjà menacés par les perturbations humaines et une maladie fongique dévastatrice. La conservation des chauves-souris passe inévitablement par l'éducation afin de redorer leur réputation et par une meilleure compréhension des menaces auxquelles font face ces animaux trop longtemps restés dans l'ombre. . .

Introduction

0.1. Maladies émergentes de la faune

La crise de la biodiversité actuelle, avec l'extinction de masse des espèces, est sans précédent depuis l'apparition de la vie il y a 3,5 milliards d'années (Western, 1992). Dans ce contexte, les maladies de la faune, qui sont en augmentation partout sur la planète, ont des conséquences dramatiques pour la biodiversité déjà fragilisée (Daszak, 2000; Jones et al., 2008; Fisher et al., 2012). L'activité humaine est la principale responsable des maladies émergentes puisqu'elle favorise l'introduction de nouveaux pathogènes, intensifie leur dispersion en modifiant les environnements naturels et crée de nouvelles possibilités d'évolution pour ceux-ci (Fisher et al., 2012). Depuis plusieurs décennies, des scientifiques sonnent l'alarme sur les conséquences de ces maladies pour la conservation et la santé des écosystèmes (Scott, 1988; Lyles & Dobson, 1993; Hess, 1996; Real, 1996). Cette menace est désormais prise au sérieux en raison de la reconnaissance des services écologiques rendus par la faune dont bénéficient la santé publique et l'économie (Daszak, 2000; Singh, 2002; Jones et al., 2008; Boyles et al., 2011; Fisher et al., 2012; Maine & Boyles, 2015).

L'émergence d'infections fongiques de la peau ayant des conséquences physiologiques graves est particulièrement préoccupante pour la biodiversité (Fisher et al., 2020). Découverte en 1997, la chytridiomycose causée par le champignon *Batrachochytrium dendrobatidis* (Berger et al., 1998) a contribué au déclin de près de la moitié des espèces d'amphibiens dans le monde (Stuart et al., 2004). Un champignon du même genre (*B. salamandrivorans*), découvert en 2012, a causé un déclin massif de populations de salamandre du nord-ouest de l'Europe (Martel et al., 2013). Découvert en 2006, l'ophidiomycose, causé par le champignon *Ophidiomyces ophiodiicola*, a engendré le déclin de populations de serpents en Amérique du Nord et est une menace potentielle pour les populations d'Europe (Allender et al., 2011, 2015; Clark et al., 2011; Franklinos et al., 2017). Ces infections cutanées présentent de nouveaux défis pour la science, car elles agissent par le biais de mécanismes qui étaient jusqu'à présent inconnus, autant chez l'homme que chez les animaux (Fisher et al., 2020).

Depuis 2006, les chauves-souris (Chiroptera) d'Amérique du Nord sont également menacées par une maladie fongique émergente, le syndrome du museau blanc (SMB) (Gargas et al., 2009; Lorch et al., 2011). Le SMB qui affecte la peau des chauves-souris est causé par le champignon *Pseudogymnoascus destructans* (Pd) (Gargas et al., 2009; Lorch et al., 2011). L'ampleur de l'extinction causée par le SMB est sans précédent chez un ordre de mammifères de l'ère moderne et elle aura des conséquences graves sur les écosystèmes, l'agriculture et la santé humaine (Tuttle et al., 2009; Boyles et al., 2011; Coleman, 2012; Maine & Boyles, 2015; Frick et al., 2016). En effet, les chauves-souris insectivores contribuent au contrôle des populations d'insectes ravageurs et permettent annuellement de sauver des milliards de dollars en agriculture (Boyles et al., 2011; Maine & Boyles, 2015).

Les chiroptères ont une grande valeur pour la science puisqu'ils représentent le seul ordre de mammifères volants. Avec plus de 1400 espèces connues, les chauves-souris forment le groupe de mammifères le plus diversifié après les rongeurs. Leur longue espérance de vie malgré leur petite taille (jusqu'à 40 ans pour certaines espèces (Podlutsky et al., 2005)), leur métabolisme élevé (Wilkinson & South, 2002; Brunet-Rossinni & Austad, 2004; N. M. Foley et al., 2018), ainsi que leur capacité à tolérer des virus mortels en font des sujets d'étude importants pour l'avancée de la science en santé humaine (O'shea et al., 2014; Brook & Dobson, 2015; Kacprzyk et al., 2017; Mandl et al., 2018). En plus du SMB, la pollution, les changements climatiques, les parcs éoliens et la perte d'habitat agissent en synergie et menacent le rétablissement des populations (Environnement et changement climatique Canada, 2018).

0.2. Propagation et transmission du syndrome du museau blanc

Le champignon Pd est présent en Europe et dans l'ensemble de la zone paléarctique, y compris le nord-est de la Chine (Wibbelt et al., 2010; Puechmaille et al., 2011; Hoyt et al., 2016; Zukal et al., 2016). La souche nord-américaine proviendrait d'Europe (Warnecke et al., 2012; Leopardi et al., 2015). Or, les chauves-souris européennes ne souffriraient pas d'une mortalité importante liée à l'infection (Puechmaille et al., 2011; Fritze & Puechmaille, 2018) due à une possible coévolution avec le pathogène (Wibbelt et al., 2010).

Initialement répertorié en 2006 dans l'état de New York (D. M. Reeder & Turner, 2008; Blehert et al., 2009; Turner & Reeder, 2009) le SMB est retrouvé dans 38 États américains et sept provinces canadiennes (Terre-Neuve-et-Labrador, Manitoba, Nouveau-Brunswick, Nouvelle-Écosse, Ontario, Québec, Île-du-Prince-Édouard) en 2020 (Fig. 0.1). La vitesse de propagation du SMB au Canada est en moyenne de 200 à 250 km par année (Canadian

Wildlife Service & Committee on the Status of Endangered Wildlife in Canada, 2013). Entre 5,7 et 6,7 millions de chauves-souris sont mortes dans les 6 années suivant la découverte de la maladie (Coleman, 2012). L'ampleur de ces ravages en fait l'une des épidémies de la faune les plus dévastatrices jamais enregistrées au niveau mondial (Tuttle et al., 2009; Coleman, 2012; Frick et al., 2016).
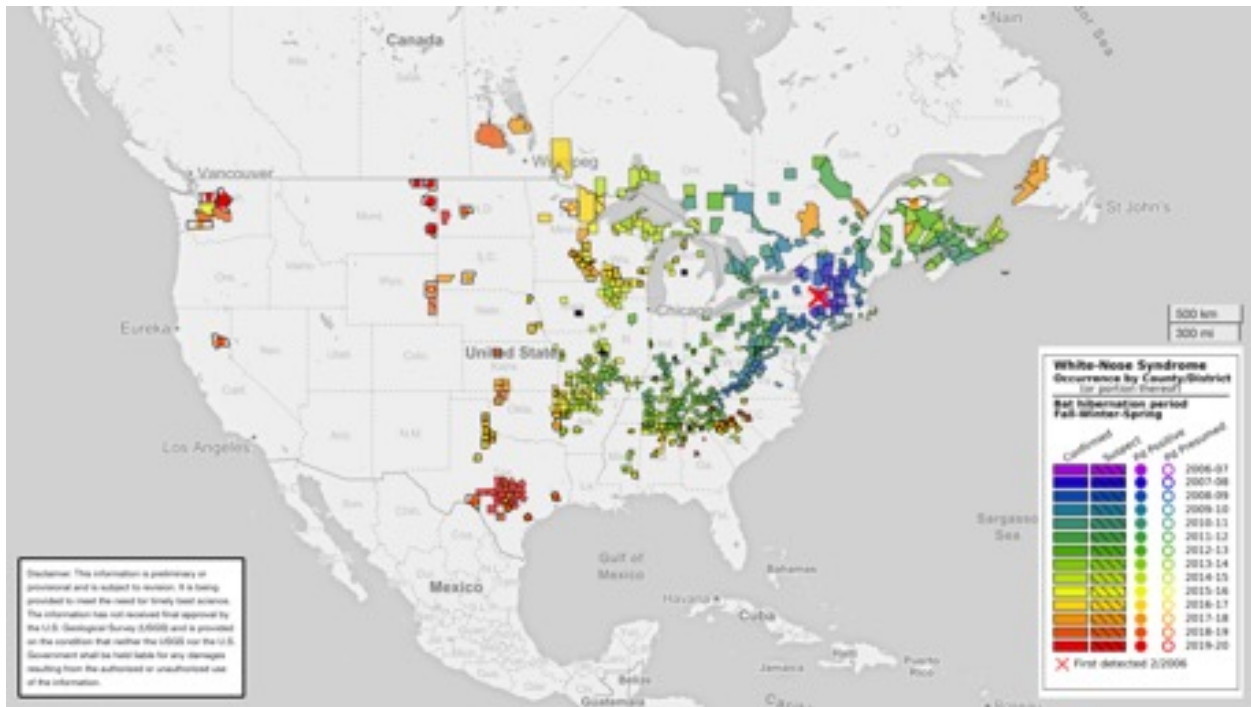
Fig. 0.1. Dispersion du SMB en Amérique du Nord depuis sa découverte à l'hiver 2006-2007 dans l'état de New York. La maladie est maintenant présente dans 38 états américains et sept provinces canadiennes. Source : White-nose syndrome occurence map - by year (2019). Data Last Updated: 8/30/2019. `https://www.whitenosesyndrome.org/static-spread-map/august-30-2019`.

Le mycète Pd est psychrophile, c'est-à-dire qu'il est adapté aux températures froides et qu'il peut croître dans les conditions rencontrées à l'intérieur des hibernacles de chauves-souris, telles que des mines abandonnées, des grottes, des puits et des tunnels. La température de l'hibernacle se situe généralement entre 2°C et 10°C (Fenton, 1970; Vanderwolf et al., 2012) et le taux d'humidité relative est supérieur à 80% (Davis, 1970). La température de la peau des chauves-souris durant l'hibernation est similaire à la température ambiante de l'hibernacle (Hock, 1951). Le champignon Pd qui est adapté pour croître à des températures basses, peut donc croître sur la peau des chauves-souris durant cette période (Gargas et al., 2009). La germination du champignon au sein de l'hibernacle serait également synchronisée avec la période d'hibernation (Fischer et al., 2020). Grâce à leurs

conditions stables dans le temps, les mêmes hibernacles sont généralement utilisés d'une année à l'autre par les chauves-souris (Environnement et changement climatique Canada, 2018).

La transmission du champignon peut se faire par contact entre chauves-souris, par contact avec un hibernacle contaminé ou par l'entremise de l'homme (tourisme, spéléologie et recherches scientifiques) (Lorch et al., 2013; Frick et al., 2016; Ballmann et al., 2017; J. E. Foley et al., 2011). Des études suggèrent que ce champignon serait apte à se propager dans le milieu sans la présence de chauves-souris et que les spores pourraient rester viables pendant plusieurs années même dans des hibernacles abandonnés (Hoyt, Langwig, et al., 2015; Reynolds et al., 2015; Ballmann et al., 2017). L'accumulation de guano dans les hibernacles pourrait également constituer un réservoir du champignon (Mulec et al., 2013; Raudabaugh & Miller, 2013; Reynolds & Barton, 2014)

0.3. Hibernation et pathophysiologie du SMB

En Amérique du Nord, Pd s'attaque aux chauves-souris insectivores lors de l'hibernation en créant des lésions, des nécroses et des ulcères sur les ailes, les oreilles et le museau (Meteyer et al., 2009; Reichard & Kunz, 2009; Coleman & Reichard, 2014) (Fig. 0.2). En colonisant les follicules pileux, les glandes sébacées et apocrines, les muscles, les tissus conjonctifs et les vaisseaux sanguins (Meteyer et al., 2009; Cryan et al., 2010), il perturbe potentiellement les sécrétions contribuant à l'intégrité de la peau qui protègent contre les pathogènes et maintiennent la communauté de microorganismes associés (Sisk, 1957; Cortese & Nicoll, 1970; Grice & Segre, 2011).

Les chauves-souris qui hibernent doivent passer l'hiver en ne comptant que sur leurs réserves de graisse accumulée durant l'été. Elles passeront donc la majorité de la saison hivernale en état prolongé de torpeur. Ces épisodes de torpeur sont caractérisés par un métabolisme ralenti et une température corporelle drastiquement réduite afin de conserver les réserves énergétiques (Jonasson & Willis, 2012; Czenze et al., 2013; Czenze & Willis, 2015). Il a été suggéré que le système immunitaire fonctionnant au ralenti lors de ces périodes de torpeur faciliterait l'infection par Pd (Geiser, 2004; Bouma et al., 2010; Moore et al., 2011). Or, il y aurait une réponse immunitaire chez les chauves-souris tel *M. lucifugus* durant l'hibernation (Moore et al., 2011, 2013; Field et al., 2015; Lilley et al., 2017). Les données de transcriptome démontrent par ailleurs que l'hibernation n'empêche pas la réponse inflammatoire locale à une infection par Pd, mais que le recrutement des leucocytes au site de l'infection ne se produit pas. Une réponse inflammatoire offre normalement une protection, mais une inflammation excessive ou non complète peut contribuer à la mortalité,

soit en affectant le comportement de torpeur, soit en causant des dommages à l'émergence au printemps (Field et al., 2015; Lilley et al., 2017; Fuller et al., 2020).
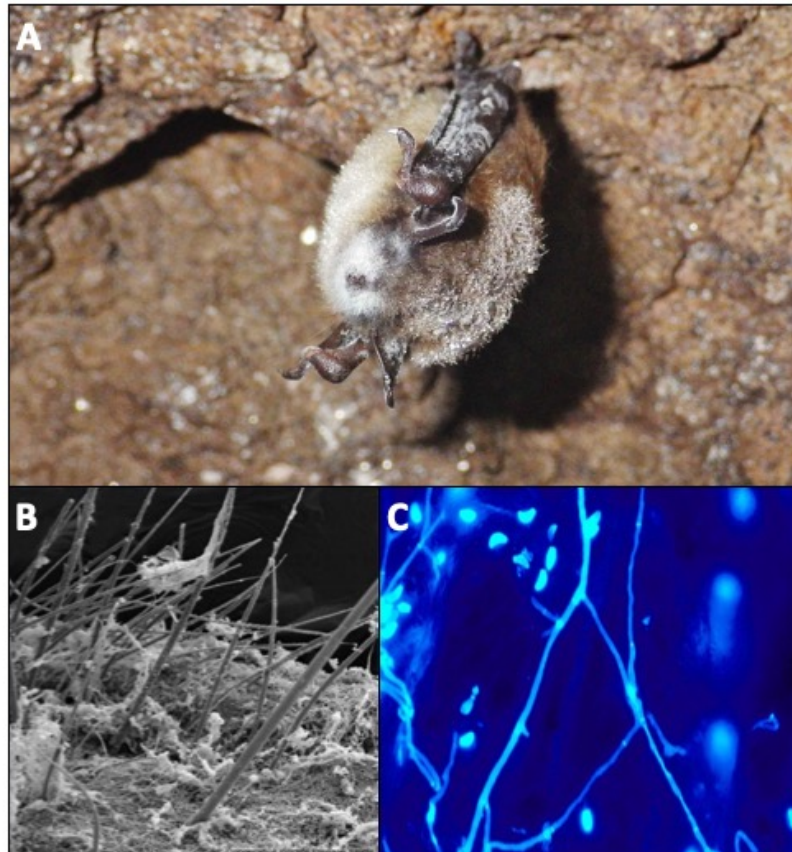
Fig. 0.2. Syndrome du museau blanc et le champignon responsable *Pseudogymnoascus destructans.* (A) Chauves-souris infectées par le SMB. Crédit: Minnesota DNR. (B) Image de microscopie électronique du champignon Pd. Crédit: K. Keel, Southeastern Cooperative Wildlife Disease Study. C) Spores et filaments de Pd sur une aile de chauve-souris. Crédit: B. E. Overton, Lock Haven University.

Il est normal que les chauves-souris s'éveillent durant la période d'hibernation pour s'hydrater, se toiletter, s'accoupler ou excréter certains métabolites (Whitaker & Rissler, 1993; D. W. Thomas, 1995), mais ces sorties de torpeur sont limitées afin de minimiser la grande quantité d'énergie dépensée durant ces périodes d'éveils (D. W. Thomas et al., 1990). Cependant, le SMB augmente le métabolisme qui stimule l'hyperventilation et augmente les périodes d'éveil. Cet état contribue à la déshydratation et à la perte d'électrolytes (Warnecke et al., 2012, 2013; Verant et al., 2014). L'infection augmente ainsi dangereusement la fréquence des sorties de torpeur, coûteuses au niveau énergétique, qui causerait la perte précoce des réserves de graisses nécessaires à la survie (D. M. Reeder et al., 2012; Warnecke et al., 2012).

L'infection des ailes par le champignon est la plus critique, car celles-ci ont un rôle important dans la thermorégulation, l'équilibre hydrique et les échanges gazeux (S. P. Thomas & Suthers, 1972; Makanya & Mortola, 2007; Cryan et al., 2010, 2013; Warnecke et al., 2013). L'infection sur les membranes alaires peut donc altérer leurs fonctions et ainsi nuire à la survie durant l'hibernation et la période active. Des ailes abîmées par le SMB représentent un danger pour les chauves-souris insectivores qui s'appuient sur leurs propriétés biomécaniques uniques pour capturer leurs proies, échapper aux prédateurs et accéder aux gîtes en période estivale (Swartz et al., 2003). Les survivantes au printemps démontrent un stress physiologique important et risquent par conséquent d'avoir un succès reproducteur réduit (Reichard & Kunz, 2009). Néanmoins, les plaies guérissent en grande partie durant l'été (Fuller et al., 2011, 2020), lorsque la température corporelle et les conditions ne sont plus propices à la croissance du champignon (Langwig et al., 2015).

0.4. Impact inter-spécifique du SMB

Douze espèces de chauves-souris sont affectées par le SMB en Amérique du Nord (Tableau 0.1) et la présence de Pd a été détecté chez six espèces sans signes cliniques de la maladie. Bien que Pd ait la capacité d'infecter plusieurs espèces, il a été démontré que l'impact du SMB n'est pas le même pour toutes les populations (Frick, Pollock, et al., 2010; Frick et al., 2015; Turner et al., 2011; Langwig et al., 2015, 2017). Au Canada, la chauve-souris nordique (*Myotis septentrionalis*), la petite chauve-souris brune (*Myotis lucifugus*) et la pipistrelle de l'Est (*Perimyotis subflavus*) ont été ajoutées à la liste des espèces menacées en raison d'un taux de mortalité estimé de 75 à 90% dans les premières années suivant l'infection (Canadian Wildlife Service & Committee on the Status of Endangered Wildlife in Canada, 2013). Généralement, le taux de mortalité dû au SMB est faible (∼20%) durant la première année où la maladie est détectée, puis il devient élevé (>70%) en l'espace de deux ans (Frick, Pollock, et al., 2010). Au Québec, en Nouvelle-Écosse et au Nouveau-Brunswick, certains hibernacles ne comptent plus aucun individu (Mainguy et al., 2011; Canadian Wildlife Service & Committee on the Status of Endangered Wildlife in Canada, 2013). La réponse de l'hôte à l'infection diffère selon l'espèce ce qui expliquerait les différents patrons de vulnérabilité (Davy et al., 2020).

La résistance (i.e. la réduction ou l'élimination de l'infection par des agents pathogènes), et/ou la tolérance à l'infection (i.e. la réduction des dommages causés par l'infection) (Råberg et al., 2007; Svensson & Råberg, 2010; Råberg et al., 2009) sont possibles dans le contexte du SMB (Frick et al., 2016; Zukal et al., 2016; Langwig et al., 2017; Cheng et al., 2019). Il est suggéré que les conditions environnementales dans l'hibernacle (Langwig et al., 2012), la

Tableau 0.1. Espèces de chauves-souris ayant des signes cliniques du SMB et leur statut de conservation selon le pays en Amérique du Nord. Les statuts ont été uniformisés entre les deux pays enfin de faciliter l'interprétation. Source : COSEPAC, Fédération canadienne de la faune et US Fish and Wildlife Service.

Espèces	Statut au Canada	Statut aux États-Unis
Grande chauves-souris brune (*Eptesicus fuscus*)	Stable	Stable
Pipistrelle de l'est (*Perimyotis subflavus*)	En voie de disparition	Menacée
Cave bat (*Myotis velifer*)	NA	Stable
Chauves-souris nordique (*Myotis septentrionalis*)	En voie de disparition	Menacée
Chauve-souris pygmée de l'Est (*Myotis leibii*)	En voie de disparition	Menacée
Chauve-souris à queue frangée (*Myotis thysanodes*)	Données insuffisantes	Stable
Chauves-souris grise (*Myotis grisescens*)	NA	En voie de disparition
Chauves-souris de l'Indianna (*Myotis sodalis*)	NA	En voie de disparition
Petite chauves-souris brune (*Myotis lucifugus*)	En voie de disparition	Menacée
Chauve-souris à longues pattes (*Myotis volans*)	Stable	Stable
Chauve-souris à longues oreilles (*Myotis evotis*)	Stable	Stable
Chauve-souris de Yuma (*Myotis yumanensis*)	Stable	Stable

physiologie (Cheng et al., 2019), le génome (Auteri & Knowles, 2020), et le comportement d'hibernation (Wilder et al., 2011) peuvent jouer un rôle dans la tolérance ou résistance variable à Pd (Puechmaille et al., 2011; Willis & Wilcox, 2014; Frick et al., 2016; Harazim et al., 2018). La grande chauve-souris brune (*Eptesicus fuscus*) semble résistante à la maladie, car elle présente des symptômes de SMB quasi-inexistants par rapport aux espèces plus sensibles (Frank et al., 2014; Moore et al., 2018). Cette espèce est d'un intérêt particulier, car elle hiberne fréquemment dans des conditions environnementales similaires à celles d'espèces de chauves-souris vulnérables au SMB. Elle peut donc nous informer sur les mécanismes de survie qui ne sont pas attribuables à l'environnement. Les mécanismes expliquant la variation de la sensibilité interspécifique ne sont toutefois pas encore bien compris, malgré les avantages potentiels pour la gestion de la maladie.

0.5. Situation des espèces vulnérables au SMB

L'abondance de *M. lucifugus* au Canada était d'environ 1 million d'individus avant l'apparition du SMB (Canadian Wildlife Service & Committee on the Status of Endangered Wildlife in Canada, 2013) et de 6,5 millions dans le nord-est des États-Unis (Frick, Pollock, et al., 2010). Cette espèce était la plus commune en Amérique du Nord, mais elle pourrait à présent disparaitre du nord-est des États-Unis d'ici 2026 (Frick, Pollock, et al., 2010). Les trois espèces touchées par le SMB au Canada sont longévives et ont un taux de reproduction faible. Les femelles *M. lucifugus* et *M. septentrionalis* ne produisent qu'un petit par année, alors que *P. subflavus* en produit un ou deux (Environnement et changement climatique Canada, 2018). Ces espèces dépendent donc d'un taux de survie élevé des adultes pour assurer leur pérennité (Environnement et changement climatique Canada, 2018). La situation est d'autant plus grave que le taux de survie dans la première année de vie est

assez faible pour ces animaux, celui-ci pouvant varier de 23 à 46% pour *M. lucifugus* (Frick, Reynolds, & Kunz, 2010).

Malgré un taux de mortalité important durant le stade épidémique du SMB, certains individus d'espèces vulnérables survivent à l'infection (Dobony et al., 2011; Langwig et al., 2012; Reichard et al., 2014; Frick et al., 2015; Maslo & Fefferman, 2015) et des colonies se stabilisent entre 5-30% de leur abondance avant SMB (Langwig et al., 2012; Frick et al., 2015; Dobony et al., 2011). L'intensité d'infection est notamment significativement plus basse chez les individus de colonies survivantes au SMB en comparaison aux colonies en pleine phase épidémique et en déclin (Langwig et al., 2017). Une étude a comparé le profil génétique d'individus sauvages de *M. lucifugus* ayant survécu à la maladie à celui des individus tués par le SMB (Auteri & Knowles, 2020). Une différence significative de composition génétique fut observée chez ces deux groupes pour les gènes associés à la régulation des périodes de torpeurs durant l'hibernation, à la dégradation des graisses et à l'écholocalisation. Il se pourrait que les chauves-souris génétiquement prédisposées à être un peu plus grosses ou à dormir plus profondément soient donc moins sensibles à la maladie (Auteri & Knowles, 2020). Toutefois, ces résultats pourraient être biaisés par un échantillonnage non répété avant et après l'arrivée du syndrome en un même site ou par la répartition géographique des individus échantillonnés. Une étude récente avec échantillonnage répété et contrôlant pour les différences géographiques n'a d'ailleurs pas observé de différence génétique entre les populations persistantes et celles non affectées par le SMB (Lilley et al., 2020).

La lutte au SMB passe généralement par la surveillance de la maladie, l'éducation du public à l'importance de la conservation des chauves-souris, le contrôle de la propagation, la modification du microclimat des hibernacles, ainsi que le traitement des individus (J. E. Foley et al., 2011). Tous les moyens pour assurer la bonne santé des chauves-souris doivent être appliqués, tels que maximiser la quantité et la qualité de l'habitat et réduire les effets des facteurs de stress synergiques qui accroissent la vulnérabilité des populations (J. E. Foley et al., 2011). Un moyen d'y parvenir est l'éducation du public pour encourager le signalement des cas de SMB, éviter la propagation accidentelle du champignon et éviter la perturbation les hibernacles. Les humains qui pénètrent dans des sites non infectés doivent absolument désinfecter leurs vêtements et leur équipement pour éviter la contamination. Dans les endroits où un grand nombre d'humains et de chauves-souris sont susceptibles de coexister, les grottes pourraient être fermées au public. Dans une grotte non infectée, l'interdiction d'entrée pour le public pourrait ralentir l'introduction de Pd, et dans une grotte infectée, cette interdiction pourrait réduire la propagation (J. E. Foley et al., 2011). Toutefois, il n'est pas possible de contrôler les contacts entre chauves-souris qui accélèrent la propagation.

La modification des hibernacles peut également permettre de lutter contre le SMB. Il peut être possible de manipuler la température et l'humidité des hibernacles pour qu'ils soient moins propices à la croissance ou à la transmission du Pd ou pour atténuer les effets de l'infection. Cependant, les chauves-souris hibernantes ont évolué pour survivre à l'hiver dans les conditions de croissance du Pd et la modification des hibernacles pour diminuer la croissance du champignon pourrait également réduire la survie des chauves-souris (J. E. Foley et al., 2011).

Finalement, les options de traitement par des agents chimiques ou biologiques à action fongicide sont envisagées (J. E. Foley et al., 2011). Un vaccin est également sous étude afin d'aider les chauves-souris à lutter contre la maladie (Rocke et al., 2019). Un obstacle majeur aux traitements est toutefois l'application en conditions naturelles. L'administration manuelle du traitement à chacun des individus serait impossible de par la taille des populations et la difficulté d'accès à certains hibernacles. Les chauves-souris affectées pourraient être traitées en captivité, mais la procédure est assez complexe et non optimale (J. E. Foley et al., 2011). De nombreuses grottes et mines touchées se trouvent sur des terres privées, dont l'accès est restreint. Elles ont également un grand volume interne et une complexité structurelle qui rendraient l'échantillonnage extrêmement difficile (J. E. Foley et al., 2011). De plus, la vaporisation de fongicide dans les hibernacles affecterait certainement les microorganismes de la grotte, alors que ceux-ci pourraient contribuer à la santé globale et même à la résistance des chauves-souris.

0.6. Microbiome, conservation et maladie de la faune

L'épiderme héberge une communauté de microorganismes diversifiée, composée en majeure partie de bactéries, d'archées, de champignons, de virus et même d'acariens (Grice & Segre, 2011). Cette communauté qui vit en symbiose avec un organisme dans un environnement défini se nomme le microbiote. Le terme microbiome est utilisé lorsqu'en plus du microbiote (taxonomie), on s'intéresse aux gènes (fonctions) ainsi qu'aux conditions environnantes à cette communauté de microorganismes (Marchesi & Ravel, 2015). Le microbiote est étudié par des gènes marqueurs, tels que les gènes de l'ARNr 16S et de l'ITS afin d'obtenir un portrait de la diversité taxonomique (Marchesi & Ravel, 2015). La méthode permettant d'étudier la collection de gènes du microbiome se nomme la métagénomique. Dans la présente thèse, les termes microbiome et microbiote seront utilisés considérant que nous nous intéressons à la communauté taxonomique (microbiote), mais également aux fonctions présentes dans la communauté de la peau (microbiome).

Le microbiome se divise en une flore résidente (organismes directement associés à la peau) et une flore transitoire (organismes libres provenant majoritairement de l'environnement) (Roth & James, 1988). Il est reconnu comme un élément essentiel de la santé de l'hôte, influençant directement une gamme de processus biochimiques et physiologiques, y compris la défense contre les agents pathogènes (Cho & Blaser, 2012). Cette communauté contribue à la défense de l'hôte en limitant la colonisation et la persistance d'agents pathogènes par compétition pour les ressources et en produisant des inhibiteurs de pathogènes (Grice & Segre, 2011; Walter et al., 2018; Woo et al., 2019). Il interagit également avec le système immunitaire inné et adaptatif et contribue au maintien de l'intégrité de la peau et à la réparation des tissus (Lai et al., 2009; Curtis & Sperandio, 2011; Naik et al., 2012).

Or, un débalancement de la communauté microbienne est souvent associé à la maladie (Gilbert et al., 2016; Mackenzie et al., 2017). De même, l'apparition ou le développement de nombreuses maladies peuvent être causés par le microbiome (Belkaid & Hand, 2014; McLean et al., 2015; Mackenzie et al., 2017). Une fonction majeure du système immunitaire est de réguler et de maintenir les communautés microbiennes et de prévenir les activités ou réactions indésirables qui mettraient l'hôte en danger. Cependant, ces fonctions sont altérées lorsque la réponse immunitaire est incontrôlée ou mal dirigée, ce qui entraîne des réactions inflammatoires et allergiques (Belkaid & Hand, 2014). De plus, certains microorganismes du microbiome sont des pathogènes opportunistes lorsqu'ils ne sont pas régulés par le système immunitaire (Xu et al., 2018). La perturbation des communautés microbiennes pourrait créer un microbiome sensible aux infections et aux maladies. Compte tenu du rôle essentiel du microbiome dans la santé de l'hôte, le débalancement de la communauté microbienne pourrait contribuer aux problèmes de conservation d'espèces animales menacées (West et al., 2019).

Dans le contexte des maladies de la faune, des études ont mis en évidence le rôle potentiel du microbiome cutané dans les schémas de résistance et de sensibilité aux pathogènes fongiques (Harris et al., 2009; Bletz et al., 2013, 2017, 2018; Jani & Briggs, 2014; Woodhams et al., 2014; Bataille et al., 2016; Rebollar et al., 2016, 2019, 2020; Ange-Stark et al., 2019). L'interaction compétitive entre les microbes du microbiome cutané et les pathogènes pourrait jouer un rôle dans la dynamique de maladies infectieuses chez de nombreuses espèces (Belden & Harris, 2007). Par exemple, la bactérie *Janthinobacterium lividum* retrouvée sur la peau d'une espèce de salamandre semble conférer une protection contre le champignon *B. dendrobatidis* qui décime les populations d'amphibiens (Brucker et al., 2008). Toutefois, la perturbation du microbiome cutané peut aussi contribuer à la gravité de la maladie chez certaines salamandres (Bletz et al., 2018).

La manipulation du microbiome, grâce au probiotiques ou prébiotiques, pourrait théoriquement améliorer l'état de santé global des animaux (Mueller & Sachs, 2015; Bahrndorff et al., 2016). Toutefois, pour gérer ou manipuler efficacement le microbiome, il faut une connaissance préalable du profil microbien sain (Brüssow, 2016). L'inclusion de méthodes métaomiques peut aider à élucider les rôles fonctionnels du microbiome (Rebollar et al., 2016) et identifier des zones cibles pour des tentatives de manipulation (Mueller & Sachs, 2015). Considérant les nombreux aspects positifs pour la santé qui n'ont pas encore été découverts, il est essentiel d'adopter un changement de paradigme dans la façon dont nous abordons la protection des espèces et leur microbiome (West et al., 2019).

0.7. Microbiome cutané des chiroptères

Le microbiome cutané des chauves-souris semble évoluer différemment que chez les autres groupes de mammifères. Leur structure alaire unique est peut-être à la base de cette différence. En effet, la membrane alaire comprend deux couches d'épiderme mince de chaque côté d'un derme/hypoderme relativement mince contenant des nerfs, des fibres musculaires des vaisseaux sanguins, et un réseau complexe de faisceaux de fibres de tissu conjonctif (Quay, 1970; Sokolov, 1982) (Fig. 0.3). Les ailes peuvent être couvertes de deux types de poils dont un est invisible à l'œil nu (Sterbing-D'Angelo et al., 2011). En revanche, la peau du corps est monocouche, relativement épaisse et, en général, pas très différente de celle des mammifères non volants (Sokolov, 1982).
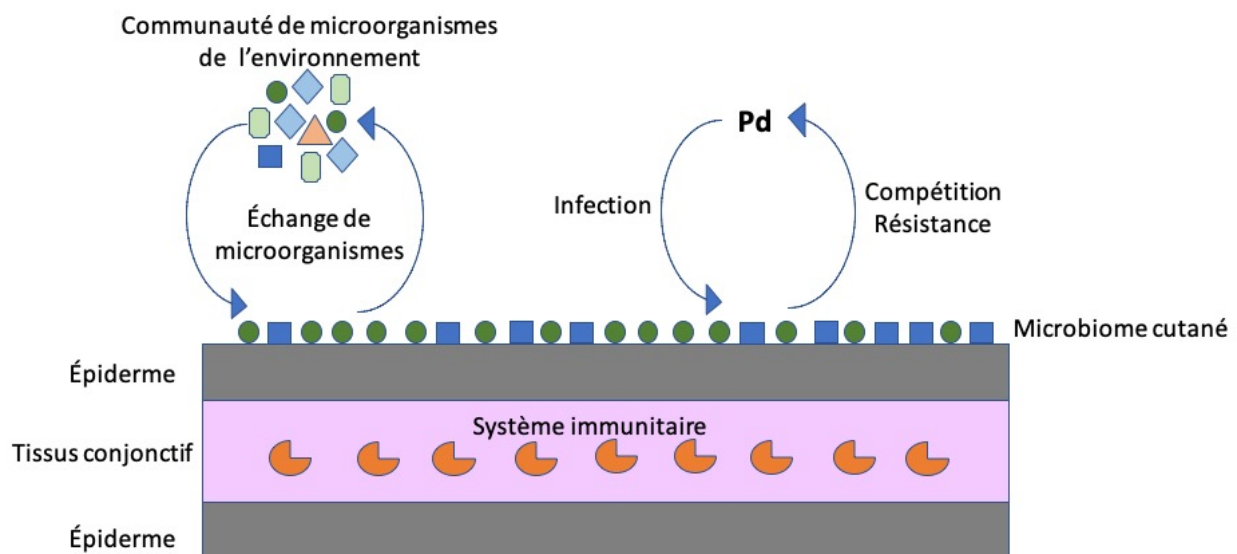
Fig. 0.3. Schéma conceptuel simplifié de la structure de la peau des ailes de chauves-souris ainsi que des relations du microbiome cutané avec l'environnement et le champignon Pd.

L'environnement et l'espèce-hôte sont de bons prédicteurs de la variation du microbiome cutané chez les chauves-souris (Annexe A) (Avena et al., 2016; Lemieux-Labonté et al., 2016; Winter et al., 2017). Une étude a cependant détecté une forte influence du site et du type d'habitat sur le microbiome de treize espèces de chauves-souris de l'ouest des États-Unis, sans toutefois détecter d'influence de l'espèce et du sexe (Kooser et al., 2015). Chez les chauves-souris et les amphibiens, l'environnement semble servir de réservoir pour les microorganismes et la peau pourrait offrir un habitat qui favorise l'enrichissement de certains taxons (Loudon et al., 2014; Walke et al., 2014; Avena et al., 2016) (Fig. 0.3). En conséquence, l'hôte et son environnement local semblent interagir étroitement pour influencer le microbiome cutané. Contrairement aux humains et autres mammifères, le microbiome cutané des chauves-souris grégaires évoluerait dans le temps au niveau de la colonie. Une paire d'échantillons de microbiome de fourrure de deux individus prélevé à la même date au sein d'une même colonie sont plus similaires qu'une paire d'échantillons du même individu prélevés à différents moments (Kolodny et al., 2019). La colonie pourrait donc être l'unité biologique appropriée pour comprendre certains des rôles du microbiome de l'hôte pour l'écologie et l'évolution des chauves-souris (Kolodny et al., 2019).

Dans une optique de traitement au SMB, des microorganismes probiotiques, c'est-à-dire pouvant avoir un bénéfice pour la santé (Sanders, 2008), ont démontré un potentiel inhibiteur sur le SMB. La bactérie environnementale *Rhodococcus rhodochrous* souche DAP96253 (Cornelison et al., 2014) et la levure *Candida albicans* (Raudabaugh & Miller, 2015) ont en effet des propriétés antifongiques contre Pd. Les microorganismes du microbiome des chauves-souris semblent également avoir un potentiel dans la lutte contre l'infection par Pd. Les bactéries antifongiques contre Pd cultivées in vitro seraient d'ailleurs significativement plus abondantes sur la peau des chauves-souris par rapport à l'environnement (Grisnik et al., 2020). Des centaines de microorganismes inhibiteurs de Pd ont été isolés à partir de chauves-souris sauvages et de leurs habitats (Hamm et al., 2017; Micalizzi et al., 2017; Grisnik et al., 2020). Leurs effets inhibiteurs in vitro, se feraient par l'action de composés sécrétés, par l'inhibition par contact ou par l'entremise de molécules volatiles (Hamm et al., 2017; Micalizzi et al., 2017; Grisnik et al., 2020). Une souche de la bactérie *Pseudomonas fluorescens* isolée de la peau d'une espèce résistante au SMB (*E. fuscus*) a démontré une action inhibitrice sur la croissance de Pd in vitro (Hoyt, Cheng, et al., 2015) et in vivo chez *M. lucifugus* (Cheng et al., 2017; Hoyt et al., 2019). L'utilisation de microorganismes constitue une perspective intéressante dans le contexte de la lutte contre la maladie. Or, il y a des dangers potentiels à l'utilisation de tels traitements. L'application de *Pseudomonas* sur des *M. lucifugus* infectées a permis de guérir les individus, mais seulement si le traitement était appliqué au même moment que l'infection par Pd (Cheng et al., 2017). Lorsque le traitement était appliqué plusieurs semaines avant l'infection (comme il serait

avantageux de la faire pour protéger les chauves-souris avant l'hibernation), l'infection était aggravée comparativement aux chauves-souris infectées non traitées. Une explication de cet effet est que le traitement préventif a perturbé le microbiome cutané d'une façon qui a facilité l'invasion par le pathogène. Cette étude souligne l'importance de mieux comprendre l'interaction entre le microbiome et le champignon Pd chez les chauves-souris affectées par le SMB et l'effet potentiel des traitements chimiques ou biologiques sur le microbiome cutané.

Ces découvertes suggèrent que le microbiome pourrait contribuer à la survie des chauves-souris face au champignon. Cependant, des études récentes indiquent plutôt que celui-ci est affecté après l'invasion et la colonisation du Pd (Ange-Stark et al., 2019; Grisnik et al., 2020). Grisnik et al. (2020) ont constaté que les chauves-souris non infectées ont un assemblage microbien contenant plus de taxons antifongiques que les chauves-souris positives, ce qui est incohérent avec une hypothèse d'acquisition antifongique sous la contrainte du Pd. Si les microorganismes commensaux diminuent en abondance tout au long de la progression de l'infection, leurs capacités collectives à produire des fonctions qui inhibent ou empêchent la croissance d'agents pathogènes et/ou de bactéries opportunistes conduisent potentiellement à une augmentation de la gravité de la maladie. Par conséquent, la chauve-souris *M. lucifugus* ayant un microbiome perturbé par l'invasion pourrait être plus vulnérable à la colonisation par Pd (Ange-Stark et al., 2019). Ces données suggèrent qu'il est encore impossible de déterminer si la communauté microbienne de l'hôte peut influencer ou être influencée par l'invasion de pathogènes fongiques.

0.8. Problématique et cadre conceptuel de la thèse

Le SMB est la cause d'un déclin sans précédent chez les chiroptères d'Amérique du Nord. Alors que le champignon continue sa propagation et qu'il est encore impossible de traiter efficacement l'infection en nature, les chauves-souris pourraient avoir un potentiel de résistance ou de tolérance naturelle. Bien que plusieurs mécanismes sont susceptibles d'être en cause, le microbiome cutané pourrait être d'une grande importance dans le patron de vulnérabilité ou de survie des populations en étant la première ligne de défense contre Pd (Belden & Harris, 2007; West et al., 2019). Obtenir des connaissances fondamentales sur le microbiome des chauves-souris pourrait aider à identifier les changements de la communauté microbienne qui peuvent entraîner la vulnérabilité ou la résistance à la maladie.

Plusieurs études ont été menées sur le microbiome cutané de chauves-souris d'Amérique du Nord, mais la majorité ont porté sur des individus non affectés par le SMB (Kooser et al., 2015; Winter et al., 2017) ou se sont basées sur de petits échantillons (Lueschow, 2015; Avena et al., 2016). Deux études ont exploré plus spécifiquement le lien entre la

communauté de microorganismes de la peau et le SMB (Ange-Stark et al., 2019; Grisnik et al., 2020). En dépit de ces travaux, le gouffre des connaissances sur le microbiome cutané des chauves-souris dans le contexte du SMB persiste et il n'est toujours pas possible d'élucider son rôle face à cette maladie.

La petite chauve-souris brune (*M. lucifugus*) et la grande chauve-souris brune (*E. fuscus*) sont des espèces modèles pertinentes afin d'étudier les interactions du microbiome avec le champignon Pd. En effet, les données récoltées sur des espèces vulnérables et résistantes pourraient aider à comprendre la dynamique de l'infection et la résistance potentielle via le microbiome (Fig. 0.4). Afin de caractériser le microbiome de la peau et sa relation avec le SMB chez ces deux espèces, il est cependant primordial de les échantillonner en période d'hibernation. L'étude du microbiome cutané et de ses influences permettront de mieux comprendre son rôle dans les patrons de virulence du pathogène, tant à l'échelle intraspécifique qu'interspécifique. Il est d'autant plus urgent de s'intéresser au microbiome en raison de l'effervescence entourant la recherche de traitements contre cette maladie de la faune. Notamment, l'utilisation de traitements biologiques ou chimiques pourrait perturber le microbiome cutané des chauves-souris et nuire à leur survie.

La présente thèse vise à caractériser le microbiome cutané de chiroptères affectés par le SMB afin d'identifier les facteurs de vulnérabilité ou de résistance à la maladie. L'objectif principal est de déterminer comment le microbiome est affectés par la maladie ainsi que de déterminer si celui-ci à un rôle dans la protection face l'infection fongique. Pour ce faire, le **Chapitre 1** traite du microbiote de colonies de *M. lucifugus* affectées et non affectées par le SMB. Le **Chapitre 2** est consacré au microbiote cutané de *E. fuscus*, une espèce qui résiste à la maladie, en conditions de laboratoire contrôlées. Finalement, le **Chapitre 3** vise à établir des différences fonctionnelles du microbiome cutané de *M. lucifugus* dans un contexte de SMB. Alors que les deux premiers chapitres utilisent une caractérisation taxonomique du microbiote cutané des chiroptères, le dernier chapitre utilise une approche métagénomique pour caractériser le potentiel fonctionnel du microbiome.
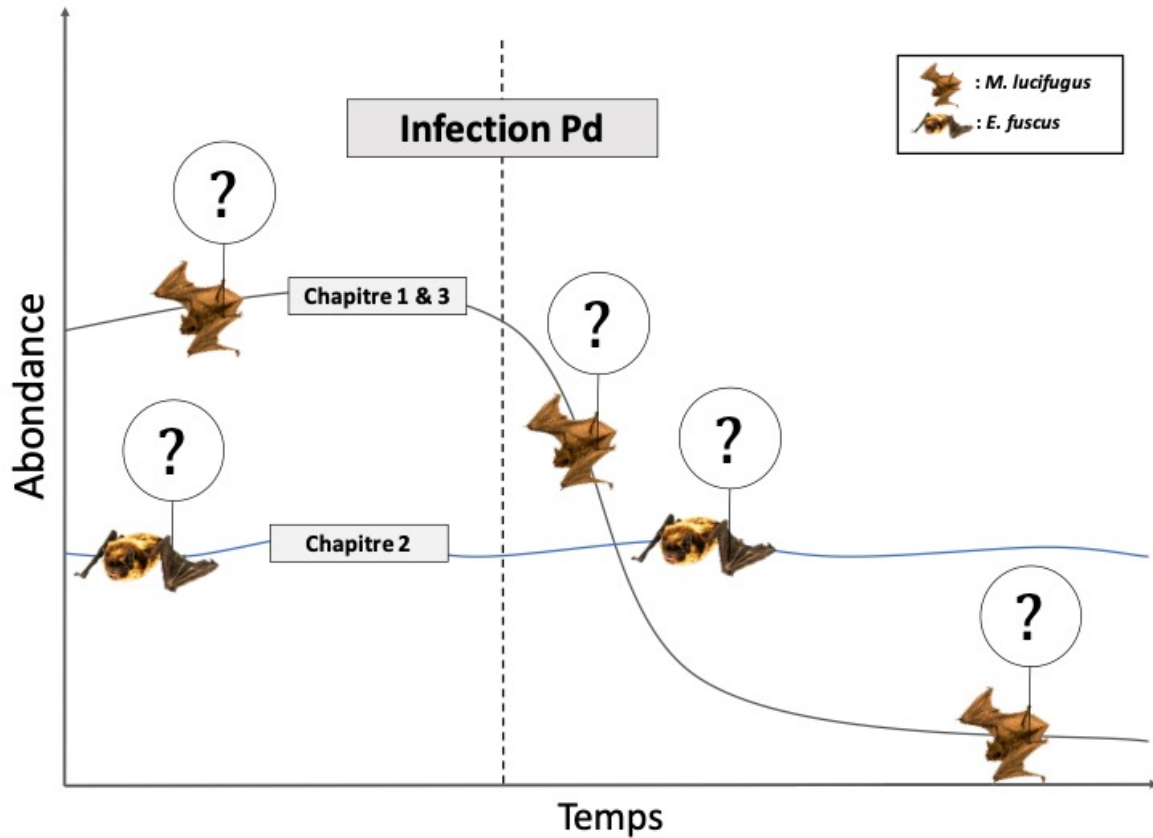
Fig. 0.4. Cadre conceptuel de la thèse. Les chapitres 1 et 3 portent sur la petite chauve-souris brune (*M. lucifugus*), une espèce vulnérable au SMB, et visent à comprendre l'effet de l'infection sur le microbiome et son potentiel dans la vulnérabilité ou la survie de l'espèce. Le chapitre 2 porte sur la grande chauve-souris brune (*E. fuscus*), une espèce non vulnérable à la maladie, et cherche à déterminer si le potentiel antifongique du microbiote cutané peut expliquer cette résistance à la maladie.

Chapitre 1

Enrichment of beneficial bacteria in the skin microbiota of bats persisting with white-nose syndrome

Virginie Lemieux-Labonté[1], Anouk Simard[2], Craig K. R. Willis[3] and François-Joseph Lapointe[1]

[1]Département de sciences biologiques, Université de Montréal, Montréal, Québec, Canada

[2]Direction de l'expertise sur la faune terrestre, l'herpétofaune et l'avifaune, Ministère des Forêts, de la Faune et des Parcs, Québec, Canada

[3]Department of Biology and Centre for Forest Interdisciplinary Research, University of Winnipeg, Winnipeg, Manitoba, Canada

Résumé. Les maladies de la faune augmentent dans le monde entier avec des conséquences graves pour la conservation et la santé humaine. Le microbiote (c'est-à-dire la communauté microbienne vivant sur un hôte ou à l'intérieur de celui-ci) joue un rôle dans la résistance ou la tolérance aux maladies de la faune. Le microbiote pourrait donc contribuer à la lutte contre le syndrome du museau blanc (SMB) causé par le champignon *Pseudogymnoascus destructans* (Pd) qui a tué des millions de chauves-souris nord-américaines depuis 2006. Dans ce contexte, nous avons comparé le microbiote cutané de petites chauves-souris brunes (*Myotis lucifugus*) non affectées par le SMB provenant de trois sites d'hibernation et des chauves-souris survivantes provenant de trois sites affectées par le SMB pour tester l'hypothèse selon laquelle le microbiote cutané est modifié par la maladie. En utilisant le séquençage haut débit du gène de l'ARNr 16S sur 66 chauves-souris et 11 échantillons environnementaux, nous avons constaté que le site d'hibernation influençait fortement la composition et la diversité du microbiote cutané. Les chauves-souris des sites SMB positifs et SMB négatifs différaient en termes de diversité alpha et bêta, ainsi qu'en termes de composition du microbiote. La diversité alpha était réduite dans le microbiote des chauves-souris survivantes des sites SMB positifs et enrichis en taxons tels que *Janthinobacterium*, Micrococcaceae, *Pseudomonas*, *Ralstonia* et *Rhodococcus*. Certains de ces taxons sont reconnus pour leur activité antifongique et des souches spécifiques de *Rhodococcus* et de *Pseudomonas* sont connues pour inhiber la croissance de Pd. La composition de la communauté microbienne dans l'environnement de l'hibernaculum et la communauté sur la peau de chauve-souris étaient similaires, mais différaient en termes d'abondance relative de certains taxons bactériens. Nos résultats sont cohérents avec l'hypothèse que l'invasion par Pd perturbe le microbiote cutané des chauves-souris survivantes et suggèrent la possibilité que le microbiote joue un rôle protecteur face au SMB. La détection de ce qui semble être l'enrichissement en bactéries bénéfiques dans le microbiote cutané des chauves-souris survivantes au SMB est une découverte prometteuse pour le rétablissement des espèces. Nos résultats mettent en évidence non seulement la valeur potentielle des actions de gestion qui pourraient encourager la transmission, la croissance et l'établissement de bactéries bénéfiques sur les chauves-souris et dans les hibernacles, mais également les risques potentiels de telles mesures de gestion. **Mots clés** : microbiote cutané, syndrome du museau blanc, *Myotis lucifugus*, espèces menacées, conservation et gestion, gène ARNr 16S.

Abstract. Infectious diseases of wildlife are increasing worldwide with implications for conservation and human public health. The microbiota (i.e. microbial community living on or in a host) could influence wildlife disease resistance or tolerance. White-nose syndrome (WNS), caused by the fungus *Pseudogymnoascus destructans* (Pd), has killed millions of hibernating North American bats since 2006. We characterized the skin microbiota of naïve, pre-WNS little brown bats (*Myotis lucifugus*) from three WNS-negative hibernation sites and persisting, previously exposed bats from three WNS-positive sites to test the hypothesis that the skin microbiota of bats shifts following WNS invasion. Using high-throughput 16S rRNA gene sequencing on 66 bats and 11 environmental samples, we found that hibernation site strongly influenced the composition and diversity of the skin microbiota. Bats from WNS-positive and WNS-negative sites differed in alpha and beta diversity, as well as in microbiota composition. Alpha diversity was reduced in persisting, WNS-positive bats, and the microbiota profile was enriched with particular taxa such *Janthinobacterium*, Micrococcaceae, *Pseudomonas*, *Ralstonia*, and *Rhodococcus*. Some of these taxa are recognized for their antifungal activity, and specific strains of *Rhodococcus* and *Pseudomonas* are known to inhibit Pd growth. Composition of the microbial community in the hibernaculum environment and the community on bat skin was superficially similar but differed in relative abundance of some bacterial taxa. Our results are consistent with the hypothesis that Pd invasion leads to a shift in the skin microbiota of surviving bats and suggest the possibility that the microbiota plays a protective role for bats facing WNS. The detection of what appears to be enrichment of beneficial bacteria in the skin microbiota of persisting bats is a promising discovery for species reestablishment. Our findings highlight not only the potential value of management actions that might encourage transmission, growth, and establishment of beneficial bacteria on bats, and within hibernacula, but also the potential risks of such management actions.
Key words: skin microbiota, white-nose syndrome, *Myotis lucifugus*, endangered species, conservation and management, 16S rRNA gene

1.1. Introduction

Infectious diseases of wildlife are on the rise worldwide with dramatic consequences for wildlife conservation and human public health (Daszak, 2000; Jones et al., 2008; Fisher et al., 2012). In North America, insectivorous bats provide important ecosystem services by limiting insect pests and potentially saving billions of dollars annually for agriculture (Boyles et al., 2011; Maine & Boyles, 2015). However, a number of ecologically important species are threatened by white-nose syndrome (WNS). This skin disease, caused by the fungus *Pseudogymnoascus destructans* (Pd) (Gargas et al., 2009; Lorch et al., 2011), has killed millions of North American bats since 2006 (Coleman, 2012).

White-nose syndrome involves invasion of exposed skin by Pd, and the disease is defined by cup-shaped erosions and ulcerations on the tissue of the flight membranes (wings and tail), ears, and muzzle (Meteyer et al., 2009). Infection of the flight membranes is thought to be the most pathologically significant aspect of the infection because this tissue is involved in fluid balance, thermoregulation, and gas exchange (Cryan et al., 2010). Pd invades hair follicles, sebaceous and apocrine glands (Meteyer et al., 2009). This likely disrupts secretions that contribute to skin integrity (Sisk, 1957; Cortese & Nicoll, 1970) with consequences for defense against pathogens and important skin commensal microorganisms (Grice & Segre, 2011). Hibernating bats survive the winter on just a few grams of stored fat by using prolonged energy-saving bouts of torpor characterized by dramatically reduced body temperatures and metabolism (Jonasson & Willis, 2012; Czenze et al., 2013; Czenze & Willis, 2015). Pd is adapted for growth at the low temperature characteristic of bat skin during torpor (Gargas et al., 2009), and infection causes hibernating bats to warm up too frequently during winter and deplete their fat reserves (D. M. Reeder et al., 2012; Warnecke et al., 2012). The immune system is downregulated during hibernation (Geiser, 2004; Bouma et al., 2010; Moore et al., 2011) which, in turn, facilitates infection.

Seven species of bats have suffered impacts from WNS in North America (Frick et al., 2016) but not all bat species are equally affected (Turner et al., 2011; Langwig et al., 2012). It has been suggested that environmental conditions inside hibernacula, physiology, and behavior could all play a role in the variable tolerance of, or resistance to, infection with Pd among species (Puechmaille et al., 2011; Langwig et al., 2012; Willis & Wilcox, 2014; Frick et al., 2016). In Canada, the northern long-eared bat (*Myotis septentrionalis*), the little brown bat (*Myotis lucifugus*), and the tricolored bat (*Perimyotis subflavus*) are listed as federally endangered (Frick et al., 2016) due to mortality rates of 75–90% during the several-year invasion stage of the disease (Canadian Wildlife Service & Committee on the Status of Endangered Wildlife in Canada, 2013).

Despite extremely high mortality during the epidemic stage of WNS, some hibernating colonies of at least one highly vulnerable species (e.g., *M. lucifugus*) seem to have persisted following disease invasion (Dobony et al., 2011; Langwig et al., 2012; Frick et al., 2015; Maslo & Fefferman, 2015) with colony counts stabilizing at about 5 to 30% of their initial size (Langwig et al., 2012; Frick et al., 2015). Recently, it was observed that intensity of infection with Pd, based on swabs of bat forearms and quantitative PCR, was significantly lower for persisting colonies in which Pd had become established, compared to colonies in the midst of the epidemic phase and massive declines (Langwig et al., 2017). One mechanism that could explain this pattern is a fundamental shift in the microbial community living on bat skin due to selection for Pd antagonists. Strong selection for microbial taxa that

inhibit Pd could provide resistance to the fungus and increase bat survival.

Animal skin is an ecosystem inhabited by highly variable and complex communities of microorganisms (Grice & Segre, 2011). This community, called microbiota, can be divided into a resident flora, defined as a relatively stable assemblage in size and composition, and a transient flora, acquired from the local environment and that only temporarily colonizes the skin (P. B. Price, 1938). A healthy skin microbiota can directly contribute to host fitness by occupying pathogen adhesion sites and producing pathogen inhibitors (Roth & James, 1988; Grice & Segre, 2011). Competitive interactions between beneficial and pathogenic skin microbes are hypothesized to play a role in disease dynamics for wild animals (Belden & Harris, 2007). For example, the bacterium *Janthinobacterium lividum*, which lives on salamander skin, appears to confer resistance to the devastating fungal pathogen *Batrachochytrium dendrobatidis* (Brucker et al., 2008) and could explain why some salamander populations decline while others do not. Recently, a strain of the bacterium *Pseudomonas fluorescens* isolated from the skin of a bat species thought to be resistant to WNS (*Eptesicus fuscus*) was shown to inhibit Pd growth in vitro (Hoyt, Cheng, et al., 2015) as well as in vivo for *M. lucifugus* (Cheng et al., 2017). It has been hypothesized that WNS could cause a shift in microbiota communities of the skin (Lueschow, 2015), and this could be one mechanism underlying resistance in persisting bats. However, it could also have negative consequences for bat populations if a shift in the microbiota makes it easier for opportunistic pathogens other than Pd to invade the skin. A detailed characterization of the skin microbiota for WNS-positive and WNS-negative bats is, therefore, needed to fully understand potential implications of skin microbial communities in the context of WNS.

Due to its direct exposure to the local environment, the skin microbiota is more dynamic and should be more strongly influenced by the environment, than the gut microbiota (Romano-Bertrand et al., 2015). Environment and host species are strong predictors of variation in the skin microbiota among bats (Avena et al., 2016; Lemieux-Labonté et al., 2016; Winter et al., 2016). However, one study (Kooser et al., 2015) found a strong influence of site and habitat type on the skin microbiota of 13 bat species in the western USA but was not able to detect an influence of host species or sex. For bats and amphibians, the local environment appears to act as a reservoir for skin microbiota, while conditions on the skin may lead to selection favoring or enriching particular taxa (Loudon et al., 2014; Walke et al., 2014; Avena et al., 2016). Consequently, host and local environmental factors appear to interact closely to shape the skin microbiota. This suggests that the skin microbiota could exhibit dramatic temporal variation for species characterized by seasonal shifts in physiology and habitat selection. Bats exhibit enormous changes in metabolism and habitat selection between winter and summer. Therefore, to fully characterize the skin microbiota

and its relevance to WNS, bats must be sampled at the appropriate time during hibernation.

Several studies have reported on the skin microbiota of North American bats, but, to date, these have involved individuals not yet affected by WNS (Kooser et al., 2015; Winter et al., 2016) or have been based on relatively small sample sizes (Lueschow, 2015; Avena et al., 2016). Our objective was to understand the potential interaction between Pd and the skin microbiota of bats by comparing individuals from WNS-positive and WNS-negative regions. We used high-throughput 16S amplicon sequencing to characterize the composition and diversity of the skin microbiota of *M. lucifugus* sampled from WNS-positive (Québec) and WNS-negative (Manitoba) hibernacula in the northern part of this species' range, in Canada. We tested two predictions of the hypothesis that WNS is causing selection favoring Pd antagonists on the skin microbiota of bats in the affected region. First, we predicted that bats persisting in WNS-affected sites would exhibit reduced diversity of their microbiota consistent with strong selection for a subset of pre-WNS microbial species (Lueschow, 2015). Second, we predicted that the microbiota of persisting bats from WNS-affected sites would show a proportional increase in antifungal/anti-Pd bacterial species such as those identified in previous studies (Cornelison et al., 2014; Hoyt, Cheng, et al., 2015; Cheng et al., 2017). We also tested the third hypothesis that variation in the skin microbiota of hibernating bats relates to environmental variation in the microbial community of a given cave. We predicted that the diversity and composition of the microbial community living on individual bats would be similar to that found on substrates in the local environment of their hibernaculum and would differ from that on bats and the local environment in other hibernacula.

1.2. Material and Methods

1.2.1. Samples collection

During winter 2015–2016, we sampled the skin microbiota of 33 *M. lucifugus* from three WNS-negative hibernacula in central Manitoba (Canada) about 50 km north of the town of Grand Rapids ($53°30'N$, $99°24'W$) and another 33 individuals from three sites known to be WNS-positive since 2010 in Québec (Canada) within 60 km north of Gatineau city ($45°28'N$, $75°42'W$). The temperature within sites ranged from -3 to 7 °C at sampling time. Site and colonies information are specified in Table 1.1.

Bats in a given hibernaculum were always sampled from within the same area (i.e., room, gallery, corridor). We selected bats at random from among those we could reach from the ground. Little brown bats are highly gregarious during hibernation, and most individuals spend at least part of their time huddling or clustering during hibernation. We defined bats

Table 1.1. *M. lucifugus* hibernaculum sites information in Manitoba and Québec provinces.

Sites	Province	Substrate	Pre-WNS count	Total count 2015-2016	Sampling dates
Abyss	Manitoba	Dolomite	NA	399	08/02/2016
Dale's	Manitoba	Dolomite	NA	385	08/02/2016
Microwave	Manitoba	Dolomite	NA	30	09/02/2016
Emerald	Québec	Pyroxenite	735[a]	18	04/03/2016
Laflèche	Québec	Calcite	450[a]	155	23/11/2015
Lames	Québec	Calcite	Unknown[b]	105	24/11/2015

[a] 2009–2010; [b] First count of 96 bats was in 2012–2013, after the arrival of WNS in the area.

in direct contact with each other as being members of the same cluster. Sixty-four of the 66 bats we sampled were clustering with other bats, and cluster sizes ranged in size from 2 to 11 individuals. We sampled two bats at Emerald that were roosting solitarily (Table S1.1). We swabbed 11 individual bats per site. Samples were collected by swabbing in linear strokes the back and forearm of each bat for 20 s with a sterile Whatman Omniswab (Fisher Scientific) soaked in sterile 0.15M NaCl (Lemieux-Labonté et al., 2016). Swab tips were ejected into MoBio Powersoil DNA isolation Kit tubes (MoBio Laboratories), which were transferred to -20 °C within 24 h of sampling until DNA extraction. Local environment samples were also collected by swabbing cave walls adjacent to clusters of sampled bats for 20 s in linear strokes (approx. 5 cm). As a negative control, a humidified sterile swab was exposed to open air for 20 s, prior to ejecting its tip into a MoBio tube.

Bats are vulnerable to disturbance during hibernation, and we were careful to minimize the impact of our visits. Only two people entered hibernacula for sampling, and bats were not handled during swabbing so we did not determine their sex. A previous study established that sex was not a significant predictor of the external microbiota of bats (Kooser et al., 2015). Therefore, differences among hibernacula are likely to reflect the influence of the local habitat (e.g., differences in temperature, humidity, and environmental bacteria), rather than difference in sex ratio among sites. All methods were approved by the Animal Welfare and Ethics Committee at Université de Montréal (Protocol Number 16-015) and the University of Winnipeg Animal Care Committee (Protocol Number AEO5639).

1.2.2. DNA extraction, amplification, and sequencing

Bacterial genomic DNA was extracted from each swab using the MoBio Powersoil DNA isolation Kit according to the manufacturer's protocol. Extractions were randomized for site and region to avoid detecting false patterns (Salter et al., 2014). Extraction, amplification blanks, and the HM-782D Human Microbiome Project mock community (BEI Resources) were also included to detect possible contamination and assess sequencing accuracy (Salter et al., 2014; Glassing et al., 2016). Amplification and sequencing were

then performed as previously described (Preheim, Perrotta, Friedman, et al., 2013b). Libraries were prepared using a two-step PCR. The first PCR amplified the hypervariable region V4 of the 16S small subunit ribosomal gene with forward primer U515f: ACAC-GACGCTCTTCCGATCTYRYRGTGCCA GCMGCCGCGGTAA and reverse primer E786R: CGGCATTCCTGCTGAACCGCTCTTCC GATCTGGACTACHVGGGTWTC-TAAT (Caporaso et al., 2011). Two microliters of extracted DNA (equivalent DNA amount by sample) was added to the PCR reaction containing 14.25 μl of sterile water, 5 μl HF buffer, 0.5 μl DNTPs, 0.25 μl Phusion High-Fidelity DNA Polymerase (New England Biolabs Inc.), and 1.5 μl of forward and reverse primers. Amplifications were performed with a Mastercycler Nexus GSX1 (Eppendorf) under the following conditions: initial denaturation at 98 °C for 30 s; 30 cycles alternating 98°C for 25 s, 40 s at 54 °C, 35 s at 72 °C, and final elongation step for 1 min at 72 °C. Each sample was amplified in quadruplicate and pooled to limit possible PCR artifacts. All PCR products were then purified by PCR purification Agencourt AMPure XP (Beckman Coulter). The second PCR step consisted of adding primers containing a barcode (index) and Illumina adapter sequences to each DNA amplicon. To do so, 4 μl of the first step amplification product was added to a PCR reaction containing 10.25 μl of sterile water, 5 μl HF buffer, 0.5 μl DNTPs, 0.25 μl Phusion High-Fidelity DNA Polymerase, and 2.5 μl of forward primer PE−III−PCR−F: AATGATACGGCGAC-CACCGAGATCTACACTCTTTCCCTACACGACGCTCTTCCATCT and reverse primer PE−III−PCR−001−096: CAAGCAGA AGACGGCATACGAGATNNNNNNNNNCG-GTCTCGGCATTCCTGCTGAACCGCTCTTCCGATCT (N indicating the unique barcode) (Preheim, Perrotta, Friedman, et al., 2013b). Indexing was performed under the following thermal conditions: initial denaturation at 98 °C for 30 s, 7 cycles alternating 98 °C for 30 s, 30 s at 83 °C, and finally 30 s at 72 °C. This second amplification was performed in triplicate. Samples were pooled and purified with the PCR purification Agencourt AMPure XP (Beckman Coulter). Qubit 2.0 Fluorometer (Invitrogen) was used to measure the DNA concentration of each sample. Indexed samples were then pooled to obtain a final concentration range between 10 and 20 ng/μl. DNA was next diluted and denatured according to the manufacturer's protocol for paired-end sequencing using MiSeq Reagent Kit v2 (500 cycles) 2 × 250 bp on MiSeq (Illumina).

1.2.3. Data analysis

We amplified 4,072,792 sequences classified into 13,224 operational taxonomic units (OTUs) from the 66 swabs of bat skin and 11 environmental samples (one or two per site). A total of 3,729,096 sequences classified in 11,812 OTUs were amplified from bat samples with a mean of 56,501 sequences per sample (range 9,920–100,812). A total of 343,696 sequences classified in 9,302 OTUs were obtained from the 11 environmental samples, with

a mean of 31,245 sequences per sample (range 10,325–73,877). We were able to match all expected sequences in the mock positive control, except for *Helicobacter pylori*, which genus was nonetheless the most abundant in the compositional data (Table S1.2). The genera or families of the 20 expected mock taxa were also the most abundant in the mock profile. We detected 36 false positives, with very low abundances (<0.3%) (Table S1.2). After filtering out OTUs with abundance values smaller than 3, sampling controls, extraction controls, and library negative controls were dominated by *Halomonas* (5–75%, mean of 56%) and *Shewanella* genera (1–26%, mean 18%) (Table S1.3).

Preclustering, quality filtering, primer removal, merging of raw sequences, and post-clustering dereplication were performed with the SmileTrain scripts (Almlab, 2015) for 16S data processing using USEARCH v.7.0.1090 (Edgar, 2010). Distribution-based clustering using the dbOTUcaller algorithm was performed to cluster sequences into OTUs by considering the distribution of DNA sequences across samples and distances between sequences (Preheim, Perrotta, Martin-Platero, et al., 2013). The corresponding OTU table, providing abundances of bacterial taxa in the different samples was assigned with QIIME version 1.9.0 (Caporaso et al., 2010) using GreenGenes database release 13_5 (DeSantis et al., 2006). For alpha diversity and compositional analysis of bat samples, mitochondrial and chloroplastic DNA sequences, as well as OTUs with abundance values smaller than 3, were filtered out, leaving 3,716,672 sequences classified into 9,897 OTUs. In addition, the genera *Halomonas* and *Shewanella*, present in negative controls, were filtered out from all bat samples for compositional analysis, resulting in 3,145,399 sequences classified into 9,575 OTUs.

The diversity of the skin microbial community (alpha diversity) of each sample was computed using the Shannon index (Shannon, 1948). The Shannon index, which includes both OTU richness and evenness, was selected due to its reduced sensitivity to sample depth differences (Haegeman et al., 2013; Preheim, Perrotta, Friedman, et al., 2013b) (Fig. S1.1). R version 3.1.3 (Team, 2018) was used for all statistical analyses. Log-transformed alpha diversity values were compared between WNS-positive and WNS-negative regions, using a linear mixed-effect model (lme() function), and significance was tested with anova.lme() of the nlme package (Pinheiro et al., 2017). Hibernaculum and clusters were included as a random effect. Variation in diversity among sites within the WNS-positive and WNS-negative regions was tested using a one-way ANOVA (function aov()) and post hoc Tukey test (function TukeyHSD()) of the package stats (Team, 2018).

The change in diversity among skin microbial community (beta diversity) was calculated among skin microbiota samples and environmental samples. Two distinct phylogenetic

distances, unweighted UniFrac (qualitative) and weighted UniFrac (quantitative) (Lozupone & Knight, 2005; Lozupone et al., 2007), were computed on rarefied data, as such measures could be sensitive to differences in sequencing depth (Lozupone et al., 2011; Weiss et al., 2017). UniFrac distances were computed from bat samples rarefied at 9,886 sequences/sample and from environmental + bat samples rarefied at 9,898 sequences/sample after retrieving OTUs in low abundance (<3 sequences). Computations were performed with the phyloseq package (McMurdie & Holmes, 2013). All beta diversity results were visualized with principal coordinates analysis (PCoA) (Gower, 1966) using the ordinate() function. The UniFrac distance matrix was checked with is.euclid() function of the ade4 package (Dray & Dufour, 2007) prior to the ordination to ensure that all distances were Euclidian and properly represented by PCoA (Gower & Legendre, 1986). When required, square-root transformations were applied to obtain distance matrices satisfying the Euclidian condition. All phylogeny-based UniFrac distances were calculated using a phylogenetic tree constructed with FastTree 2.1.8 (M. N. Price et al., 2010).

To assess the influence of explanatory variables on the microbiota composition, we used distance-based redundancy analysis (db-RDA), a method intended to conduct a redundancy analysis (RDA) on distance matrices (Legendre & Anderson, 1999). It is computed by first decomposing UniFrac distances (weighted or unweighted) into principal coordinates and then applying RDA to the corresponding principal coordinates using the capscale() function of the R package vegan (Oksanen et al., 2019). Four distinct models were constructed to test the relative importance of (1) WNS status (i.e., WNS-negative vs. WNS-positive), (2) sampling sites (i.e., the six different hibernacula), (3) types of samples (i.e., bat samples vs. local environment samples), and (4) clusters (i.e., bat clusters within each hibernaculum). To better understand the relationships among explanatory models in the variation of the microbial assemblages, partial db-RDA was also computed (Davies & Tso, 1982). This form of RDA allows for exploration of the contribution of an explanatory variable model while controlling for other explanatory models. Adjusted R-squared (R^2) values (Ezekiel, 1930) were calculated to compare the explanatory power of such models containing different numbers of variables. Significance of db-RDA and partial db-RDA was tested via 9999 permutations with the anova.cca() function of the R package vegan .

The microbiota composition was explored down to genus level to assess differences among hibernacula and between WNS-positive and WNS-negative sites. To emphasize these differences, Indicator Value tests (IndVal) (Dufrene & Legendre, 1997) were performed on relative abundance data, using the 26 taxa with a relative abundance larger than 1 % for the analysis. The IndVal indicator value is based on the comparison of occurrences and abundances of taxa across predefined groups of bats (e.g., grouped by sites or WNS status). The analysis

for any given taxon is not influenced by other taxa present in the dataset. It provides an index ranging between 0 and 1, the maximum value indicating a taxon exclusively present in one group. IndVal is calculated as the product of A (specificity, i.e., the probability that a site belongs to the group given the fact that a given species is found in that site) and B (fidelity, i.e., the probability of finding a given taxon at a site when the site belongs to that group) (Dufrene & Legendre, 1997). The multipatt() function of the R package indicspecies (De Cáceres & Legendre, 2009) was used to compute indicator values, and significance was assessed with 9999 permutations of object between groups. The p.adjust() function of the R package stats was used to correct p values for multiple comparisons (Holm, 1979). A corrected *p*-value threshold of 0.05 was considered significant in all tests, and only significant taxa with a specificity of A ≥ 0.4 were retained as indicators.

1.3. Results

1.3.1. Alpha diversity in WNS-positive and WNS-negative regions

After controlling for sites and bat clusters using a linear mixed-effects model, we found significant differences in Shannon diversity between our pooled set of WNS-positive hibernacula in Québec and WNS-negative hibernacula in Manitoba (ANOVA: $F_{1,4} = 16.27$, $p \leq 0.05$) (Fig. 1.1A). WNS-positive sites had significantly lower Shannon diversity than WNS-negative sites (Fig. 1.1A). We also found significant variation in alpha diversity between some of the hibernacula in the WNS-negative region (ANOVA: $F_{2,30} = 22.84$, $p \leq 0.001$), whereas all the three WNS-positive sites in Québec were statistically indistinguishable from each other and had relatively low alpha diversity (ANOVA: $F_{2,30} = 0.96$, $p = 0.395$) (Fig. 1.1B). Within the WNS-negative region in Manitoba, Abyss cave harbored particularly high alpha diversity and was significantly different from Dale's (Tukey's: $p \leq 0.0014$) and Microwave (Tukey's: $p \leq 0.001$).
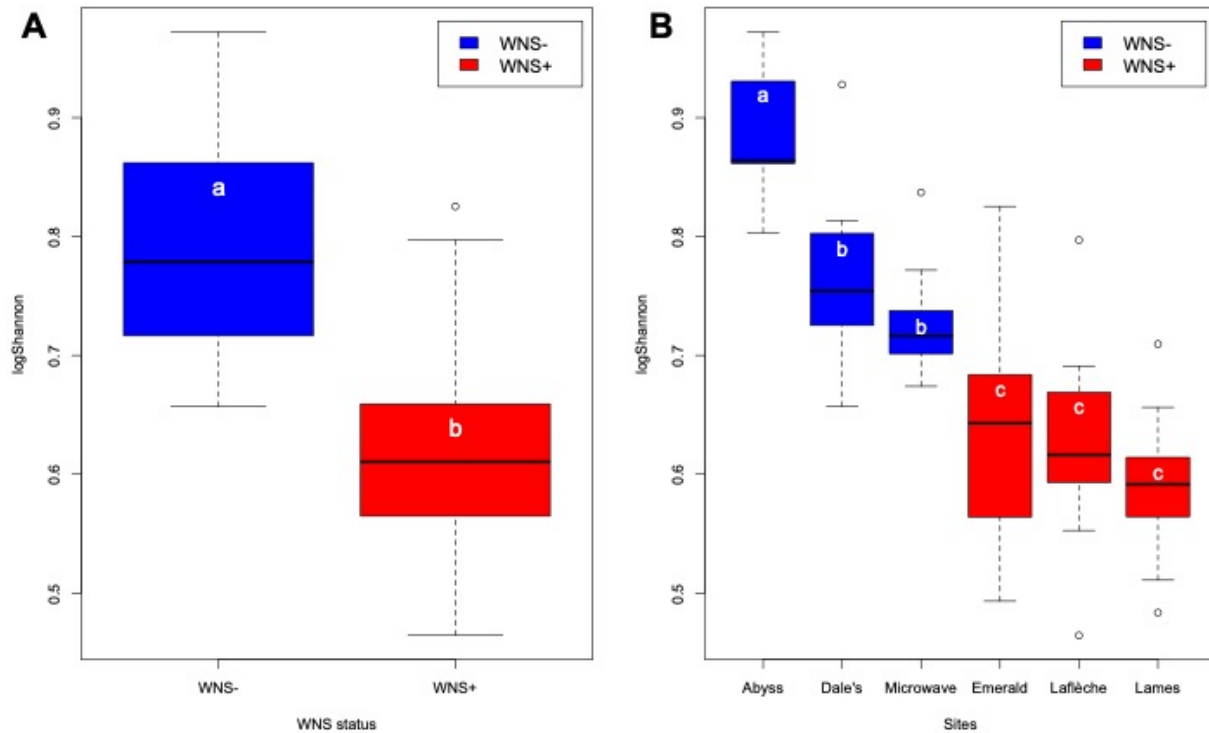
Fig. 1.1. Alpha diversity of *M. lucifugus* skin microbiota in WNS-positive and WNS-negative sites in Canada. Distribution of alpha diversity within groups as estimated by the Shannon index for (A) hibernacula pooled by WNS status (positive vs. negative) and (B) all six hibernacula sampled in the study. Error bars represent standard deviations. Significant differences in alpha diversity among groups are indicated by different letters according to model effect, ANOVA, and Tukey's test ($p \leq 0.05$).

1.3.2. Beta diversity analysis of microbial community assemblage

We first used beta diversity analysis to explore compositional differences among skin microbiota samples alone, that is, after removing all environmental samples from the analysis. The PCoA, based on unweighted UniFrac, revealed a clear separation between WNS-positive sites in Québec and WNS-negative sites in Manitoba, and also grouped samples from within the same hibernaculum (Fig 1.2A). This pattern was not observed with weighted UniFrac (Fig 1.2B), which implies that accounting for differential abundances (weighted UniFrac), and not just the presence/absence of bacterial OTUs between samples (unweighted UniFrac), affected our results. However, the first principal axes, accounting for 20.1% of the variation in the data, support the separation of microbiota samples according to WNS status (Fig. 1.2A).
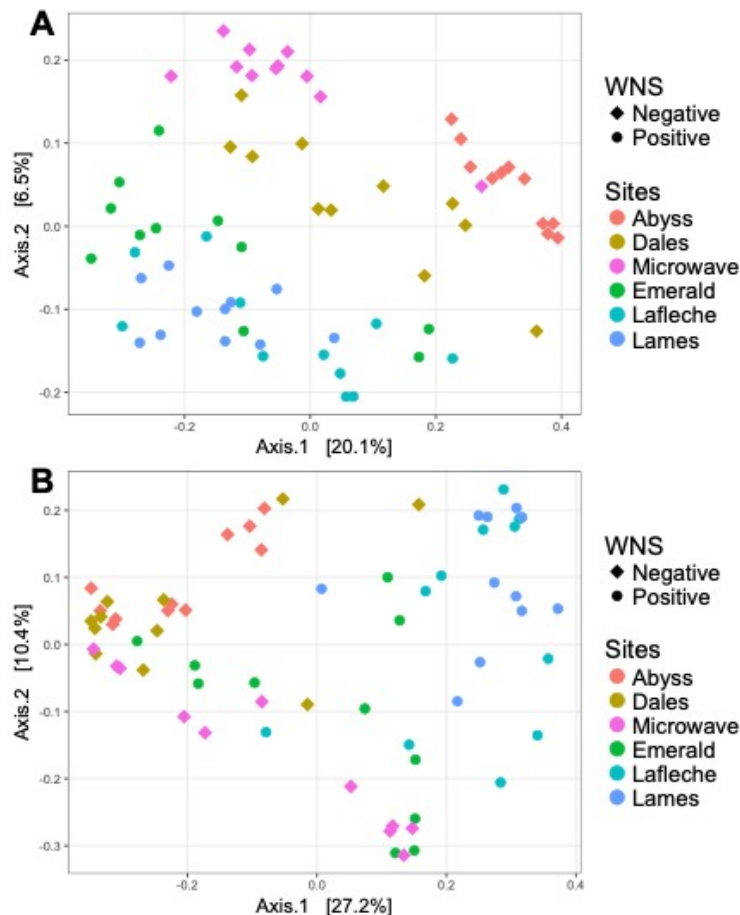
Fig. 1.2. Principal coordinate analysis of *M. lucifugus* skin microbiota in WNS-positive and WNS-negative sites. (A) Principal coordinate analysis of unweighted UniFrac distances. (B) Principal coordinate analysis of weighted UniFrac distances. Each point represents a sample from an individual bat hibernating in one of the six different hibernacula that differed in WNS status.

In order to better relate these patterns to different variables, we used a distance-based redundancy analysis (db-RDA) to compute from UniFrac distances among skin microbiota samples using three distinct explanatory models: (1) WNS status, (2) sampling sites (hibernacula), and (3) clusters (bat clusters within each hibernaculum). Unweighted UniFrac distances revealed that each of these models explained a significant fraction of microbiota community variation (Table 1.2). The WNS status model explained 8%, sites explained 22%, and bat cluster explained 28% of microbiota community variation among samples. Weighted UniFrac distances accounting for abundance of taxa revealed similar patterns with WNS status explaining 14%, sites explaining 26%, and cluster explaining 30% of the variation in the microbiota samples (Table 1.2).

Table 1.2. db-RDA of unweighted and weighted UniFrac distances of *M. lucifugus* skin microbiota samples.

	Model	Test	Adjusted R^2	F statistic
db-RDA unweighted UniFrac	WNS	Global	0.08***	7.03
		Partial: sites	0	0
		Partial: clusters	0	0
	Sites	Global	0.22***	4.68
		Partial: clusters	0	0
		Partial: WNS	0.14***	3.78
	Clusters	Global	0.28***	2.98
		Partial: sites	0.06***	1.67
		Partial: WNS	0.19***	2.48
db-RDA weighted UniFrac	WNS	Global	0.14***	11.70
		Partial: sites	0	0
		Partial: clusters	0	0
	Sites	Global	0.26***	5.45
		Partial: clusters	0	0
		Partial: WNS	0.11***	3.45
	Clusters	Global	0.30***	3.18
		Partial: sites	0.05***	1.53
		Partial: WNS	0.16***	2.24

WNS, sites, and clusters model redundant variation with UniFrac beta diversity variation among *M. lucifugus* skin microbiota. Global test for one model redundant variation on microbial community whereas the partial test for the model controlling variation from the other model. ***$p \leq 0.001$. Total inertia of response variable matrix is 0.21286 for unweighted UniFrac db-RDA and 0.10555 for weighted UniFrac db-RDA.

In light of these results, we conducted partial RDA to better distinguish the relative influence of our three explanatory models (Table 1.2). This analysis revealed that WNS status explained no variation after controlling for sites and/or clustering. Similarly, the sites model explained none of the variation after controlling for bat cluster. The cluster model, on the other hand, explained a significant fraction of variation in microbiota community after controlling for sites, both with weighted and unweighted UniFrac distances. These results suggest that bat clustering within each hibernaculum exerts strong influence on the

composition of the skin microbiota. Controlling for WNS status, however, greatly reduced the variation explained by sites and cluster models alone, regardless of UniFrac distances (unweighted or weighted). Taken together, the results of simple and partial db-RDA analyses suggest that sites, combined with a local effect of bat clustering within sites, contribute to shaping the skin microbiota, whereas WNS status have much less influence.

We next used unweighted and weighted UniFrac to explore the relationship between skin microbiota samples and environmental samples collected at each site. The first PCoA, based on unweighted UniFrac distances, grouped skin microbiota samples and environmental samples by sites, with some overlap between them (Fig. 1.3A). The second PCoA based on weighted UniFrac distances revealed a different pattern, however. In that case, the PCoA plot clearly distinguished between environmental samples and skin microbiota samples collected at all sites (Fig. 1.3B), except for three bat samples from Abyss and one from Dale's. The results of PCoA suggest that the presence/absence of OTUs in bat skin samples is influenced by the local environment within each hibernaculum. Yet, the same analyses also reveal differences in abundance patterns of some OTUs in bat skin samples compared to local environmental samples.

We then used RDA to explore the influence of site (hibernaculum) and sample type (bat vs. environment samples) on variation in microbial community assemblage. Both of these models were significant (Table 1.3), but the sites model accounted for the most variation in the data, explaining 18% of the microbial community variation in both UniFrac distances employed (Table 1.3). The sample type model only explained 5% of microbial variation for unweighted UniFrac distances and 8% for weighted distances. The higher explanatory power of the weighted UniFrac model indicates that differences observed between environmental samples and bat samples partly depend on the relative abundance of each taxon within the corresponding microbial communities. This is consistent with patterns revealed by the PCoA plots (Fig. 1.3).

We used a partial db-RDA to better understand the relationship between the two explanatory models, and their influence on the composition of microbial communities. In both cases, when variation of one model was controlled for using partial db-RDA, the ability of the models to explain variation in microbial community composition was slightly increased by 1% (Table 1.3). These results suggest that both sample type and sites models had a non-redundant influence on microbial community variation and that the local environment is an important factor explaining skin microbiota patterns of hibernating bats in our study sites.
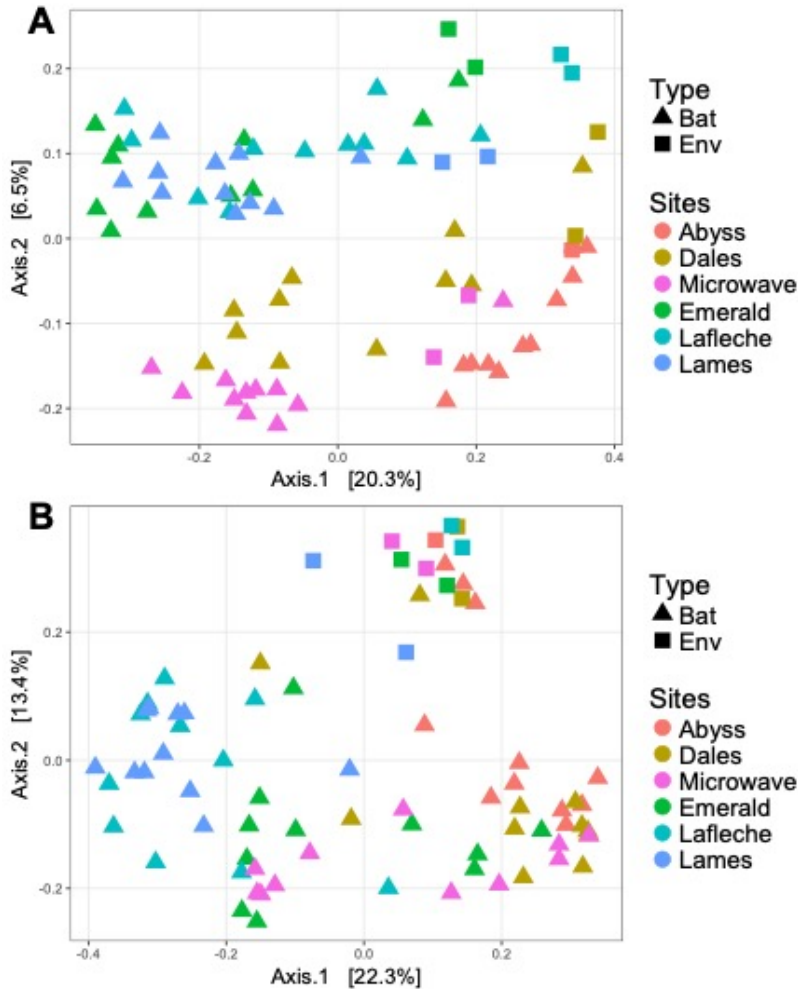
Fig. 1.3. Principal coordinate analysis comparing local environment sites samples and *M. lucifugus* skin microbiota in Canada. (A) Principal coordinate analysis of unweighted UniFrac distances. (B) Principal coordinate analysis of weighted UniFrac distances. Each point represents a single sample.

Table 1.3. db-RDA of unweighted and weighted UniFrac distances among local environment and bat skin microbiota samples.

	Model	Test	Adjusted R^2	*F* statistic
db-RDA unweighted UniFrac	Sites	Global	0.18***	4.35
		Partial: type	0.19***	4.82
	Type	Global	0.05***	4.78
		Partial: sites	0.06***	6.65
db-RDA weighted UniFrac	Sites	Global	0.18***	4.25
		Partial: type	0.19***	4.86
	Type	Global	0.08***	7.18
		Partial: sites	0.09***	9.51

Sites and type model redundant variation with UniFrac beta diversity variation among *M. lucifugus* skin microbiota and site environmental microbial assemblage. Global test for one model redundant variation on microbial community whereas the partial test for the model controlling variation from the other model. ***$p \leq$ 0.001. Total inertia of response variable matrix is 0.21818 for db-RDA unweighted UniFrac and 0.22375 db-RDA weighted UniFrac.

1.3.3. Taxonomic indicators of WNS status

We found that the most abundant bacterial taxa were shared among all hibernacula, but we also identified indicator taxa present more often and more abundant at particular sites. At the phylum level, the dominant taxa accounting together for 86 to 98% of overall profiles in a given cave were Actinobacteria (23 to 53%), Proteobacteria (24 to 51%), and Bacteroidetes (6 to 38%) (Table S1.4). At the class level, the six principal taxa accounting for 80 to 98% of the total abundance were Actinobacteria, Gammaproteobacteria, Flavobacteriia, Sphingobacteriia, Alphaproteobacteria, and Betaproteobacteria (Table S1.5).

Generalist genera such as *Arthrobacter*, *Chryseobacterium*, *Flavobacterium*, Intrasporangiaceae, *Pedobacter*, *Mycoplana*, Pseudonocardiaceae, *Ralstonia*, *Rhodococcus*, *Sinobacteraceae*, and *Sphingobacterium* were identified from all sites (Fig. S1.2). Significant representatives were found among the 26 more abundant taxa representing more than 1% of the total composition profile (Fig. 1.4, Table S1.6). Among the more abundant taxa identified at three WNS-positive sites in Québec, only *Pseudomonas* and *Acinetobacter* were indicators of one site (Fig. 1.4, Table S1.6). On the other hand, the more abundant taxa at three WNS-negative sites in Manitoba, *Knoellia*, Brucellaceae:Other, *Microbacterium*, and Pseudomonadaceae were all indicators of the Microwave site (Fig. 1.4, Table S1.6). The largest indicator value was obtained for *Nitrosovibrio* at the Abyss site. Cytophagaceae and Flavobacteriaceae were also associated with Abyss. Representative taxa were identified from all hibernacula, except for Emerald, Laflèche and Dale's.

We compared skin microbiota profiles based on WNS status in order to highlight possible differences in microbial composition related to the fungal disease. Here, again, some of the most abundant taxa such as *Pedobacter* and Intrasporangiaceae were not significant representatives as they were identified in both areas in similar relative abundance (Fig. S1.2). However, a large number of significant indicators were detected, some with high indicator values. At WNS-negative sites in Manitoba, significant indicators were *Knoellia*, Brucellaceae:Other, *Nitrosovibrio*, Flavobacteriaceae, Enterobacteriaceae, *Microbacterium*, *Sphingobacterium*, Cytophagaceae, *Chryseobacterium*, and Xanthomonadaceae (Fig. 1.5, Table S1.7). On the other hand, significant indicators of WNS-positive sites in Québec were *Ralstonia*, *Janthinobacterium*, *Rhodococcus*, Micrococcaceae, and *Pseudomonas* (Fig. 1.5, Table S1.7).
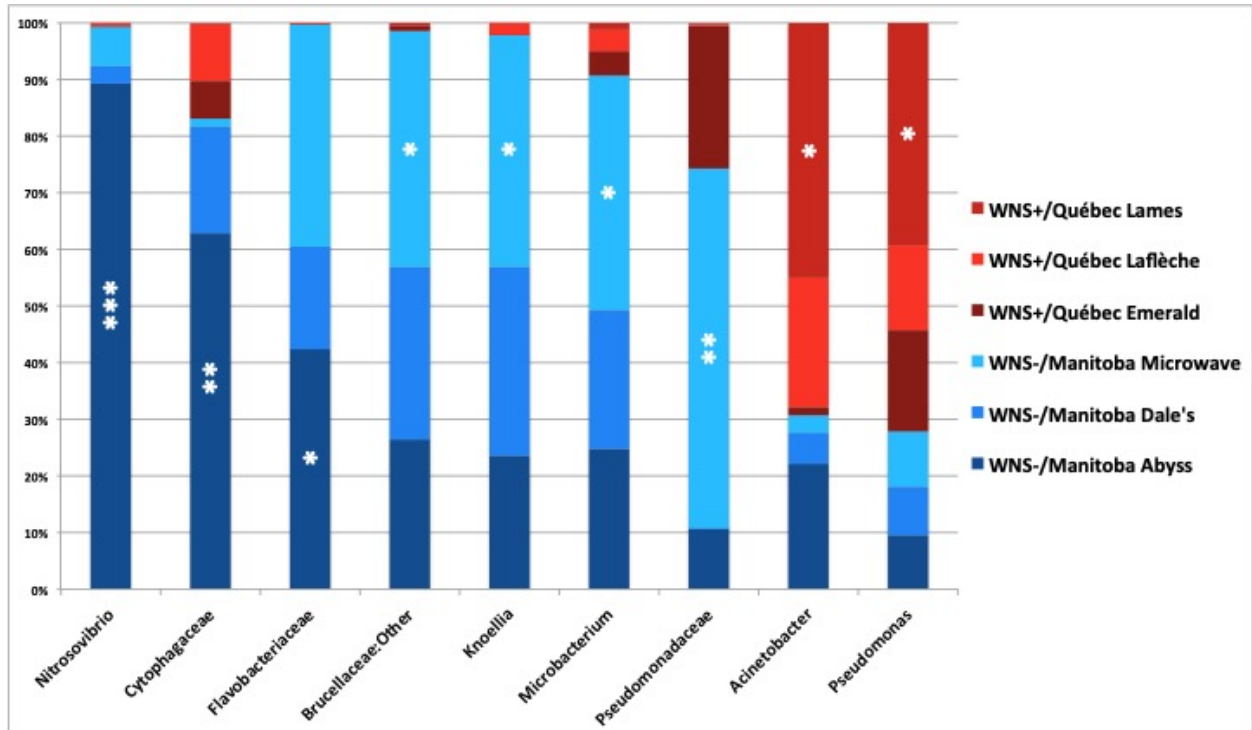
Fig. 1.4. *M. lucifugus* skin microbiota taxa indicator of the six hibernacula of different WNS status in Canada. The sites from WNS-negative (Manitoba, Canada) and WNS-positive (Québec) regions are presented. The significant indicators were identified by IndVal analysis among the 26 more abundant taxa representing more than 1% of total abundance. Stars indicate hibernacula with significant representative taxa. *IndVal $\geq$ 0.60, **IndVal $\geq$ 0.75, ***IndVal $\geq$ 0.89.
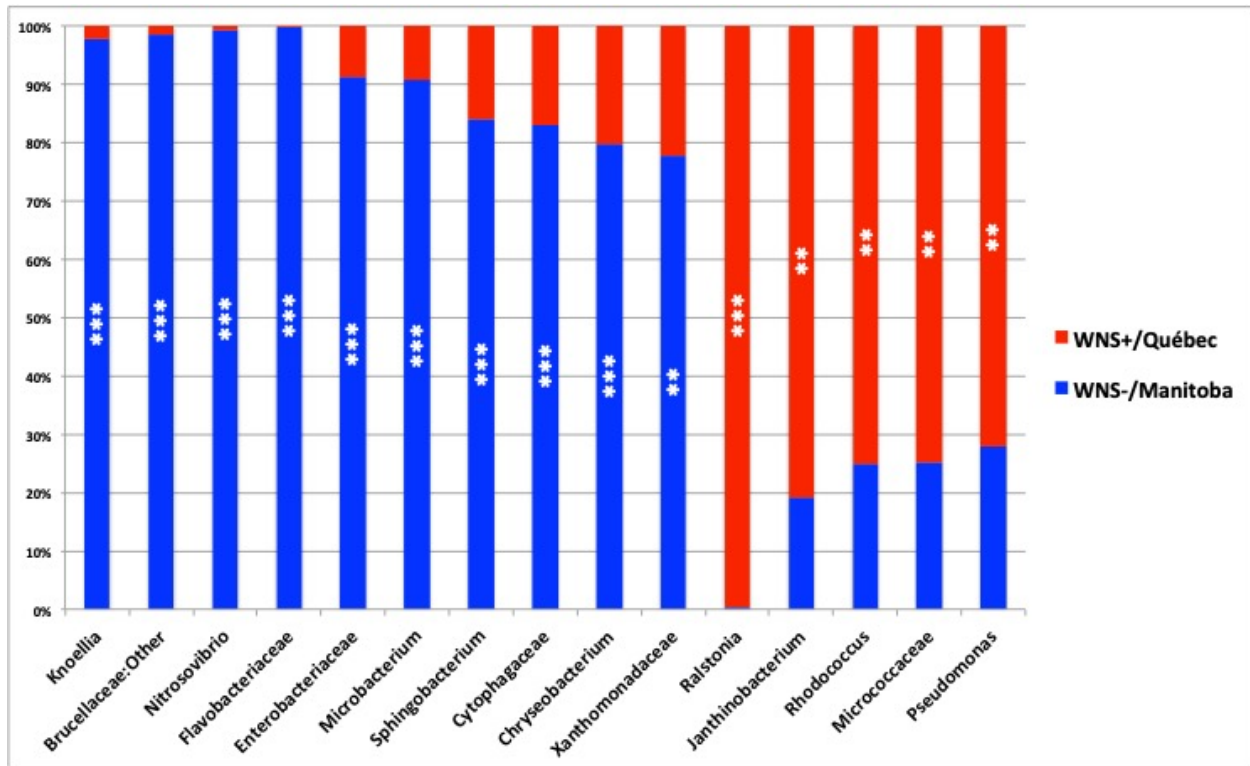
Fig. 1.5. *M. lucifugus* skin microbiota taxa indicator of WNS-positive (Québec) and WNS-negative regions (Manitoba) in Canada. Significant indicators were found among the 26 more abundant taxa representing more than 1% of total abundance with IndVal analysis. Stars indicate regions with significant representative taxa. **IndVal ≥ 0.75, ***IndVal ≥ 0.89.

1.4. Discussion

We compared the skin microbiota of bats from WNS-positive and WNS-negative sites to better understand the role of the microbiota as a factor in the host-pathogen interaction associated with WNS. We found support for the hypotheses that WNS has contributed changes in the skin microbiota for bats that are persisting in affected regions and that the skin microbiota is strongly influenced by the local environment within hibernacula. Although we cannot rule out the role of geographic variation confounded here with WNS status we believe that our results are more consistent with the proposal that WNS has led to a shift in the microbiota of bats inhabiting WNS-positive sites. For one, our analyses based on weighted UniFrac distances show no clustering environmental samples by province when analyzed together with bat samples, supporting that region is not a major driver of microbiota communities. Second, because Pd affects and interacts with the skin so directly and because higher levels of bacteria known to inhibit Pd growth in vitro (Cornelison et al., 2014; Hoyt, Cheng, et al., 2015) and in vivo (Cheng et al., 2017) were observed, it seems more likely that WNS status, and not geography, explains the compositional patterns. As predicted by our first hypothesis, the diversity of the skin microbiota was indeed smaller at WNS-positive sites compared to WNS-negative sites, which is consistent with a shift in microbiota caused by Pd. In addition, WNS status was a strong predictor of variation in Shannon diversity values across sites. A previous study on tricolored bats (*P. subflavus*) affected by WNS also revealed a trend for lower diversity values at WNS-positive sites (Lueschow, 2015), as shown here for little brown bats persisting after WNS invasion. Phylogenetic beta diversity analysis was also consistent with selection on the microbiota by Pd and WNS. Future studies, assessing diversity of the microbiota on bats from the same sites, before and after Pd invasion, would help resolve the WNS influence in microbiota diversity patterns of persisting bats.

At the compositional level, the skin microbiota of hibernating little brown bats is dominated by the classes Actinobacteria, Gammaproteobacteria, Flavobacteriia, Alphaproteobacteria, and Betaproteobacteria, a pattern consistent with previous investigation of the skin microbiota in several species of bats (Winter et al., 2016) and particularly *M. lucifugus* (Avena et al., 2016). Our analysis also identified Sphingobacteriia as a predominant class. IndVal analysis revealed that one interesting genus, *Rhodococcus*, was significantly more abundant in skin microbiota samples collected at WNS-positive sites in Québec. This genus has previously been identified on bats (Voig et al., 2005; Lueschow, 2015) and is known for its antifungal activity (Chiba et al., 1999; Nakayama et al., 2000). Most interesting, a volatile organic chemical produced by *R. rhodochrous* strain DAP 96253 has been shown to inhibit Pd growth in vitro (Cornelison et al., 2014). Several other

genera, reported as antifungal agents, were also identified as significant indicators of bat samples collected at WNS-positive sites. Namely, *Pseudomonas* was enriched at all WNS-positive sites, whereas *Acinetobacter* was enriched at a single WNS-positive site. Both taxa are known for their antifungal activity (Liu et al., 2007; Lauer et al., 2008) and have been previously identified on the skin of North American bats (Lueschow, 2015; Avena et al., 2016). Moreover, one strain of *Pseudomonas fluorescens* has been shown to inhibit Pd growth in vitro and reduce disease severity and improve survival of bats with WNS in a laboratory challenge experiment (Hoyt, Cheng, et al., 2015; Cheng et al., 2017). Another lesser-known antifungal bacterial genus, *Janthinobacterium*, was also identified as a significant representative at WNS-positive sites in Québec. Some species from the same genus isolated from the skin of wild amphibians confer resistance against the fungal pathogen *Batrachochytrium dendrobatidis* (Brucker et al., 2008; Lauer et al., 2008). Enrichment of multiple taxa with potential antifungal and anti-Pd activity in bats persisting following WNS invasion is consistent with our second hypothesis that the skin microbiota of bats provides a mechanism for resistance to, or tolerance of, Pd infection. Further studies should focus on any functional influence of these bacteria on the host-pathogen interaction between bats and Pd.

Consistent with our third hypothesis, we found that the skin microbiota of hibernating little brown bats is related to the microbial community composition of the nearby environmental substrates. That is, bacteria living on bats and bacteria living on adjacent cave walls are very likely exchanged by contact. However, bat skin samples and local environmental samples were by no means identical when considering abundance and compositional profiles, indicating that microbial communities on the skin of hibernating bats are probably not regulated in the same way as in the environment (Table S1.8). These results are consistent with other studies of bats (Avena et al., 2016) or frogs (Loudon et al., 2014; Walke et al., 2014) showing that skin microbiota assemblages do not exactly mirror the microbial communities in the immediate environment. Although we did not detect any related variation within sites of microbial communities of the skin and that of the substrates, we found that individual bats strongly differ across sites. Moreover, the tendency for hibernating little brown bats to cluster, often in large groups of hundreds to thousands of individuals, is likely to reduce variation in the microbiota among individuals because of transfer within clusters, as shown by our analysis. Homogenization of the skin microbiota by close contact among individuals has also been observed in previous studies of bats and humans (Song et al., 2013; Lemieux-Labonté et al., 2016). Taken together, these results suggest that bat populations could differ in their susceptibility to WNS depending on the microbial community in their immediate environment, their reliance on clustering behavior, and the potential for clustering to homogenize the bacterial community. In this study, we did not attempt to quantify the potential

influence of abiotic variables, such as pH, temperature, and humidity, and considered these factors as possible contributors to site effects. It would be interesting in future studies to analyze these factors separately to understand their relative influence on the microbial community on bats and in the environment. Temporal variation may also have influenced the compositional patterns observed in this study, but our experimental protocol was designed to reduce this effect as much as possible. All sites were sampled within a relatively short period of time (less than 3.5 months), and we avoided the start of hibernation when the experience of bats prior to hibernation might be expected to more strongly influence their skin microbiota. Moreover, the microbiota on bats or in the environment for the single WNS-positive site we sampled in March (Emerald) was not different from the two WNS-positive sites we sampled in November (Lames and Laflèche).

1.5. Conclusion

This study highlights the role of skin microbiota for wildlife population health, conservation, and management in the face of emerging infectious diseases. The enrichment of potentially beneficial bacteria in skin microbiota samples collected at WNS-positive hibernacula is an encouraging discovery for the prospect of bat population recovery after WNS becomes endemic in a given region. This finding highlights the potential value of management actions that might encourage transmission, growth, and establishment of beneficial bacterial taxa on bats and within hibernacula (Cheng et al., 2017). However, our findings also highlight a potential risk of some proposed management actions. Considerable funding and time is currently being devoted to development and testing of potential chemical or biological treatments for WNS that could be applied to hibernating bats or hibernaculum substrates. Our results not only support previous work highlighting the potential of some bacteria as biological control agents for Pd (e.g., (Cornelison et al., 2014; Hoyt, Cheng, et al., 2015; Cheng et al., 2017)) but also highlight a potential risk of biological or chemical treatments. Treatments that disrupt the skin microbiota or attenuate selection for a beneficial skin community could cause more harm than good for recovery of bat populations and the establishment of stable, long-term resistance to WNS in the wild. Thus, an important component of testing any potential treatment for WNS should be to confirm that it is selective for Pd and has minimal negative impacts on the whole non-target microbiota on bats or in hibernacula.

1.6. Availability of data and materials

The datasets generated and analyzed during the current study are available in the Figshare repository. Raw sequence data and metadata are available

at DOI: `https://figshare.com/s/623a1e47b4bed20459a7` and DOI: `https://figshare.com/s/74d9497a792f9c0c76df`

1.7. Acknowledgements

1.8. Supplementary files

The supplementary files are available here: `https://figshare.com/s/a044498ddcb83ad5550c`.
Table S1.1 to S1.5 and S1.8 are too wide to be presented in this section.

Table S1.1. Clusters of bats sampled within each hibernaculum and coded as dummy variables for db-RDA analysis.

Table S1.2. Positive control mock community analysis. Sequence set comparisons of the mock community to what is expected. File 1 shows the matching sequences and related taxa identified. File 2 shows the taxa composition of the mock in relative abundance, the matching taxa at the genus or family level, and the false positive taxa.

Table S1.3. Main taxa relative abundance (>0.1%) in negative control samples. File 1 presents DNA extraction control samples, file 2 the library control, file 3 the negative site controls, and file 4 presents all controls together.

Table S1.4. Main phyla identified in bat skin microbiota samples. The 8 more abundant phyla across all hibernacula are provided.

Table S1.5. Main classes identified in bat skin microbiota samples. The 6 more abundant classes across all hibernacula are provided.

Table S1.6. *M. lucifugus* skin microbiota taxa indicator test and related association measure (A, B) of six hibernaculum groups with different WNS status in Canada. Indicator value tests were computed with the multipatt() function of the indicspecies package in R. Only taxa with A $\geq$ 0.4 were retained as indicators.

Hibernaculum group	Associated taxa	A	B	IndVal	*P*-value	Holm corrected *P*-value
Abyss	*Nitrosovibrio*	0.892	1.000	0.945	0.0001***	0.0026**
	Cytophagaceae	0.630	1.000	0.793	0.0011**	0.0187*
	Flavobacteriaceae	0.425	1.000	0.652	0.0009***	0.0162*
Microwave	Pseudomonadaceae	0.635	1.000	0.797	0.0001***	0.0026*
	Brucellaceae:Other	0.416	1.000	0.645	0.0024**	0.0336*
	Microbacterium	0.413	1.000	0.643	0.0002***	0.0044**
	Knoellia	0.408	1.000	0.639	0.0012**	0.0192*
Lames	*Acinetobacter*	0.450	1.000	0.671	0.0003***	0.0060**
	Pseudomonas	0.392	1.000	0.626	0.0001***	0.0026**

A, the specificity, is the probability that a site belongs to the group given the fact that the species is found and B, the fidelity, is the probability of finding a given taxon when the sites belong to that group. $^{*}p \leq 0.05$, $^{**}p \leq 0.01$, $^{***}p \leq 0.001$.

Table S1.7. *M. lucifugus* skin microbiota taxa indicator and related association measure (A, B) of WNS-positive (Québec) and WNS-negative (Manitoba) sites in Canada. Indicator value tests were computed with the multipatt() function of the indicspecies package in R. Only taxa with A ≥ 0.4 were retained as indicators.

WNS status and Province group	Associated taxa	A	B	IndVal	*P*-value	Holm corrected *P*-value
WNS positive sites (Québec)	*Ralstonia*	0.997	0.879	0.936	0.0001***	0.0026*
	Janthinobacterium	0.808	0.939	0.871	0.0023**	0.0288*
	Rhodococcus	0.751	1.000	0.867	0.0001***	0.0026**
	Micrococcaceae	0.750	1.000	0.866	0.0001***	0.0026**
	Pseudomonas	0.720	1.000	0.849	0.0001***	0.0026**
WNS negative sites (Manitoba)	*Knoellia*	0.979	1.000	0.989	0.0001***	0.0026**
	Brucellaceae:Other	0.986	0.970	0.978	0.0001***	0.0026**
	Nitrosovibrio	0.992	0.970	0.981	0.0001***	0.0026**
	Flavobacteriaceae	0.997	0.909	0.952	0.0001***	0.0026**
	Enterobacteriaceae	0.912	1.000	0.955	0.0001***	0.0026**
	Microbacterium	0.906	1.000	0.952	0.0001***	0.0026**
	Sphingobacterium	0.839	1.000	0.916	0.0001***	0.0026**
	Cytophagaceae	0.831	1.000	0.911	0.0007***	0.0091**
	Chryseobacterium	0.798	1.000	0.893	0.0001***	0.0026**
	Xanthomonadaceae	0.778	1.000	0.882	0.0001***	0.0026**

A, the specificity, is the probability that a site belongs to the group given the fact that the species is found and B, the fidelity, is the probability of finding a given taxon when the sites belong to that group. $^*p \leq 0.05$, $^{**}p \leq 0.01$, $^{***}p \leq 0.001$.

Table S1.8. OTUs table resulting from the analysis of 66 bat skin microbiota samples and 11 environmental samples.
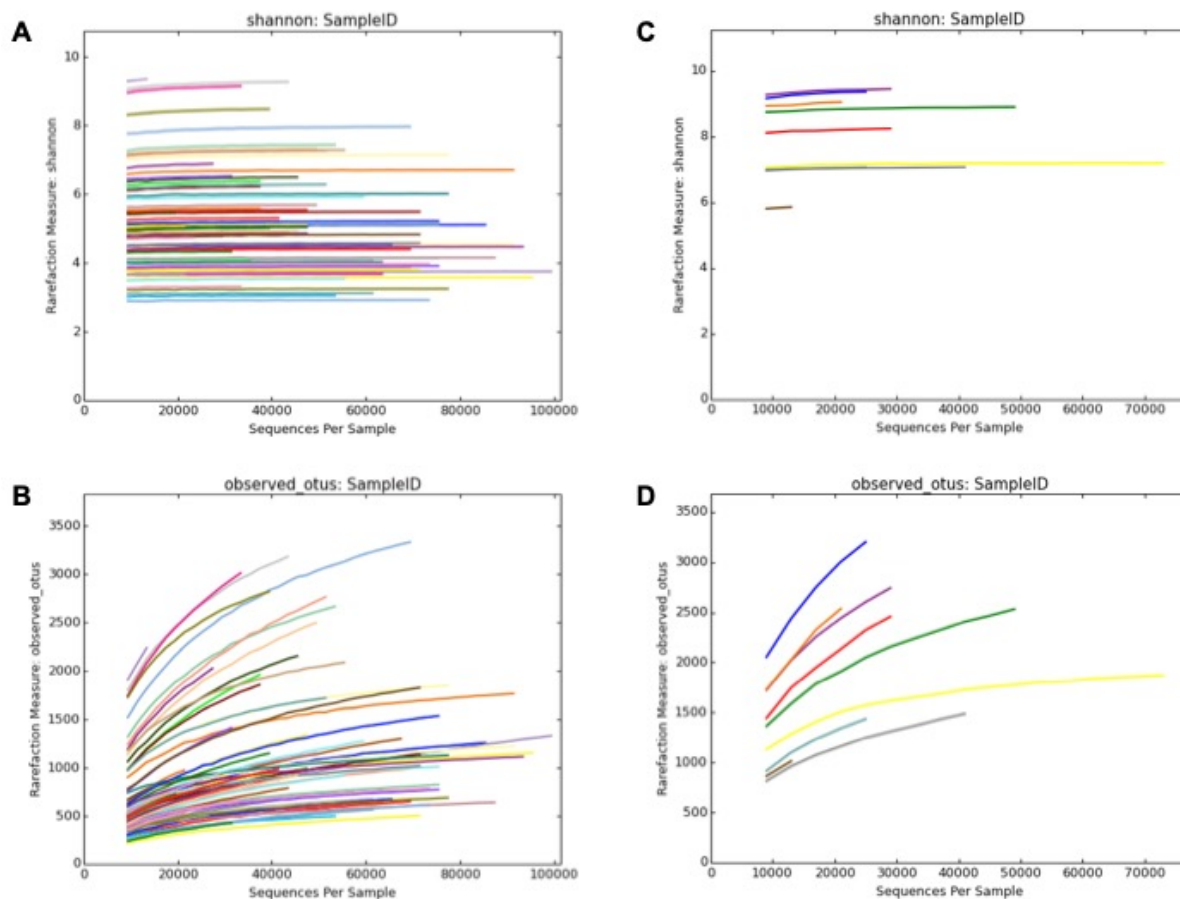
Fig. S1.1. Rarefaction curves of alpha diversity calculated on multiple rarefied data table for each of the 66 bat skin microbiota samples and 11 environmental samples. (A) Shannon diversity of bat skin samples. (B) Overall richness (OTUs observed) of bat skin samples. (C) Shannon diversity of environmental samples. (D) Overall richness (OTUs observed) of environmental samples.
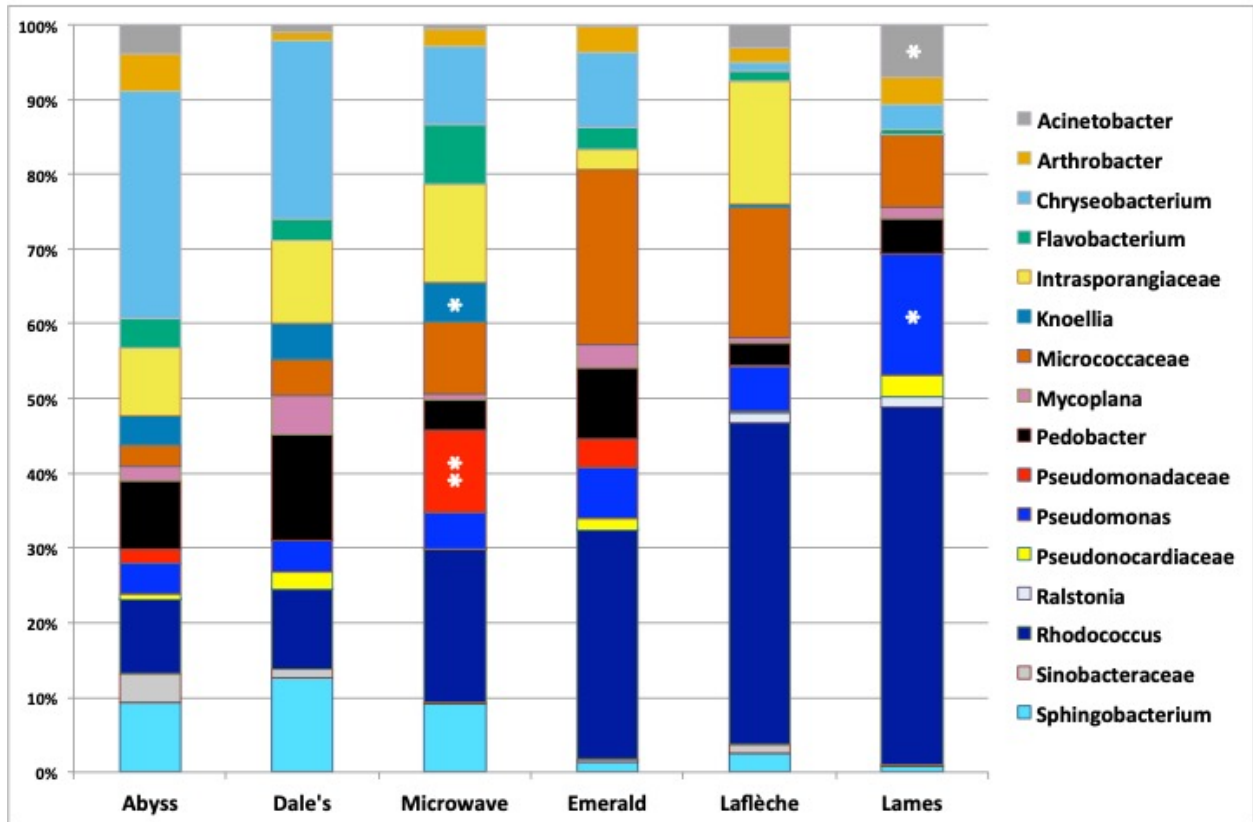
Fig. S1.2. Major bacterial taxa identified in bat skin microbiota samples. The 16 more abundant taxa across all hibernacula are provided. Stars represent significant indicator taxa. *IndVal < 0.50, **IndVal ≥ 0.50, ***IndVal ≥ 0.89.

Chapitre 2

Antifungal potential of the skin microbiota of hibernating big brown bats (*Eptesicus fuscus*) infected with the causal agent of white-nose syndrome

Virginie Lemieux-Labonté[1], Nicole A. S.-Y. Dorville[2], Craig K. R. Willis[2] and François-Joseph Lapointe[1]

[1]Département de sciences biologiques, Université de Montréal, Montréal, Québec, Canada

[2]Department of Biology and Centre for Forest Interdisciplinary Research, University of Winnipeg, Winnipeg, Manitoba, Canada

Résumé. Le syndrome du museau blanc (SMB) causé par le champignon *Pseudo-gymnoascus destructans* (Pd) a provoqué des ravages considérables dans les populations de chauves-souris nord-américaines au cours de la dernière décennie. Certaines espèces hibernantes telle que la grande chauve-souris brune (*Eptesicus fuscus*) semblent néanmoins résistantes à la maladie et leur microbiote cutané pourrait jouer un rôle de protection. Pourtant, une analyse approfondie du microbiote cutané d'*E. fuscus* dans le contexte de l'infection par Pd n'a encore jamais été réalisée. En janvier 2017, nous avons donc capturé des grandes chauve-souris brunes en hibernation, échantillonné leur microbiote cutané et les avons inoculés avec le champignon Pd ou un traitement contrôle en laboratoire. Nous avons laissé les chauves-souris hiberner en captivité pendant 11 semaines, puis avons échantillonné leur microbiote cutané pour tester les hypothèses suivantes : 1) l'inoculation par le champignon Pd ne devrait pas perturber le microbiote cutané des grandes chauve-souris brunes puisque cette espèce est résistante ; et 2) les taxons microbiens possédant des propriétés antifongiques devraient être abondants avant et après l'inoculation par le champignon. En utilisant le séquençage à haut débit du gène de l'ARNr 16S, nous avons observé que la diversité bêta du microbiote des chauves-souris inoculées au Pd a davantage été modifié au fil du temps que la diversité bêta du microbiote des chauves-souris contrôles. Or, les taxons les plus abondants de la communauté sont demeurés stables tout au long de l'expérience. Parmi les taxons les plus abondants, *Pseudomonas* et *Rhodococcus* sont connus pour leur potentiel antifongique contre Pd et d'autres champignons. Ainsi, contrairement à l'hypothèse 1, l'inoculation par le champignon Pd a déstabilisé le microbiote cutané, mais conformément à l'hypothèse 2, les bactéries aux propriétés antifongiques connues n'ont pas été affectées par le traitement. Cette étude est la première à caractériser le microbiote cutané d'*E. Fuscus*, démontrant les associations potentielles entre le microbiote cutané des chauves-souris et la résistance au SMB. Ces résultats ouvrent la voie à des études métegénomiques, afin de mieux comprendre les mécanismes de résistance au SMB et aider à développer des stratégies de conservation.

Mots clés : microbiote, syndrome du museau blanc, resistance, *Eptesicus fuscus*, grande chauves-souris brune, gène ARNr 16S.

Abstract. Little is known about skin microbiota in the context of the disease white-nose syndrome (WNS), caused by the fungus *Pseudogymnoascus destructans* (Pd), that has caused enormous declines of hibernating North American bats over the past decade. Interestingly, some hibernating species, such as the big brown bat (*Eptesicus fuscus*), appear resistant to the disease and their skin microbiota could play a role. However, a comprehensive analysis of the skin microbiota of *E. fuscus* in the context of Pd has not been done. In January 2017, we captured hibernating *E. fuscus*, sampled their skin microbiota, and inoculated them with Pd or sham treatment. We allowed the bats to hibernate in the lab under controlled conditions for 11 weeks and then sampled their skin microbiota to test the following hypotheses: 1) Pd infection would not disrupt the skin microbiota of Pd-resistant *E. fuscus*; and 2) microbial taxa with antifungal properties would be abundant both before and after inoculation with Pd. Using high-throughput 16S rRNA gene sequencing, we discovered that beta diversity of Pd-inoculated bats changed more over time than that of sham-inoculated bats. Still, the most abundant taxa in the community were stable throughout the experiment. Among the most abundant taxa, *Pseudomonas* and *Rhodococcus* are known for antifungal potential against Pd and other fungi. Thus, in contrast to hypothesis 1, Pd infection destabilized the skin microbiota but consistent with hypothesis 2, bacteria with known antifungal properties remained abundant and stable on the skin. This study is the first to provide a comprehensive survey of skin microbiota of *E. fuscus*, suggesting potential associations between the bat skin microbiota and resistance to the Pd infection and WNS. These results set the stage for future studies to characterize microbiota gene expression, better understand mechanisms of resistance to WNS, and help develop conservation strategies. **Key words**: microbiota, white-nose syndrome, resistance, *Eptesicus fuscus*, big brown bat, 16S rRNA gene.

2.1. Introduction

The skin is the first physical and immunological barrier against invading pathogens. It is also a complex and dynamic ecosystem inhabited by a rich community of microorganisms composed of bacteria, archaea, fungi and viruses. This community contributes to host defenses by limiting colonization and persistence of pathogens that compete for resources, and by producing pathogen inhibitors (Grice & Segre, 2011; Walter et al., 2018; Woo et al., 2019). Here, we use the term "microbiota" to refer to the taxonomic diversity of Bacteria and Archaea assessed using marker genes, rather than "microbiome", which refers to both taxonomic and functional diversity of the complete community (Marchesi & Ravel, 2015). The microbiota also interact with the innate and adaptive immune system and contributes to maintenance of skin integrity and tissue repair (Lai et al., 2009; Curtis & Sperandio, 2011; Naik et al., 2012). Despite this importance, the complex interactions among the skin microbiota, skin invading pathogens and hosts remain

poorly documented in animals, especially for newly emerged wildlife diseases causing population declines around the globe (Daszak, 2000; Belden & Harris, 2007; Jones et al., 2008; Fisher et al., 2012). Introduced fungal pathogens such as *Batrachochytrium dendrobatidis* and *Batrachochytrium salamandrivorans* have caused global declines and even extinctions in amphibians (Longcore et al., 1999; Martel et al., 2013). In recent decade, studies have highlighted the potential role of skin microbiota in patterns of resistance and susceptibility to these fungal pathogens and have pointed to potential management practices that might help conserve host populations (Harris et al., 2009; Bletz et al., 2013, 2017; Jani & Briggs, 2014; Woodhams et al., 2014; Bataille et al., 2016; Ange-Stark et al., 2019; Rebollar et al., 2019). However, despite this potential, management actions based on the skin microbiota have still not been widely applied in response to wildlife disease.

Similar to amphibians, hibernating North American bats have suffered dramatic impacts from a newly introduced fungal disease, white-nose syndrome (WNS) (Blehert et al., 2009; Frick et al., 2016). WNS is caused by the fungus *Pseudogymnoascus destructans* (Pd) (Gargas et al., 2009; Lorch et al., 2011) and has caused widespread declines of hibernating bats since being introduced from Eurasia sometime around 2006 (Frick et al., 2015, 2017; Warnecke et al., 2012; Hoyt et al., 2016; Drees et al., 2017; Trivedi et al., 2017; Frick, Pollock, et al., 2010). In vulnerable bat species, Pd invades the skin creating lesions that alter fluid balance, thermoregulation, and gas exchange (Meteyer et al., 2009; Cryan et al., 2010; Warnecke et al., 2012; Verant et al., 2014; McGuire et al., 2017). Hibernating bats survive the winter using stored body fat and prolonged energy-saving bouts of torpor characterized by dramatically reduced body temperature and metabolism (Jonasson & Willis, 2012; Czenze et al., 2013; Czenze & Willis, 2015). The fungal infection causes bats to warm up too frequently which, in turn, depletes their fat reserves (D. M. Reeder et al., 2012; Warnecke et al., 2012). Understanding how bat species respond to this disease is important for designing management strategies to protect bat populations both for biodiversity conservation, and preservation of the ecosystem services that bats provide (Boyles et al., 2011; Maine & Boyles, 2015; Wray et al., 2018). There is enormous variation in the impacts of WNS for different bat species, with some exhibiting little to no mortality, and others facing local extinction (Frick, Pollock, et al., 2010; Frick et al., 2015; Langwig et al., 2015, 2017). Mechanisms underlying this variation in susceptibility are not fully understood, despite potential benefits for disease management. Variation in susceptibility to Pd could reflect mechanisms that allow for resistance to infection (i.e., reduction or elimination of pathogen infection) and/or tolerance of infection (i.e., reduction of the harm caused by infection) (Råberg et al., 2007, 2009; Svensson & Råberg, 2010) and potential mechanisms of resistance and tolerance are beginning to

be addressed in the WNS context (Frick et al., 2016; Langwig et al., 2017; Cheng et al., 2019).

Big brown bats (*Eptesicus fuscus*) exhibit evidence of resistance with mild WNS symptoms compared to more susceptible species (Frank et al., 2014; Moore et al., 2018). *E. fuscus* are of particular interest as they often hibernate under similar environmental conditions as species that are highly vulnerable to WNS, including the little brown bat (*Myotis lucifugus*), the tricolored bat (*Perimyotis subflavus*), and the northern long-eared bat (*M. septentrionalis*), all three of which are now listed as endangered in Canada due to WNS (Canadian Wildlife Service & Committee on the Status of Endangered Wildlife in Canada, 2013). Physiological and behavioral factors could play a role in this resistance (Willis & Wilcox, 2014; Langwig et al., 2015; Frick et al., 2016) and understanding these mechanisms could help fulfill an important knowledge gap by identifying traits that contribute to WNS survival.

One underexplored factor that could affect resistance to WNS is the skin microbiota. Differences in lipid profiles affecting WNS-resistance (Frank et al., 2016, 2018) may contribute to different microbial profiles by providing different nutritional substrates. Hundreds of microorganisms isolated from wild bats and their corresponding habitats have been tested in controlled laboratory conditions for their inhibitory effects on Pd, by focussing on the actions of secreted compounds, contact inhibition or volatile molecules (Hamm et al., 2017; Micalizzi et al., 2017). *M. lucifugus* bats persisting with Pd have proportionally more abundant *Rhodococcus* and *Pseudomonas* in their skin microbiota (Lemieux-Labonté et al., 2017), suggesting a possible role for these microorganisms in bat survival. Moreover, antifungal strains of *Pseudomonas* isolated from the skin of *E. fuscus* inhibit Pd growth in vitro (Hoyt, Cheng, et al., 2015; Hamm et al., 2017), and improve survival of WNS-infected *M.lucifugus* bats when applied as a probiotic treatment in vivo (Cheng et al., 2017; Hoyt et al., 2019). All of these results are promising but they do not provide a complete picture of the complex skin community and its potential role in Pd resistance of some species.

We explored the skin microbiota of WNS-resistant *E. fuscus* inoculated with Pd. This species can hibernate under the same environmental conditions as more susceptible species like *M. lucifugus* but survives Pd infection with limited skin colonization (Walke et al., 2015; Moore et al., 2018). Therefore, *E. fuscus* represents a good model to study potential resistance mechanisms resulting from the skin microbiota in a controlled environment that accounts for variation in hibernation conditions. We tested two hypotheses about the skin microbiota of *E. fuscus* in the context of Pd infection: 1) that Pd inoculation is not a strong selective force on the skin microbiota of this species and would therefore not disrupt the microbial community, and 2) that microbial taxa with antifungal properties, which are common in the hibernation sites of bats persisting after WNS (e.g., *Rhodococcus* and *Pseudomonas*,

(Lemieux-Labonté et al., 2017), would be abundant both before and after infection with Pd in this resistant species.

2.2. Material and Methods

2.2.1. Bats collection

On 18 January 2017, we visited Richard Lake Mine, a hibernaculum approximately 100 km east of Kenora, Ontario, Canada ($49°45'N$, $-94°28'W$), which houses several hundred *M. lucifugus* and *E. fuscus* each winter. We first sampled 8 bats in the cave to ensure that transportation has no effect on the skin microbiota (Table S2.1 and 2.2). We then collected 32 adult *E. fuscus* (16 males and 16 females), suspended them in cloth bags in a cooler lined with wet towels to maintain hibernation conditions, and transported them by car to a bio-secure animal facility at the University of Winnipeg. All handling of bats in the lab occurred in a biosafety cabinet. We swabbed the left wing of each torpid bat immediately after arrival in the lab to sample the "pre-captivity" hibernation microbiota. We swabbed the dorsal face of the right wing (forearm and under forearm) in linear strokes for 20 s with a sterile Whatman Omniswab (Fisher Scientific) soaked in sterile 0.15M NaCl (Lemieux-Labonté et al., 2017). Swabs tips were ejected into MoBio Powersoil DNA isolation Kit tubes (MoBio Laboratories), which were then transferred to 4°C within 2hr and to -20°C within 12hr of sampling. As a negative control, a humidified sterile swab was exposed to open air for 20 s, prior to ejecting its tip into a MoBio tube. The other wing was swabbed to determine Pd status.

All individuals were then randomly assigned to one of 4 cages with 8 individuals/cage in a 1:1 sex ratio (i.e., 4 males and 4 females/cage). We replicated the experiment in two incubators with one cage of Pd-inoculated bats, and one cage of sham-inoculated controls per incubator. Incubators were maintained at 8°C and 98% relative humidity. Pd-inoculated bats received 20 μl of inoculum, containing 500,000 conidia suspended in phosphate buffered saline (PBS) with Tween20 to prevent clumping, pipetted onto the ventral side of their wings (Lorch et al., 2011; Warnecke et al., 2012; McGuire et al., 2016). Healthy controls were inoculated only with PBS-Tween20 (Warnecke et al., 2012; McGuire et al., 2016). We analyzed the skin microbiota between the two treatments at the beginning of the experiment to control for any pre-existing difference and how it may affect the result interpretation.

After 11 weeks of captive hibernation, bats were swabbed again, as described above, to assess the "post-captivity" skin microbiota (left wing) and Pd load (right wing). We recorded body temperature immediately after removing bats from the incubator at the

end of the study using a digital thermometer accurate to ± 0.1°C (SPER Scientific, Model 80008, Arizona USA) and inserting a 1 mm diameter l-type thermocouple probe 4 mm into the rectum (Table S2.3). Bats were then swabbed within ∼1-2 min of body temperature measurement. Only a maximum of couple of minutes would have elapsed from the time bats started rewarming in response to our disturbance until the time we swabbed them. After obtaining additional measurements and samples for a range of complementary studies, bats were euthanized by CO_2 inhalation under isoflurane anesthesia.

Pd swabs were processed and analyzed at the Pathogen and Microbiome Institute at the Northern Arizona University, whereas skin microbiota samples were shipped to Université de Montréal (Québec, Canada) for further processing. Areas of the wing that are infected and colonized by Pd hyphae fluorescence orange under UV lightning (Turner et al., 2014; Cheng et al., 2017). We took UV photographs of every bat's wings using a digital camera (Olympus© Tough TG-830) using a Canadian dime as a sizing reference, and then digitally quantified these areas as a measure of Pd load and infection intensity using the Image-J© software. All methods were approved by the University of Winnipeg Animal Care Committee (Protocol Number AEO08399).

2.2.2. DNA extraction, amplification and sequencing

Bacterial genomic DNA was extracted from each swab using the MoBio Powersoil DNA isolation kit. We followed the manufacturer's protocol, modified by adding a 15-min incubation period at 70°C after the addition of buffer C1 to increase the efficiency of microbial cell lysis (Castelino et al., 2017). All procedures were conducted in a laminar flow hood to limit potential sample contamination, and extractions were randomized to avoid detecting false patterns (Salter et al., 2014). Four extraction blanks, two amplification blanks, and the HM-782D Human Microbiome Project mock community (BEI Resources) were also included to detect possible contamination and assess sequencing accuracy (Salter et al., 2014; Glassing et al., 2016). Because of contamination and low input DNA, 23 pre- and post-captivity *E. fuscus* skin microbiota samples, and five sampling negative controls were retained for subsequent analysis. Amplification and sequencing were performed as previously described (Preheim, Perrotta, Friedman, et al., 2013b; Lemieux-Labonté et al., 2017). Briefly, libraries were prepared using a two-step PCR. The first PCR amplified the hypervariable region V4 of the 16S small subunit ribosomal gene with forward primer U515 F and reverse primer E786 R (Caporaso et al., 2011). The amplifications were performed with a Mastercycler Nexus GSX1 (Eppendorf). Each sample was amplified in quadruplicate and pooled to limit possible PCR artifacts. The second PCR step consisted of adding primers containing a barcode (index) and Illumina adapter sequences to each DNA amplicon, and used forward primer PE-III-PCR-F

and reverse primer PE-III-PCR-001-096 (Preheim, Perrotta, Martin-Platero, et al., 2013). This second amplification was performed in triplicate. After each PCR step, samples were pooled and purified with the PCR purification Agencourt AMPure XP (Beckman Coulter). Indexed samples concentration was measured with Qubit 2.0 Fluorometer (Invitrogen), and samples were pooled to obtain a final concentration range between 10 and 20 ng/μl. DNA was next diluted and denatured according to the manufacturer's protocol for paired-end sequencing using MiSeq Reagent Kit v2 (500 cycles) 2x250bp on MiSeq (Illumina).

2.2.3. Data analysis

For all sequences, quality filtering, trimming, dereplication, sample inference and merging of paired-end sequences, were performed in DADA2 version 1.14.1 (Callahan et al., 2016). The corresponding amplicon sequence variants (ASV) table providing ASV abundances was assigned in DADA2 using SILVA database release 128 (Quast et al., 2012).

We amplified 8,282,605 sequences classified into 43,436 ASV from the 67 samples sequenced. We filtered out mitochondrial and chloroplastic DNA sequences, as well as sequences from the genera *Halomonas* and *Shewanella*, the two most abundant taxa in negative controls. ASVs with abundance values smaller than 10 were filtered out leaving 5,176,773 sequences in 17,162 ASVs. After these filtration steps, only a small number of sequences (less than 11,000) were identified in the sampling control, extraction and PCR negative controls, and these samples were also excluded. One sampling negative control had 47,608 sequences, but it was excluded from our analysis because it diverged dramatically in composition from bat samples collected (Fig. S1.1). A total of 5,098,811 sequences, classified in 17,162 ASVs, were amplified and analyzed from the 46 bat samples (from 23 bats pre- and post-infection), with a mean of 110,843 sequences per sample (range: 34,416 – 300,474). We were able to match all expected genera in the mock positive control (Fig. S2.2). The genera of the 20 expected mock taxa were the most abundant in the mock profile (Fig. S2.2). We detected 733 false positives, but with very low relative abundance values (<0.1%). All analyses were conducted in R version 3.5.0 (Team, 2018).

2.2.4. Alpha diversity

We first quantified diversity of the skin microbial community for all samples based on alpha diversity using the Shannon index (Shannon, 1948). The Shannon index, which includes both ASVs richness and evenness, was selected due to its reduced sensitivity to sample depth differences (Fig. S2.3) (Haegeman et al., 2013; Preheim, Perrotta, Friedman, et al., 2013b). Normally distributed alpha diversity values were compared using linear models and linear

mixed-effect models (lm() and lme() function) in R with Shannon index as the response variable, Pd-inoculation versus control (hereafter "inoculation") and pre- versus post-captivity (hereafter "captivity") as fixed effects and cage ID as a random effect. Significance was tested using ANOVA for linear model and a likelihood ratio test with a chi-square distribution for linear mixed-effect models (Pinheiro et al., 2017).

2.2.5. Beta diversity

We used two distance measures to account for the phylogeny of microbiota in our samples (i.e., unweighted UniFrac and weighted UniFrac) (Lozupone & Knight, 2005; Lozupone et al., 2007). Distances were computed on rarefied data, as such measures could be sensitive to differences in sequencing depth (Lozupone et al., 2011; Weiss et al., 2017). Computations were performed with the phyloseq package (McMurdie & Holmes, 2013) and results were visualized with principal coordinates analysis (PCoA) (Gower, 1966) using the ordinate() function in R. Distance matrices were checked with the function is.euclid() of the ade4 package (Dray & Dufour, 2007) prior to the ordination to ensure that all distances were Euclidian and properly representable by PCoA (Gower & Legendre, 1986). When required, square-root transformations were applied to obtain distance matrices satisfying the Euclidian condition (e.g., Weighted UniFrac). All phylogeny-based UniFrac distances were calculated using a phylogenetic tree constructed with FastTree 2.1.8 (M. N. Price et al., 2010).

To test for effects of inoculation and captivity we used distance-based redundancy analysis (db-RDA) (Legendre & Anderson, 1999). It is computed by first decomposing UniFrac distances (weighted or unweighted) into principal coordinates, and then applying RDA to the corresponding principal coordinates using the capscale() function of the R package vegan (Oksanen et al., 2019). We computed partial db-RDA to better understand the influence of Pd-inoculation and captivity on variation in microbial assemblages while controlling for possible confounding factors (i.e., incubator, sex and cage ID) (Davies & Tso, 1982). Adjusted R^2 values (Ezekiel, 1930) were calculated to compare the explanatory power of different models. Significance of db-RDA and partial db-RDA was tested via 9999 permutations with the anova.cca() function of the R package vegan. We then performed an analysis of multivariate homogeneity (PERMDISP) (Anderson, 2006) with the betadisper() function to test whether groups differed in their dispersion. The null hypothesis of this test is that the average within-group dispersion is identical in all groups (Anderson, 2001). For these two tests, the number of permutations was set to 9999. To test for an effect of inoculation on any change in the microbiota from pre- to post-captivity, we calculated distances between paired pre- and post-captivity samples for each individual, and then used linear mixed-effects models to test for the fixed effect of inoculation on this distance while controlling for cage

ID as a random effect (Pinheiro et al., 2017). For all analyses, a *p*-value threshold of 0.05 was considered significant.

2.2.6. Analysis of skin microbiota composition

We assessed the effect of inoculation and captivity on the composition of microbial taxa down to the genus level using the Analysis of Composition of Microbiomes (ANCOM 2.0) (Mandal et al., 2015). ANCOM is based on nonparametric tests (i.e., either Kruskal-Wallis test for independent samples, or Friedman test for dependent samples) and is appropriate for compositional data (Gloor et al., 2017). The test relies on point estimates of data transformed by an additive log ratio, where presumed invariant taxa are selected as the denominator. To identify differences between samples, the analysis was performed using an unrarified ASVs table only including taxa with a relative abundance larger than or equal to 0.1%. The relative composition of skin microbiota was assessed using the same ASVs table.

2.3. Results

2.3.1. Pd status and bat data

We selected Richard Lake Mine for our study, in part, because, based on our surveillance in winter 2016 (swabs from bats and substrates) and fall 2016 (swabs from swarming bats), it was negative for Pd the year before this study. It was also > 350 km from the nearest known WNS-positive hibernaculum at the time of our study (U.S. Geological Survey, 2019) and we observed no signs of WNS at the time of capture. We swabbed bats to confirm Pd-negative status as soon as we returned to the lab after capture, but it was not possible to wait for result of these swabs before assigning bats to experimental groups. Unfortunately, after we began the experiment, qPCR results revealed that eight of the 23 study animals selected for microbiota analysis were just above the threshold (40 C_t) to be considered Pd positive (McGuire et al., 2016) at the time of collection (39.3 $\pm$ 0.744 C_t, mean $\pm$ SD; Table 2.1, Table S2.4). Half of these eight bats had been randomly assigned to the inoculated group and half to the control group. Among the bats assigned to the control group, three Pd-negative bats remained negative throughout the experiment, but four bats that started in the control group as negative were positive by the end of the experiment presumably because of transfer of Pd from naturally infected control bats. One control bat that was Pd-positive at the time of capture was Pd-negative by the end of the experiment (Table S2.1). We do not expect this infection of captured bats, or contamination of the control group, influenced our results because loads at capture were extremely low, near the limit of detection and, on average, 18-fold lower than loads for the bats we experimentally infected (Table S2.4). Moreover, proportion of the wing exhibiting orange UV fluorescence (Table

S2.4) of contaminated control bats at the end of the experiment (0.2 ± 0.4%) was 14-fold lower than that of inoculated bats (2.8 ± 3.3%) (Wilcox test, W = 6, $p < 0.001$). The Pd load of the inoculated bats (0.0003 ± 0.0003 ng) was six-fold that of the contaminated control bats at the end of the experiment (0.00005 ± 0.0001 ng) (Wilcox test, W = 24, $p = 0.01$). All bats that we inoculated with Pd in the laboratory, and used for subsequent analysis of the microbiota (n = 12), were Pd-positive at the end of the experiment.

After experiment, we detected orange fluorescence typical of Pd infection on *E. fuscus* skin of all bats we inoculated and on four control bats (Table 2.1). Interestingly, green and/or blue fluorescence was also detected. Green was always detected with co-occurrence of orange and/or blue fluorescence, whereas blue fluorescence was detected in the presence of orange, or alone.

Table 2.1. Information from *E. fuscus* individuals sampled skin microbiota.

Sample ID	Inoculation[1]	Incubator	Sex	Pd status qPCR Pre	Pd loads Pre (ng) 10^{-6}	Pd status qPCR Post	Pd loads Post (ng) 10^{-6}	Fluorescence Post
EPFU11	PBST	2	Female	Negative	0	Positive	55.3	Nothing
EPFU13	PBST	1	Female	Negative	0	Negative	0	Nothing
EPFU15	PBST	1	Female	Negative	0	Positive	33.1	Nothing
EPFU18	PBST	2	Male	Negative	0	Positive	45.0	Nothing
EPFU19	PBST	1	Male	Negative	0	Negative	0	Blue
EPFU24	PBST	1	Male	Negative	0	Negative	0	Blue
EPFU26	PBST	2	Female	Positive	5.2	Positive	60.4	Blue
EPFU30	PBST	2	Male	Positive	5.2	Positive	30.5	Orange-blue
EPFU31	PBST	1	Male	Positive	5.9	Negative	0	Orange-blue
EPFU4	PBST	2	Female	Positive	40.6	Positive	37.5	Orange-blue-green
EPFU7	PBST	1	Female	Negative	0	Positive	5.3	Orange-blue
EPFU1	Pd	1	Female	Negative	0	Positive	389.0	Orange-blue
EPFU10	Pd	1	Female	Positive	6.0	Positive	722.1	Orange-blue-green
EPFU12	Pd	2	Male	Negative	0	Positive	69.5	Orange-blue
EPFU16	Pd	1	Female	Negative	0	Positive	94.8	Orange-blue
EPFU2	Pd	2	Female	Negative	0	Positive	794.6	Orange-blue-green
EPFU20	Pd	1	Male	Negative	0	Positive	208.4	Orange
EPFU23	Pd	1	Male	Positive	6.7	Positive	139.2	Orange-green
EPFU27	Pd	1	Male	Negative	0	Positive	10.9	Orange
EPFU29	Pd	2	Male	Negative	0	Positive	44.6	Orange
EPFU3	Pd	2	Female	Positive	5.7	Positive	42.5	Orange-blue-green
EPFU32	Pd	2	Male	Positive	5.1	Positive	642.7	Orange-green
EPFU5	Pd	2	Female	Negative	0	Positive	9.8	Orange

[1]Pd: Pd inoculated bats PBST: sham inoculated bats PBS + 05% Tween 20.

2.3.2. Alpha diversity

After assuring no difference in Shannon diversity between inoculation groups prior to the experiment ($F = 0.62$, $p = 0.44$), no effect of inoculation was detected on Shannon diversity at the end of the experiment while controlling for cage ID ($\chi^2 = 0.05$, $p = 0.82$). There was also no effect of inoculation on the change in alpha diversity from capture to the end of the experiment ($F = 0.74$, $p = 0.40$). Although there was no effect of inoculation, we did detect a significant difference in alpha diversity between the start and the end of the experiment ($F = 93.15$, $p < 0.0001$). Mean Shannon diversity values decreased by 24% (1.59 ± 0.16) in post-inoculated samples indicating a strong effect of either hibernation or

captivity (or both) on alpha diversity of the skin microbiota.

2.3.3. Beta diversity

By chance, the inoculation group factor explained redundant variation in weighted UniFrac distances when we controlled for sex pre-captivity (Table 2.2). However, this redundant variation was not persistent throughout the experiment. Indeed, there was no redundant variation between inoculation and UniFrac distances by the end of the experiment (i.e., for post-captivity samples) after controlling for incubator, sex and cage ID (Table 2.2). This indicates that beta diversity changed over the course of the experiment, although it was not caused by inoculation. Yet, cage ID was the factor that explained most of the variation in beta diversity when included in the model post-captivity (Table 2.2). Dispersion was homogeneous according to inoculation in pre-captivity samples (PERMDISP unweighted UniFrac, $F = 0.87$, $p = 0.36$; PERMDISP weighted UniFrac $F = 3.15$, $p = 0.09$) and in post-captivity sample (PERMDISP unweighted UniFrac, $F = 2.23$, $p = 0.16$; PERMDISP weighted UniFrac, $F = 1.12$, $p = 0.30$).

Table 2.2. db-RDA of unweighted and weighted UniFrac distances of *E. fuscus* skin microbiota samples. Captivity timepoint model test for difference between pre- and post-captivity samples while sex factor is controlled. Inoculation pre model test for difference between treatment group pre-captivity while controlling sex. Inoculation post model test for difference between treatment group post-captivity while controlling incubator, sex and cage ID. Cage ID post model test for difference in cage post-captivity while controlling incubator, sex and inoculation.

Distance measure	Model	F statistic	Adjusted R^2	P-value
Unweighted UniFrac	Captivity timepoint	16.70	0.26	**0.0001**
	Inoculation pre	0.99	NA	0.46
	Inoculation post	0	NA	0
	Cage ID post	2.24	0.06	**0.0017**
Weighted UniFrac	Captivity timepoint	29.54	0.42	**0.0001**
	Inoculation pre	0	NA	0
	Inoculation post	0	NA	0
	Cage ID post	2.72	0.08	**0.02**

Significant results are in bold.

To account for temporal effect and test whether inoculation led to more or less change in the microbiota over the course of the experiment, we calculated distances between pre- and post-captivity samples, paired within each individual. After controlling for cage ID, we found significantly higher dispersion of distances for Pd-inoculated bats based on both unweighted and weighted UniFrac distances ($\chi^2 = 6.52$, $p = 0.01$, $\chi^2 = 8.92$, $p = 0.003$) (Fig. 2.1). Post-captivity samples from inoculated bats were 11% (0.09 ± 0.03) more distant

than samples from controls based on unweighted UniFrac distances, and 22% (0.10 ± 0.03) more distant based on weighted UniFrac (Fig. 2.1). In other words, the skin microbiota of Pd-inoculated bats changed more over time than that of sham-inoculated controls.
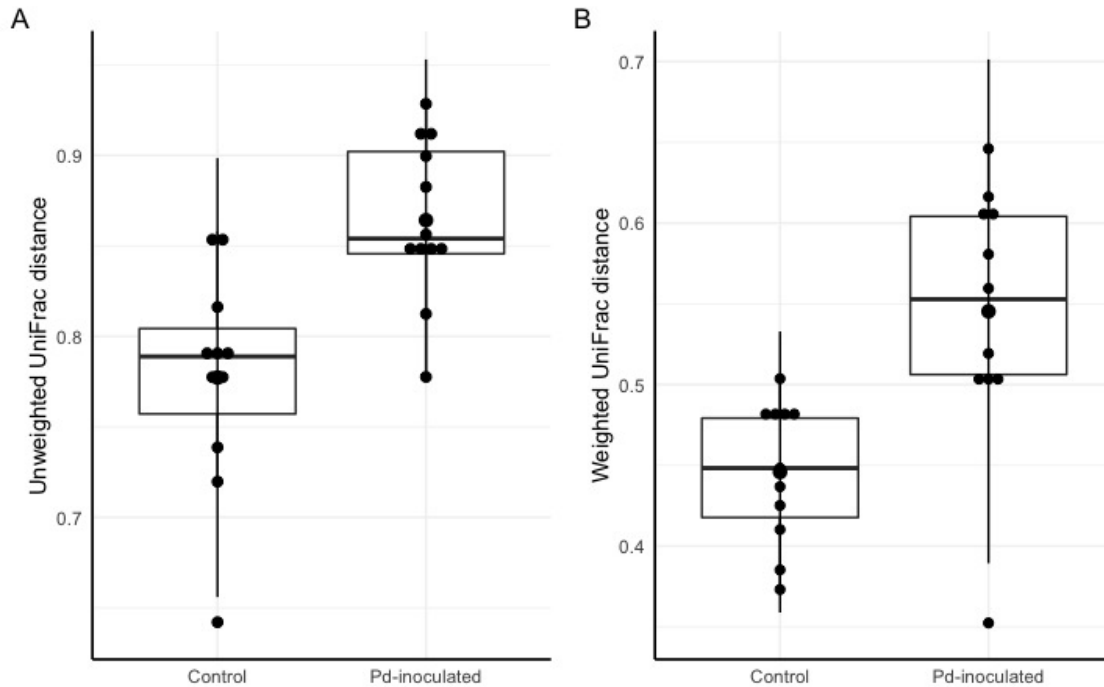
Fig. 2.1. Pre- and post-captivity paired distance grouped by inoculation. (A) Pre-and post-captivity paired Unweighted UniFrac distances grouped by inoculation (B) Pre-and post-captivity paired Weighted UniFrac distances grouped by inoculation. The black bars represent standard deviations, and the black points represent mean alpha diversity values.

Captivity was an important factor shaping community structure of the skin microbiota (Fig. 2.2). About 26% of the variation in community structure was explained by captivity based on unweighted UniFrac distances, and about 42% of this variation was explained by captivity based on weighted UniFrac (Table 2.2). Community structure of pre-captivity samples was more dispersed than that in post-inoculated samples based on unweighted UniFrac distances (PERMDISP, F = 12.34, p = 0.0008) and weighted UniFrac (PERMDISP, F = 30.33, p = 0.0001) (Fig. 2.2).
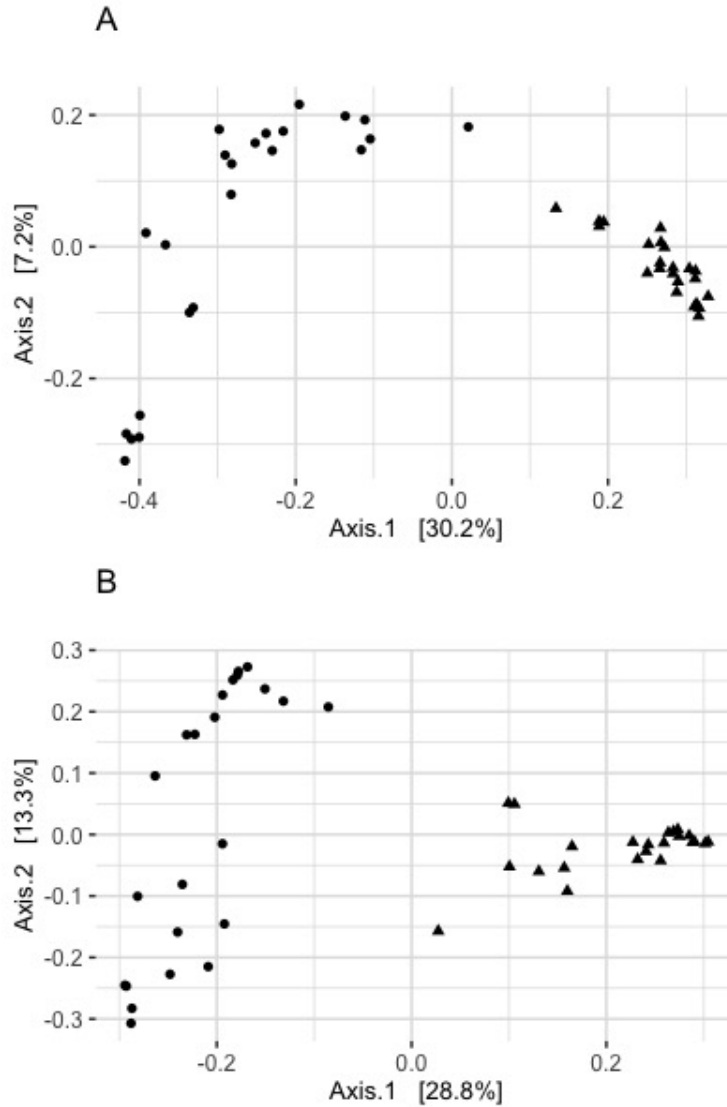
Fig. 2.2. Principal coordinates analysis of rarefied pre- (triangles) and post-captive (circles) bat samples (36,416 sequences). (A) Principal coordinate analysis of unweighted UniFrac distances. (B) Principal coordinate analysis of square rooted weighted UniFrac distances. Each point represents a sample from an individual bat.

2.3.4. Analysis of skin microbiota composition

Only one taxon (i.e., *Pseudonocardia*) changed in abundance over the course of captivity at the genus level and it was more abundant in pre-captive individuals (Table 2.3). No taxa were significantly more abundant in Pd-inoculated individuals at the end of the experiment (Table 2.3).

Table 2.3. Differently abundant taxa detected with Analysis of Composition of Micro-biomes (ANCOM) comparing paired bat pre- and post-captivity and comparing post-captive bats according to inoculation. Analysis was performed on unrarefied table at genus level with relative abundance higher or equal to 0.1%. Significant taxa obtained p< 0.05 after taxa-wise multiple correction.

Comparison	Taxa	W statistic
Captivity timepoint	***Pseudonocardia***	**12**
	Staphylococcus	10
	Hafnia.Obesumbacterium	10
	Arthrobacter	10
	Rhodococcus	10
	Pseudarthrobacter	10
	Bacillus	9
	Mycoplasma	9
	Klebsiella	8
	Actinobacillus	8
	Clostridium	8
	Pseudomonas	7
	Yersinia	7
	Flavobacterium	5
Post inoculation	*Pseudarthrobacter*	10
	Flavobacterium	9
	Pseudomonas	8
	Arthrobacter	7
	Clostridium	7
	Klebsiella	5
	Rhodococcus	5
	Pseudonocardia	4
	Staphylococcus	4
	Bacillus	4
	Actinobacillus	4
	Hafnia.Obesumbacterium	3
	Yersinia	1
	Mycoplasma	0

Significant results are in bold.

Consistent with these results, community composition of the microbiota remained similar over the course of captivity and only a higher proportion of *Pseudonocardia* was detected in pre-captivity samples (Table 2.3 and Fig. 2.3). The dominant genera we observed

in the skin microbiota of *E. fuscus* were *Mycoplasma*, *Pseudomonas*, *Staphylococcus*, *Hafnia.Obesumbacterium*, *Pseudonocardia*, *Pseudarthrobacter*, *Arthrobacter*, *Bacillus*, *Klebsiella*, *Actinobacillus*, *Clostridium*, *Yersinia*, *Flavobacterium* and *Rhodococcus*. Based on ANCOM results (Table 2.3) *Pseudomonas*, *Mycoplasma*, *Staphylococcus*, *Hafnia.Obesumbacterium*, *Pseudarthrobacter*, *Arthrobacter*, *Bacillus*, *Klebsiella*, *Actinobacillus*, *Clostridium*, *Yersinia*, *Flavobacterium* and *Rhodococcus* appeared to remain constant over the course of captivity.
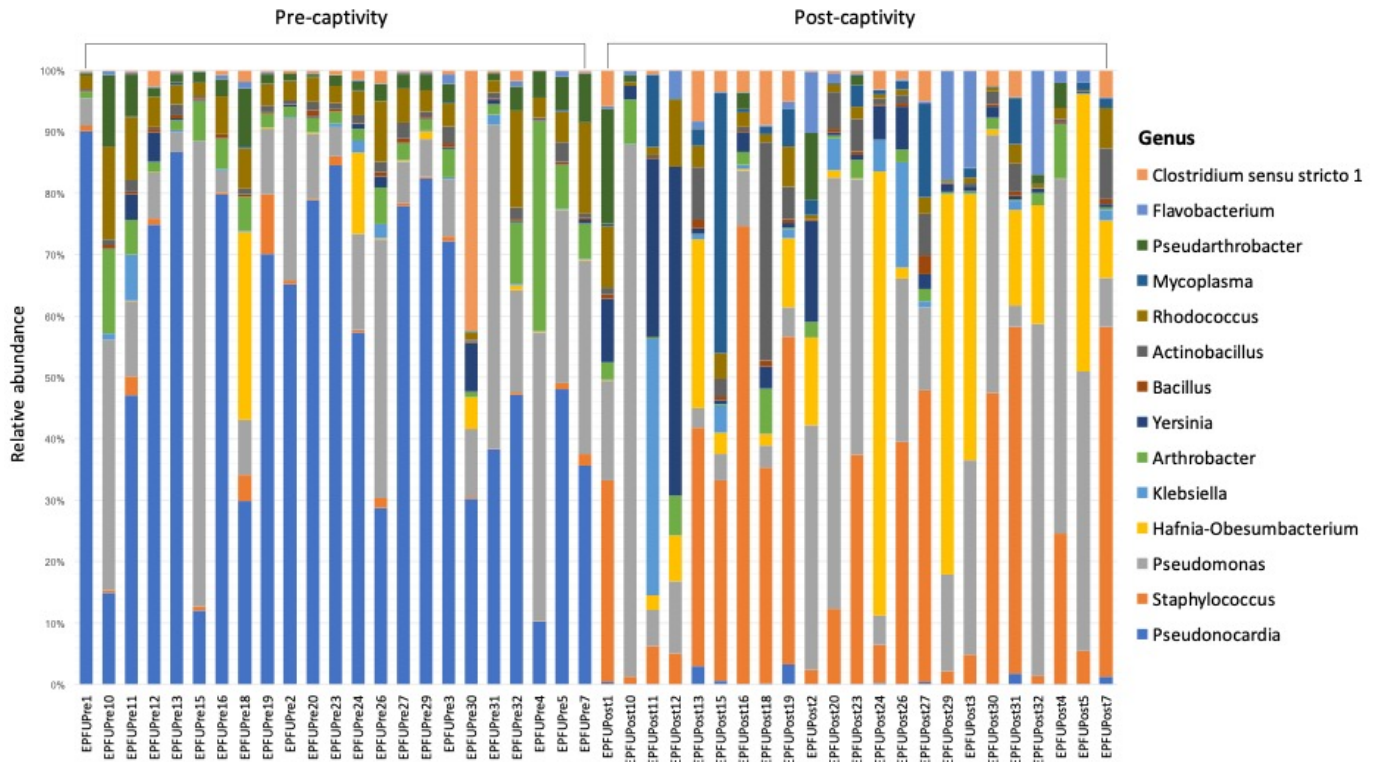
Fig. 2.3. Relative abundance of different genera in the microbiota on bat skin from before (pre-captivity) and after (post-captivity) experiment. Analysis was performed on unrarefied ASVs table of taxa with relative abundance higher or equal to 0.1%.

2.4. Discussion

Research on the skin microbiota of wildlife facing emergent skin diseases is a growing area of research (Daszak, 2000; Belden & Harris, 2007; Fisher et al., 2012; Jones et al., 2008), and in the specific context of North American bats, understanding responses of the skin microbiota could contribute to management of WNS (Cheng et al., 2017; Hoyt et al., 2019). We inoculated, or sham inoculated *E. fuscus* with Pd and maintained them under controlled conditions for three months to test whether the skin microbiota of a WNS-resistant species might evolve in response to fungal infection, and help understand the potential contribution of the microbiota to WNS resistance.

We found mixed support for our first hypothesis that Pd inoculation would have little impact on the skin microbiota of this WNS-resistant species. No taxa were significantly more abundant on Pd-inoculated bats, at the end of the experiment, compared to controls and no difference was detected in diversity as observed in the wild for this species (Ange-Stark et al., 2019). Interestingly, difference between inoculation group in weighted UniFrac distances prior to the experiment disappeared post experiment, supporting that Pd inoculation effect was not strong enough to create divergence in skin microbiota. However, our results suggest that Pd inoculation reduced the capacity of the host (or its microbiota) to regulate the skin microbiota, leading to more dispersion within and between individuals as observed in studies of Bd, the fungal pathogen affecting amphibians (Zaneveld et al., 2017). Jani and Briggs (2014) found that outbreaks of Bd increased temporal changes in the skin microbiota of *Rana sierra* and suggested that, even frogs that could tolerate Bd infection could be sensitive to disruption of the microbiota by the pathogen, although whether this disruption was protective or harmful was not clear. Similarly, our results reflect a transformation of the skin microbiota due to Pd infection, although we do not know if this disruption would be advantageous, detrimental, or neutral for infected *E. fuscus*. In *Lithobates catesbieanus*, an amphibian species with low susceptibility to Bd (Eskew et al., 2015), the fungus was a selective force on the microbial community, but the microbiota also affected Bd infectivity and, consequently, probably exhibited a negative effect on host fitness (Walke et al., 2015). Our results could not establish whether the skin microbiota affects the fungal infection, or if the fungal infection could in turn affect the microbiota, and this still needs to be investigated.

Consistent with our second hypothesis, the composition of the microbiota included several taxa known to inhibit Pd growth in vitro, and which have been found on bats persisting after WNS (e.g., *Rhodoccocus* (Cornelison et al., 2014; Hamm et al., 2017), *Pseudomonas* (Hoyt, Cheng, et al., 2015)). *Pseudonocardia* was also the most abundant microbial taxa in pre-captivity samples and, although it declined in abundance by the end of

the experiment, it is known to have antifungal activity (Sen et al., 2009). The proportional abundances of *Rhodoccocus* and *Pseudomonas* were stable from pre- to post-captivity and they were among the most abundant taxa at both time points. These bacteria may play a role in the persistence of some individuals of highly susceptible bat species (e.g., *M. lucifugus*) after Pd invasion (Lemieux-Labonté et al., 2017) and the fact that they represented a large proportion of the microbiota in the resistant species we studied also suggests their importance in the response of bats to WNS. Interestingly, the blue and green fluorescence we detected on *E. fuscus* skin, is typical of pyocyanine and pyoverdine pigments, which have been observed in some *Pseudomonas* such as *P. aeruginosa* and *P. fluorescens* (Reyes et al., 1981; Albesa et al., 1985). Pyoverdine is a molecule that scavenges iron from the environment and could compete with pathogens such as Pd that may be limited by iron availability (Mascuch et al., 2015; S. M. Reeder et al., 2017; Sass et al., 2017). Pyocyaninie is an exotoxin with antimicrobial potential and could also be detrimental to Pd (Hassan & Fridovich, 1980; Baron & Rowe, 1981). Green fluorescence (typical of pyoverdine) was always observed co-occurring with orange fluorescence (typical of Pd) and/or blue fluorescence (typical of pyocyanine), whereas blue fluorescence was detected both alone or alongside orange fluorescence. These patterns are consistent with antifungal activity by *Pseudomonas* on the skin of *E. fuscus.* However, it is important to note that strains of the potential genera discussed above are not obligatorily antifungal, and that the metabarcoding method used in our study did not allow us to assess the proportion of antifungal metabolites produced as suggested by a previous study (Antony-Babu et al., 2017). The proportional overview of the community is also biased by the different copy numbers of ribosomal 16S rRNA gene present in different microorganisms (Klappenbach, 2001). Further studies should focus on the functional influence of these bacteria and other microorganisms (e.g., fungi and viruses) on the host-pathogen interaction between bats and Pd using approaches such as whole metagenomics sequencing.

The fact that some *E. fuscus* were, unexpectedly, already Pd-positive when we collected them before the experiment could have influenced our results. Since all collected bats were roosting in the same site, it is possible that all bats sampled were either carrying Pd at levels below our detectability threshold, or had previously been exposed. However, the facts that the mine was Pd-negative the year before our study, that we observed no clinical signs of WNS during our capture session, and that intensity of infection was very low for the few positive bats we did collect, collectively suggest that the cave only recently became infected with Pd and that impacts on our results were minimal.

We also found that the skin microbiota shifted during captivity. This finding supports previous results in which samples from the same bat collected over time were more different

than samples from multiple bats collected at the same time and place (Kolodny et al., 2019). The decrease in micriobial diversity we observed in post-captivity samples likely reflects the controlled conditions in the laboratory setting. Captivity has been observed to negatively affect community diversity in the microbiota of wild amphibians (Kueneman et al., 2016; Sabino-Pinto et al., 2016) and it has been linked to sterile conditions in captivity (Loudon et al., 2014).

Our results suggest that the skin microbiota profile of *E. fuscus* may contribute to the apparent resistance of this species to Pd. Antifungal taxa predominated the microbiota prior to infection and remained stable in the skin microbiota after inoculation and three months of hibernation. However, despite apparent resistance to WNS and the abundance of anti-fungal bacteria, Pd could still affect host health in this species as it was shown to create skin lesion and inflammation (Moore et al., 2018) that may impact skin barrier integrity and lead to subsequent vulnerability to other pathogens. Although certain bacterial taxa remained abundant, there was destabilization of the microbiota that could be harmful for bats and this requires further study to truly understand impacts of infection on this species. We recommend that future studies try to better characterize post-Pd colonization patterns and, especially, characterize functional changes resulting from these patterns. WNS resistance and tolerance may reflect a range of mechanisms, from storage of extra body fat in fall (Cheng et al., 2019), endogenous fat in epidermis composition (Frank et al., 2016, 2018), variation in individual behaviour (Frick et al., 2016) to variation in immune response (Maslo et al., 2015). Our results suggest that the skin microbiota could be another mechanism helping some bats survive infection with Pd. We recommend further research on gene expression by the microbiome of resistant and susceptible bat species to help understand disease mechanisms in WNS and contribute to conservation strategies for North American bats.

2.5. Availability of data and materials

The datasets supporting the conclusions of this article are available in the Figshare repository. Raw data are available at `https://figshare.com/s/a1015374c5bccd9f9dc7`. Scripts and matrix are available at `https://figshare.com/s/87d08697f1d32aeebb86`

2.6. Acknowledgements

obtained through BEI Resources, NIAID, NIH as part of the Human Microbiome Project: Genomic DNA from Microbial Mock Community B (Even, Low Concentration), v5.1L, for 16S rRNA Gene Sequencing, HM-782D.

2.7. Supplementary files

Table S2.1. Shannon diversity of *E. fuscus* skin microbiota samples tested by ANOVA of linear model. Transport model compare 8 bats skin microbiota sampled in the cave at capture with bats sampled in lab less than 24h later.

Model	*F* statistic	*P*-value
Transport	3.36	0.08

Table S2.2. db-RDA of unweighted and weighted UniFrac distances of *E. fuscus* skin microbiota samples. Transport model compare 8 bats skin microbiota sampled in the cave at capture with bats sampled in lab less than 24h later. Sex factor was controlled.

Distance measure	Model	*F* statistic	Adjusted R^2	*P*-value
Unweighted UniFrac	Transport	1.15	NA	0.11
Weighted UniFrac	Transport	1.76	NA	0.08

Table S2.3. Rectal temperature record of *E. fuscus* at the end of captivity.

Sample ID	Inoculation[1]	Time Exit Incubator	Time Rectal Temperature	Rectal Temperature (°C)
EPFU11	PBST	12:15	12:17	10
EPFU13	PBST	11:47	11:49	9.2
EPFU15	PBST	11:42	11:45	9.2
EPFU18	PBST	12:34	12:35	9.9
EPFU19	PBST	14:10	14:10	16.7
EPFU24	PBST	14:14	14:14	29
EPFU26	PBST	14:47	14:48	13.2
EPFU30	PBST	12:24	12:24	13.5
EPFU31	PBST	11:33	11:35	10.2
EPFU4	PBST	14:53	14:54	16.3
EPFU7	PBST	14:03	14:03	13.3
EPFU1	Pd	15:26	15:26	11.3
EPFU10	Pd	15:47	15:48	33.3
EPFU12	Pd	11:40	11:41	10.1
EPFU16	Pd	15:19	12:17	10.2
EPFU2	Pd	15:50	15:50	15.7
EPFU20	Pd	15:42	15:43	30.5
EPFU23	Pd	15:34	15:35	15.9
EPFU27	Pd	12:11	12:12	10.9
EPFU29	Pd	11:46	11:47	35.3
EPFU3	Pd	15:46	15:46	35.1
EPFU32	Pd	15:39	15:40	14.4
EPFU5	Pd	11:34	11:35	12.7

[1]Pd: Pd inoculated bats PBST: sham inoculated bats PBS + 05% Tween 20.

Table S2.4. C_t score, Pd load and UV proportions of *E. fuscus* bats.

SampleID	Inoculation[1]	Pre C_t score	Pre Pd load (ng) 10^{-6}	Post C_t score	Post Pd load (ng) 10^{-6}	Orange UV proportion (%)
EPFU11	PBST	>41	0	36.30	55.3	0
EPFU13	PBST	>41	0	>41	0	0
EPFU15	PBST	>41	0	37.05	33.1	0
EPFU18	PBST	>41	0	36.60	45.0	0
EPFU19	PBST	>41	0	>41	0	0
EPFU24	PBST	>41	0	>41	0	0
EPFU26	PBST	39.73	5.2	36.17	60.4	0.072
EPFU30	PBST	39.74	5.2	37.17	30.5	0.016
EPFU31	PBST	39.55	5.9	>41	0	0.077
EPFU4	PBST	36.75	40.6	33.52	375.0	1.092
EPFU7	PBST	>41	0	39.71	5.3	0.003
EPFU1	Pd	>41	0	33.47	389.0	8.416
EPFU10	Pd	39.52	6.0	32.57	722.1	6.758
EPFU12	Pd	>41	0	35.97	69.5	1.785
EPFU16	Pd	>41	0	35.52	94.8	0.203
EPFU2	Pd	>41	0	32.43	794.6	6.956
EPFU20	Pd	>41	0	34.37	208.4	0.731
EPFU23	Pd	39.37	6.7	34.96	139.2	1.35
EPFU27	Pd	>41	0	38.66	10.9	0.517
EPFU29	Pd	>41	0	36.62	44.6	0.121
EPFU3	Pd	39.61	5.7	36.69	42.5	0.444
EPFU32	Pd	39.77	5.1	32.74	642.7	6.682
EPFU5	Pd	>41	0	38.81	9.8	0.237

[1]Pd: Pd inoculated bats PBST: sham inoculated bats PBS + 05% Tween 20.
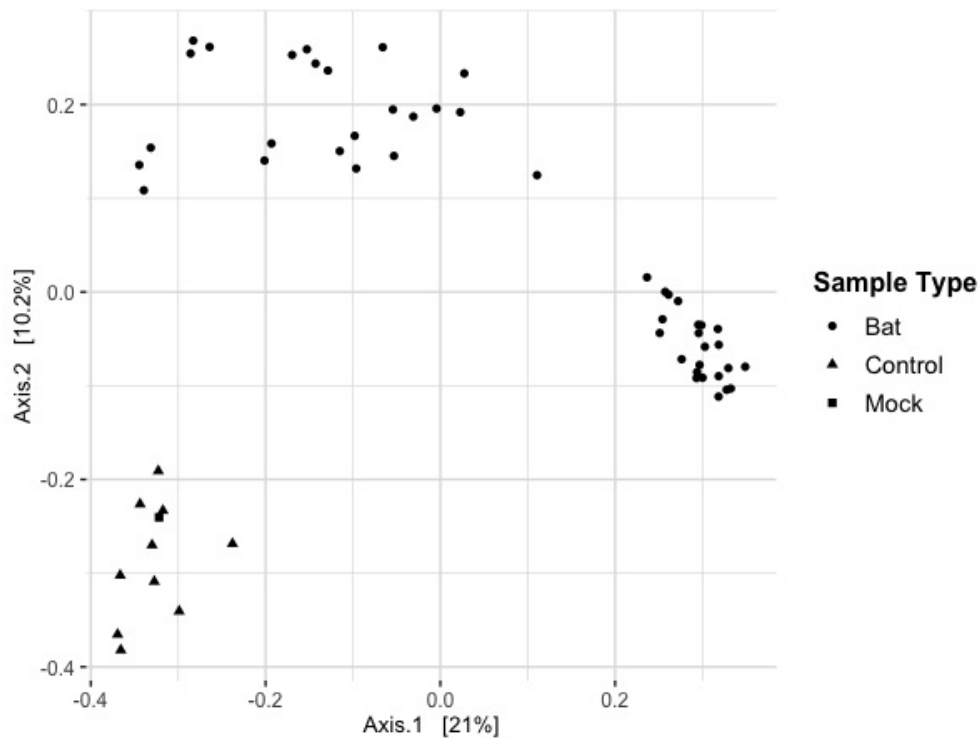
Fig. S2.1. Principal coordinates analysis of square rooted weighted UniFrac distances. Each point represents a control, mock, or individual bat sample.
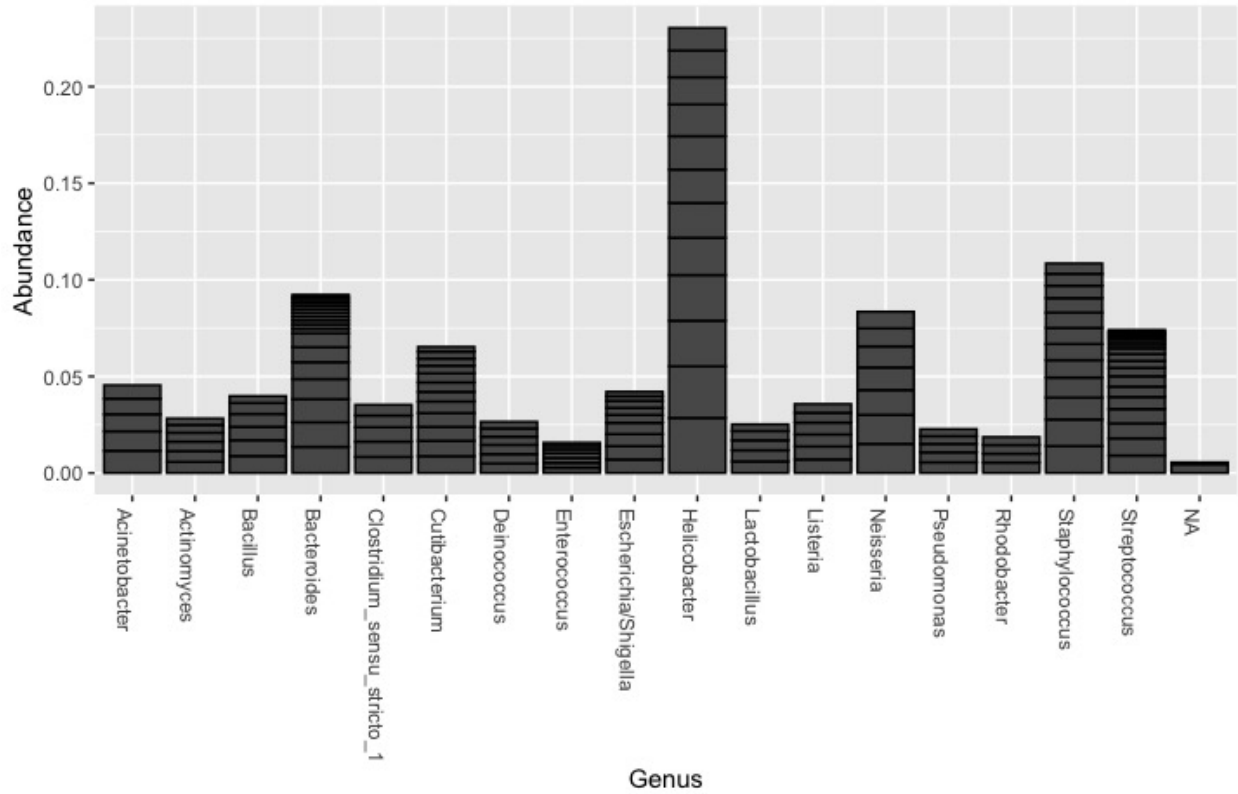
Fig. S2.2. Relative abundance of different genera in the Mock sample. The analysis was performed on unrarefied ASVs table of taxa with relative abundances higher or equal to 0.1%.
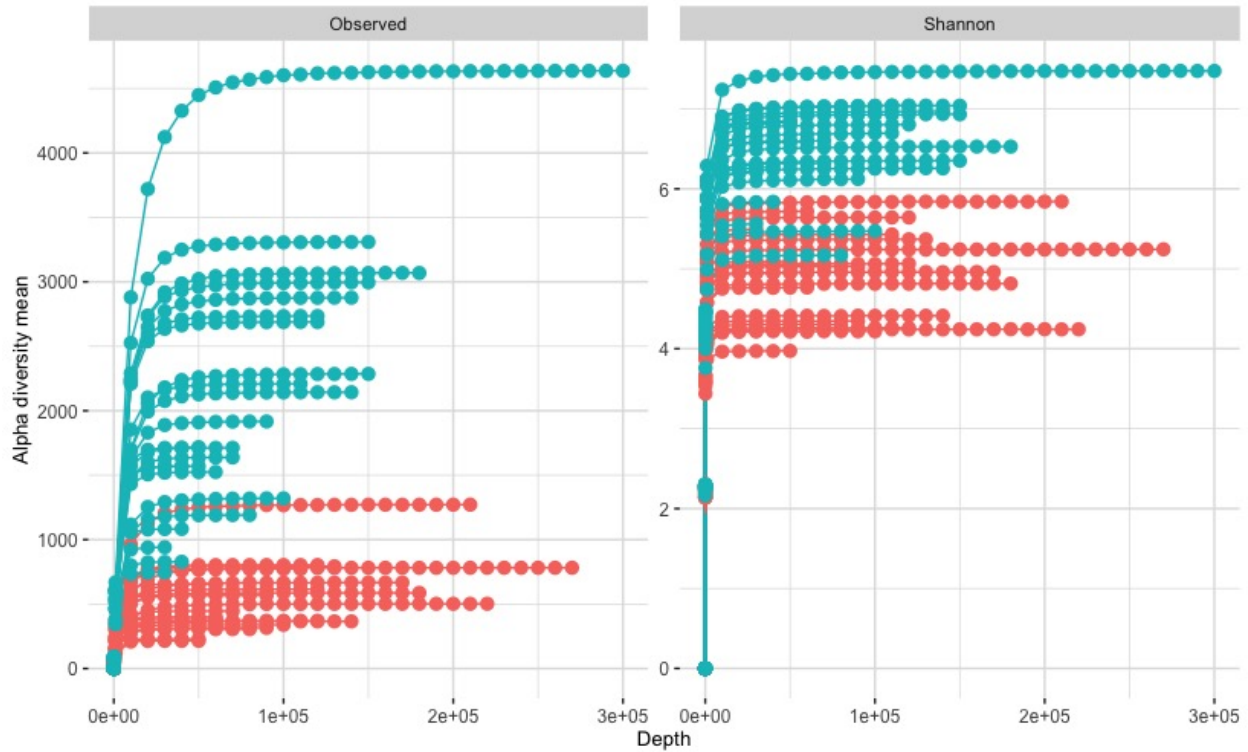
Fig. S2.3. Rarefaction curves of alpha diversity calculated on multiple rarefied data for each of the 46 pre-(blue) and post-captive(coral) bat skin microbiota samples. Left panel presents overall richness (ASV observed) and right panel presents Shannon diversity of bat skin samples.

Chapitre 3

Pseudogymnoascus destructans infection impacts the functional metagenome of highly vulnerable *Myotis lucifugus*

Virginie Lemieux-Labonté[1], Jananan Pathmanathan[2], Yves Terrat[1], Nicolas Tromas[1], Anouk Simard[3], Catherine G. Haase[4], Cori Lausen[5], Craig K. R. Willis[6] and François-Joseph Lapointe[1]

[1]Département de sciences biologiques, Université de Montréal, Montréal, Québec, Canada

[2]Rutgers School of Environmental and Biological Sciences, New Brunswick, New Jersey, United States

[3]Direction de l'expertise sur la faune terrestre, l'herpétofaune et l'avifaune, Ministère des Forêts, de la Faune et des Parcs, Québec, Canada

[4]Department of Biology Austin Peay State University, Clarksville, Tennessee, United State

[5]Wildlife Conservation Society Canada. Kaslo, British-Colombia Canada

[6]Department of Biology and Centre for Forest Interdisciplinary Research, University of Winnipeg, Winnipeg, Manitoba, Canada

Résumé. L'émergence d'infections cutanées fongiques pose de nouveaux défis en biologie de la conservation. Le champignon *Pseudogymnoascus destructans* (Pd), agent pathogène du syndrome du museau blanc (SMB), a mis en danger de nombreuses espèces de chauves-souris nord-américaines depuis 2006. Récemment, le rôle potentiel du microbiome cutané dans la résistance et la sensibilité à des champignons pathogènes a été mis en évidence, mais seulement en se basant sur l'exploration taxonomique des communautés. Dans cette étude, nous évaluons le potentiel fonctionnel du microbiome cutané (le métagénome fonctionnel) de petites chauves-souris brunes (*Myotis lucifugus*) sauvages en hibernation à l'aide de la métagénomique. Nous comparons les colonies positives et négatives au Pd à trois moments en fonction de l'infection au Pd (non infectées, première année d'infection et 10 années post-infection). Notre premier objectif est de cerner les effets du statut infectieux et du temps écoulé depuis l'infection sur le métagénome fonctionnel. Notre deuxième objectif est de détecter des différences significatives dans le métagénome qui pourraient affecter ou être affectées par le SMB. Le statut Pd n'a aucun impact sur le métagénome, mais il existe un effet important du temps écoulé depuis l'infection sur la structure et la composition de celui-ci. Les colonies de chauves-souris qui venaient d'être infectées par la maladie présentaient des valeurs plus faibles de diversité alpha, tandis que le métagénome des colonies qui survivaient à la maladie pendant au moins 10 ans était similaire à celui des colonies non infectées. Nous n'avons trouvé aucun enrichissement des fonctions antifongiques chez les colonies ayant survécu à la maladie. Or, des fonctions pour le transport et l'assimilation des métaux essentiels étaient significativement moins abondantes suite à l'infection. Bien que nos résultats soutiennent l'hypothèse d'un métagénome altéré suite à l'infection, nous ne pouvons pas exclure la possibilité que le métagénome fonctionnel puisse agir en synergie avec d'autres mécanismes pour prévenir l'infection par le champignon Pd. Dans l'ensemble, nos résultats révèlent que le métagénome fonctionnel varie considérablement juste après l'invasion du Pd, mais que celui-ci semble se rétablir après 10 ans. Une telle réponse pourrait avoir un impact sur la résilience de *M. lucifugus*. Des études futures utilisant des approches métaomiques combinées et prenant en compte d'autres mécanismes de résistance et de tolérance seront essentielles pour élucider le rôle et l'influence du du métagénome fonctionnel et du microbiome dans le contexte du SMB. **Mots clés** : métagénome fonctionnel, métagénomique, microbiome cutané, syndrome du museau blanc, *Myotis lucifugus*, petite chauve-souris brune.

Abstract. The emergence of fungal skin infections raises new challenges in conservation biology. The fungus *Pseudogymnoascus destructans* (Pd), the pathogen agent of white-nose syndrome (WNS), has endangered numerous North American bat species since 2006. Recently, the potential role of the skin microbiome in the resistance and susceptibility to multiple fungal pathogens have been highlighted, but mostly by focussing on taxonomic assessment. In this study, we assess the functional potential of the skin microbiome (functional metagenome) of vulnerable wild hibernating little brown bats (*Myotis lucifugus*) using shotgun metagenomics. We compare Pd positive and negative colonies at three-time points according to Pd infection (not infected, just infected and 10 years post infection). Our first objective was to untangle the effects of infection status and time since infection on the functional metagenome. Our second objective was to detect significant differences in the functional metagenome that could affect, or be affected by WNS. We found no effect of Pd status, but an important effect of time since infection on the functional metagenome structure and composition. Colonies just affected by the disease exhibited the lowest values of alpha diversity, whereas colonies surviving the disease for at least 10-years were more similar to pre-infected colonies than to one-year infected colonies. Although, we found no enrichment of antifungal functions in colonies surviving the disease, functions essential for metal transport and assimilation were significantly less abundant after infection. Even our results support the hypothesis of a functional metagenome disruption by Pd, we could not rule out the possibility that the functional metagenome may act synergistically with other mechanisms to prevent Pd infection. Overall, our results reveal that microbiome functional profiles vary greatly just after Pd invasion but that original functions are reestablished after 10 years. Such diversified response could impact *M. lucifugus* fitness. Future studies using combined metaomics approaches and considering other resistance and tolerance mechanisms will be key to untangle the functional metagenome and microbiome role and influence in the WNS context. **Key words**: functional metagenome, shotgun metagenomic, skin microbiome, white-nose syndrome, *Myotis lucifugus*, little brown bats.

3.1. Introduction

Fungal diseases are on the rise worldwide, causing an unprecedented decline in wildlife (Daszak, 2000; Jones et al., 2008; Fisher et al., 2012, 2020). The emergence of fungal skin infections with devastating physiological consequences is of particular concern (Fisher et al., 2020). Such emergent fungal diseases raise new challenges in conservation biology, as they operate by mechanisms not yet fully characterized (Fisher et al., 2020). The chytridiomycosis caused by the fungus *Batrachochytrium dendrobatidis* (Berger et al., 1998) has led to a 50% decrease in amphibian species worldwide (Stuart et al., 2004). Similarly, *Ophidiomyces ophiodiicola*, the fungal agent of ophidiomycosis, is a potential threat to the European snake

population and has caused important declines in North America (Allender et al., 2011, 2015; Clark et al., 2011; Franklinos et al., 2017).

The fungus *Pseudogymnoascus destructans* (Pd) (Gargas et al., 2009; Lorch et al., 2011), pathogen agent of the white-nose syndrome (WNS), has greatly affected North American bats over the last decade (Blehert et al., 2009; Frick, Pollock, et al., 2010; Frick et al., 2016). Pd invades the skin during hibernation, thus creating lesions that alter fluid balance, thermoregulation, and gas exchange, resulting in increased arousal frequency (Meteyer et al., 2009; Cryan et al., 2010; Warnecke et al., 2013; Verant et al., 2014; McGuire et al., 2017). Up to 6,7 million bats died from this disease (Coleman, 2012). In Canada, the northern long-eared bat (*Myotis septentrionalis*), the little brown bat (*Myotis lucifugus*), and the tricolored bat (*Perimyotis subflavus*) are listed as federally endangered due to mortality rates of 75–90% during the several-year invasion stage of the disease (Canadian Wildlife Service & Committee on the Status of Endangered Wildlife in Canada, 2013). Yet, some hibernating colonies of the endangered *M. lucifugus* persisted following fungal invasion (Dobony et al., 2011; Langwig et al., 2012; Canadian Wildlife Service & Committee on the Status of Endangered Wildlife in Canada, 2013; Frick et al., 2015; Maslo et al., 2015), with population counts stabilizing at about 5 to 30% of their initial sizes (Langwig et al., 2012; Frick et al., 2015). Variation in susceptibility to Pd could reflect mechanisms that allow for resistance (i.e. reduction or elimination of pathogen infection) and/or tolerance (i.e. reduction of the damage caused by infection) (Råberg et al., 2007, 2009; Svensson & Råberg, 2010). Resistance and tolerance are increasingly being studied in the WNS context, with mechanisms ranging from increase in fat accumulation, roost selection, torpor regulation and skin microbiome response (Hoyt, Cheng, et al., 2015; Frick et al., 2016; Langwig et al., 2017; Lemieux-Labonté et al., 2017; Cheng et al., 2019; Auteri & Knowles, 2020).

In fungal disease context, the microbiome could play an important role in species resistance or vulnerability. The microbiome can be defined as a collection of microorganisms (bacteria, archaea, eukaryotes, and viruses), their genomes (i.e., genes) and surrounding environmental conditions (Marchesi & Ravel, 2015). It is recognized as a critical component of host health, influencing biochemical and physiological processes, including defence against pathogens (Cho & Blaser, 2012). Namely, the microbiome contributes to host defence by limiting colonization and persistence of pathogens that compete for resources, and by producing pathogen inhibitors (Grice & Segre, 2011; Walter et al., 2018; Woo et al., 2019). It also interacts with the innate and adaptive immune system, and contributes to the maintenance of skin integrity and tissue repair (Lai et al., 2009; Curtis & Sperandio, 2011; Naik et al., 2012). In recent decades, several studies have highlighted the potential role of the skin microbiome in the resistance and susceptibility to multiple fungal pathogens

(Harris et al., 2009; Bletz et al., 2013, 2017; Jani & Briggs, 2014; Woodhams et al., 2014; Bataille et al., 2016; Ange-Stark et al., 2019; Rebollar et al., 2019; Lemieux-Labonté et al., 2017, 2020). However, previous studies have mostly focused on taxonomic composition of bacterial communities to infer microbiome functions.

Based on taxonomical analysis, the bat microbiome, contrary to other mammals, is mostly influenced by ecological factors, and not the phylogenetic relationships (Lutz et al., 2019). Particularly, community assemblage of gregarious bats changes over time at the colony level (Kolodny et al., 2019) and is predominantly influenced by the environment (Avena et al., 2016; Lemieux-Labonté et al., 2016; Grisnik et al., 2020; Winter et al., 2017). In accordance with a protective effect of the skin microbiome, hundreds of microorganisms isolated from wild bats and their corresponding habitats have shown inhibitory effects on Pd by secreted compounds, contact inhibition, or volatile molecules (Hamm et al., 2017; Micalizzi et al., 2017). Additionally, compared with the microbiome of the cave environment, the bat microbiome is enriched with antifungal taxa (Grisnik et al., 2020). Indeed, antifungal strains of *Pseudomonas* isolated from the skin of *E. fuscus* inhibit Pd growth in vitro (Hoyt, Cheng, et al., 2015; Hamm et al., 2017), and improve survival of WNS-infected little brown bats when applied to the skin as a probiotic treatment in vivo (Cheng et al., 2017; Hoyt et al., 2019). Moreover, the survival of *M. lucifugus* may be due to commensal bacteria, as persisting colonies with Pd have a less diverse microbiome, and proportionally more antifungal taxa on their skin (Lemieux-Labonté et al., 2017).

In spite of previous studies indicating that the microbiome may have a protective effect against Pd in *M. lucifugus*, at least one study has observed a significant reduction in bacterial community richness and evenness after invasion and colonization by Pd (Ange-Stark et al., 2019). This reduction could alter the microbiome ability to perform functions that inhibit or prevent the growth of pathogens and/or opportunistic bacteria, and may in turn potentially amplify disease severity. In contrast with the hypothesis that the microbiome protects against Pd, Grisnik et al. (2020) found that Pd-negative bats exhibited microbial assemblages with more antifungal taxa than Pd-positive bats. Taken together, these findings show that the response of host microbial communities with respect to fungal pathogens is still unclear. Recent work suggests that metagenomics yield greater resolution, accuracy in taxonomic assignation and in detection of putative functional genes compared to amplicon sequencing (Brumfield et al., 2020; Ranjan et al., 2016; Poretsky et al., 2014; Louca et al., 2016). Metagenomics should thus be used to study microbiome by taxonomy and/or functions (genes) (Langille, 2018). Furthermore, studies indicated that functional characterization of microbial community is more sensitive and that genes, rather than species or genera, may be the appropriate parameter for understanding patterns of

diversity in many microbial communities (Green et al., 2008; Burke et al., 2011; Louca et al., 2016; Ma et al., 2019). We believe that a functional investigation is now required to unravel the role of microbiome in vulnerable bat species facing WNS.

We will assess the functional potential of the skin microbiome (functional metagenome) of wild hibernating *M. lucifugus* colonies using shotgun metagenomics. By comparing Pd-positive and Pd-negative colonies, our main objectives are (1) to disentangle the effects of infection status and time since infection on the gene functions in the microbiome, and (2) detect significant differences in functional metagenome that could affect or be affected by WNS. Based on previous results (Lemieux-Labonté et al., 2017), we hypothesize that Pd will affect the functional metagenome structure, with a decrease in diversity following infection and in persisting bats. Moreover, we postulate that gene functions associated with antifungal properties or acting in fungal competition will be more prevalent in Pd surviving bats.

3.2. Materials and Methods

3.2.1. Skin metagenome collection

Bats were sampled according to two distinct protocols applied at different sites. For the first method (M1), bats were captured by plucking them off the wall and metagenome samples were collected while handling the bats with gloves. We swabbed the dorsal face of the right wing (forearm and under forearm) in linear strokes for 12 seconds with a sterile Puritan HydraFlock swabs (Fisher Scientific) soaked in sterile 0.15 M NaCl. 0.1% Tween-20 buffer. Swabs tips were ejected into a 1.5 ml microtube containing the same buffer. Tubes were transferred to 4°C within 2hr, and to -20°C within 24hr of sampling (See Table 3.1 for more information on the samples). All samples were shipped to Université de Montréal (Québec, Canada) for further processing. Two separate teams collected skin samples in two distinct hibernacula as part of independent studies. One hibernaculum was located 60 km south of Great Falls, Montana, USA ($47°30'N$, $-111°1'W$), whereas the second one was located in Alberta, Canada ($53°5'N$, $116°34'W$). Both hibernacula were Pd-negative at collection time in 2018 (according to qPCR results). The Montana samples were heated to 56°C for 30 min to ensure eradication of potential rabies viruses prior to being shipped on dry ice, as requested by USDA animal products export certificates 0579-0256 and Canadian Food inspection Agency importation permit A-2017-06316-4.

For the second sampling protocol (M2), we selected hibernating bats at random among those that we could reach from the ground in each hibernaculum. Samples were collected without handling the specimens by swabbing in linear strokes the back and forearm of

each bat for 20 s with a sterile Whatman Omniswab (Fisher Scientific) soaked in sterile 0.15 M NaCl. Swab tips were ejected into MoBio Powersoil DNA isolation Kit tubes (MoBio Laboratories), which were transferred to -20°C within 24 h of sampling. Bats are highly vulnerable to disturbance during hibernation, and we proceeded with caution to minimize the impact of our visits. Only two people entered the hibernaculum for sampling, and bats were not handled during swabbing. All methods were approved by the Animal Welfare and Ethics Committee at Université de Montréal (Protocol Number #16-015) and the University of Winnipeg Animal Care Committee (Protocol Number AEO5639). Using this method, we sampled the skin metagenome of specimens known to be Pd-negative at collection time in 2015 from one site (Patate), located on Anticosti island, Québec, Canada ($49°29'N$, $-63°00'W$). We also sampled the skin microbiota from one hibernaculum near St-George (SG), Manitoba, Canada ($51°22'N$, $97°14'W$) before (2016) and after (2019) Pd was first detected. The Richard Lake hibernaculum, located approximately 100 km east of Kenora, Ontario, Canada ($49°45'N$, $94°28'W$) was sampled in 2018, one year after the first Pd detection. Finally, samples were also collected in 2019 from two nearby sites (Lames and Lafleche) known to be Pd-positive since 2009-2010, and located 60 km north of Gatineau, Québec, Canada ($45°28'N$, $75°42'W$). All Pd status were determined by qPCR. See Table 3.1 for more details on the samples.

Table 3.1. Pooled skin metagenome samples information. Each sample is a mixed of five individuals collected at the same site.

Samples ID	Site	Pd status at collection time	Collection years	Year since infection	Collection method
Albpool1	Alberta	Negative	2018	0	M1
Albpool3	Alberta	Negative	2018	0	M1
Mont1pool1	Montana	Negative	2018	0	M1
Montpool3	Montana	Negative	2018	0	M1
Patpool1	Patate	Negative	2015	0	M2
Patpool3	Patate	Negative	2015	0	M2
SG163pool	St-George (SG)	Negative	2016	0	M2
Lafpool2	Lafleche	Positive	2019	10	M2
Lafpool3	Lafleche	Positive	2019	10	M2
Lamespool2	Lames	Positive	2019	10	M2
Lamespool3	Lames	Positive	2019	10	M2
RL18pool1	Richard Lake	Positive	2018	1	M2
RL18pool2	Richard Lake	Positive	2018	1	M2
RL18pool3	Richard Lake	Positive	2018	1	M2
SG192pool	St-George (SG)	Positive	2019	1	M2
SG19pool1	St-George (SG)	Positive	2019	1	M2

3.2.2. DNA extraction, purification and sequencing

Bacterial genomic DNA was extracted from each swab using The ChargeSwitch® gDNA Mini Bacteria Kit (Invitrogen™). We followed the manufacturer's protocol, modified by adding a 15 min heating period when eluting to increase DNA yield, and eluting in 50 μl of elution buffer. All procedures were conducted in a laminar flow hood to limit sample

contamination, and extractions were randomized to avoid detecting false patterns (Salter et al., 2014). Because of low input DNA, samples were pooled by sites and collection years. Therefore, each line in Table 3.1 is a mixed sample of five individuals collected at the same site. Pooled samples were purified using purification kit spin column (Zymo Research$^{\text{TM}}$), and sample concentration was measured with a Qubit 2.0 Fluorometer (Invitrogen). Samples with DNA concentration below 0.01 ng/μl were discarded, except for extraction controls that were used to keep track of contamination. We treated all pooled samples with RNase to improve samples quality. To do so, a mix of 20 μl nuclease free water, 5 μl NEB3 buffer and 3 μl RNase was added to each sample, prior to heating them at 37°C for 60 min, and at 70°C for 20 min. Samples were then sent to Génome Québec facilities at McGill University (Québec, Canada) for shotgun DNA library preparation with NEB Ultra II kit (New England BioLabs inc.). Samples failing the quality control test were discarded, including all extraction controls. DNA sequencing was then performed on NovaSeq6000 S4 flow cells and paired-end of 150bp (Illumina) at Génome Québec facilities.

3.2.3. Sequence processing

We obtained a total 320,713,730 shotgun sequence reads, and 96,855,546,460 bases for the sixteen bat sample pools under study (Table S3.1 for details on the raw sequences). Sequence reads were mapped to *M. lucifugus* genome, and unmapped reads only representing bat skin metagenome were selected for further analysis. First, quality trimming of raw reads was performed using the SolexaQA v3.1.7.1 program (Cox et al., 2010) with default parameters. Trimmed reads shorter than 75nt were removed for further analysis. Removal of artificial duplicates was performed based on the screening of identical leading 20bp. From the trimmed high-quality reads, gene fragments were predicted using FragGeneScan-Plus v3.0 (Kim et al., 2015). Predicted protein fragments were clustered at a 90% similarity level using cd-hit v4.8.1 (Fu et al., 2012). One representative of each cluster was further used for a similarity search on the M5nr database (`https://github.com/MG-RAST/myM5NR`) using the Diamond engine (Buchfink et al., 2015). To assess function of protein fragments, we retrieved predicted functions of best hits through Clusters of Orthologous Groups (COG) of proteins databases (Tatusov et al., 2000). There are three COGs levels ranging from general to more precise function. COG1 has 4 classification levels, COG2 level 22 classes, and COG3 level more than 20,324. The COG database is updated periodically as new genomes become available. A matrix of function abundance by samples was produced to analyze the diversity and composition profiles (see sections below) in R studio v1.1.447. (Team, 2018)

3.2.4. Alpha diversity

We first quantified alpha diversity of the gene functions for all samples with the Shannon index (Shannon, 1948), using the *phyloseq* package (McMurdie & Holmes, 2013) at COG2 and COG3 levels. The Shannon index, which includes both richness and evenness, was selected due to its reduced sensitivity to sample depth differences (Haegeman et al., 2013; Preheim, Perrotta, Friedman, et al., 2013a). We first transformed data to ensure normality with Tukey's ladder transformation (Tukey, 1977). Alpha diversity values were compared using linear models and linear mixed-effect models (lm and lme functions) in R, with Shannon diversity as the response variable, Pd status and time since infection at collection time as fixed effects, and site and collection years as a random effect. Significance was tested using a likelihood ratio test with a chi-square distribution for linear mixed-effect models (Pinheiro et al., 2017). Heating and collection methods (M1 and M2) were tested as fixed effects, because they could not be included as random variables. As they were not significant, both were discarded from subsequent alpha diversity analysis (Table S3.2).

3.2.5. Beta diversity

Microbiome data are compositional because they are relative. The total number of counts per sample is highly variable and constrained by the maximum number of sequence reads. This induces strong dependencies among feature abundances, as an increase of one feature implies the decrease of counts for another feature so that the total number of counts does not exceed the specified sequencing depth (Calle, 2019). Ignoring the compositional nature of microbiome data may lead to erroneous results. Consequently, we used the coherent Aitchison distance that respects the compositional properties of microbiome data (Aitchison, 1982; Aitchison et al., 2000; Gloor et al., 2017; Calle, 2019). The Aitchison distance is defined as the Euclidian distance after a centred-log transformation (clr). However, since microbiome data contain a high number of zeros, they should be corrected prior to the centred-log transformation to ensure validity of results. We used the function transform from the microbiome package to perform the clr transformation (Lahti & Shetty, 2017). This function applies a pseudocount before taking log results. Beta diversity was then visualized with principal component analysis (PCA) using the ordinate and plot ordinate function of the phyloseq package (McMurdie & Holmes, 2013).

To test for effects of Pd status and time since infection, we used a distance-based redundancy analysis (db-RDA) (Legendre & Anderson, 1999). This approach first decomposes distances into principal coordinates, and then applies RDA to the corresponding principal coordinates using the capscale function of the R package vegan (Oksanen et al., 2019). We also computed a partial db-RDA to better understand the influence of Pd status and time

since infection, while controlling for potential confounding factors (Davies & Tso, 1982). To select the constrained variables and to spare degrees of freedom, we performed first a db-RDA not controlled on potential confounding factors (i.e., sites, year of collection, collection method, heating) (Table S3.3) and only kept significant factors for further analysis. By doing so, sites and collection years were used to constrain the partial db-RDA at COG3, whereas only collection years was used at COG2 level. Significance was tested via 9999 permutations with the anova.cca function of the R package vegan. For all analyses. a p-value threshold of 0.05 was considered significant.

3.2.6. Skin metagenome composition profile

We assessed the effect of time since infection on the composition of microbial functions down to the COG3 level using the Analysis of Composition of Microbiomes (ANCOM 2.0) (Mandal et al., 2015). ANCOM is based on the analysis of difference in pairwise log-ratios of function abundance/relative abundance, between comparison groups of interest. It is appropriate for compositional data (Gloor et al., 2017), under the assumption that a minority of features ($< 25\%$) are differentially abundant (Mandal et al., 2015). This analysis does not ouput p-value. Instead for each function, we computed a W statistic indicating the number of significantly different pairwise log-ratios, while controlling for false discoveries. Significance level was set to 0.05 and multiple corrections were performed with the Benjamini-Hochberg procedure (Benjamini & Hochberg, 1995). ANCOM analysis was conducted on unrarefied COG3 level table of the more abundant functions ($>1\%$)

3.2.7. Bipartite graph analysis

We used a bipartite graph analysis to better explore the microbial functions without *a priori* group definition. A bipartite network is a collection of nodes, grouped in two separate sets, with no interactions among nodes within a set. In the present case, the bat samples were pooled by sites and year of collection to explore the relations with functional traits at COG3 level. We use the R package bipartite and bipartiteD3 to plot bipartite graphs and to compute modules that are aggregated sets of interacting components (Dormann et al., 2008; Terry, 2018). Their defining feature is that within-module interactions are more prevalent than between-module interactions (Newman, 2003; Newman & Girvan, 2004; Fortunato, 2010). In other words, modules are link-rich clusters of genes in a group. In addition, we chose to compute the species specificity index (Julliard et al., 2006; Poisot et al., 2012), that is, the coefficient of variation of interactions, normalized to values between 0 and 1 to target the most discriminant functions between modules. Values of 0 indicate low specificity, and those of 1 a high specificity. We performed the modules and species specificity index

computation on the most abundant (>1%) functions of the eight samples pooled by year and site (177 functions).

3.3. Results

3.3.1. Alpha diversity functional profile

The Pd status model at COG2 level was not significant (Table 3.2 and Fig. 3.1A), whereas time since infection model was significant (Table 3.2). Mean transformed Shannon diversity values decreased by 6% (854.463 ± 565.861) after the first year of infection and augmented by 6% (919.57 ± 576.92) after 10 years compared with pre-infection diversity (Fig. 3.1B). The model accounting for time since infection + Pd status was significant, but AIC and likelihood ratios were the same as time since infection models. No model was significant at COG3 level (Table 3.2).

Table 3.2. Linear mixed model effect of functional alpha diversity at COG2 and COG3 levels. Site and collection years as random effect.

Fixed effect	COG level	Null model AIC	Model AIC	Likelihood ratio	*P*-value
Pd status	COG2	266.12	267.84	0.29	0.59
	COG3	519.60	521.58	0.02	0.88
Time since infection	COG2	521.58	0.02	0.88	**0.04***
	COG3	519.60	523.54	0.06	0.97
Time since infection + Pd status	COG2	266.12	263.41	6.71	**0.04***
	COG3	519.60	523.54	0.05	0.97

Stars and bold indicate significant results. ***≤0.001. **≤0.01. *≤0.05.

3.3.2. Beta diversity functional profile

Clustering according to time since infection is not clearly defined for COG2 (Fig. 3.2A), but is much clearer for COG3 (Fig. 3.2B). Though, time since infection explained about 15% of the functional metagenome variation in db-RDA at COG2 level, whereas Pd status was not significant when collection years was partialled out (Table 3.3). Time since infection clusters is observable in the PCA at COG3 level, with a clear separation on the first principal axis that explained 27.4% of variation between bats infected for 10 years vs. bats infected for 1 year (Fig. 3.2B). However, according to the db-RDA, the confounding effect of sites was predominant and explained up to 9% of the functional metagenome variation (Table 3.4). These results indicate that time since infection is nested into the site factor effect, since without site, time since infection explained up to 7% of variation. Even when unconstrained by site, Pd status explained no redundant variation in the functional metagenome variation (Table 3.4).
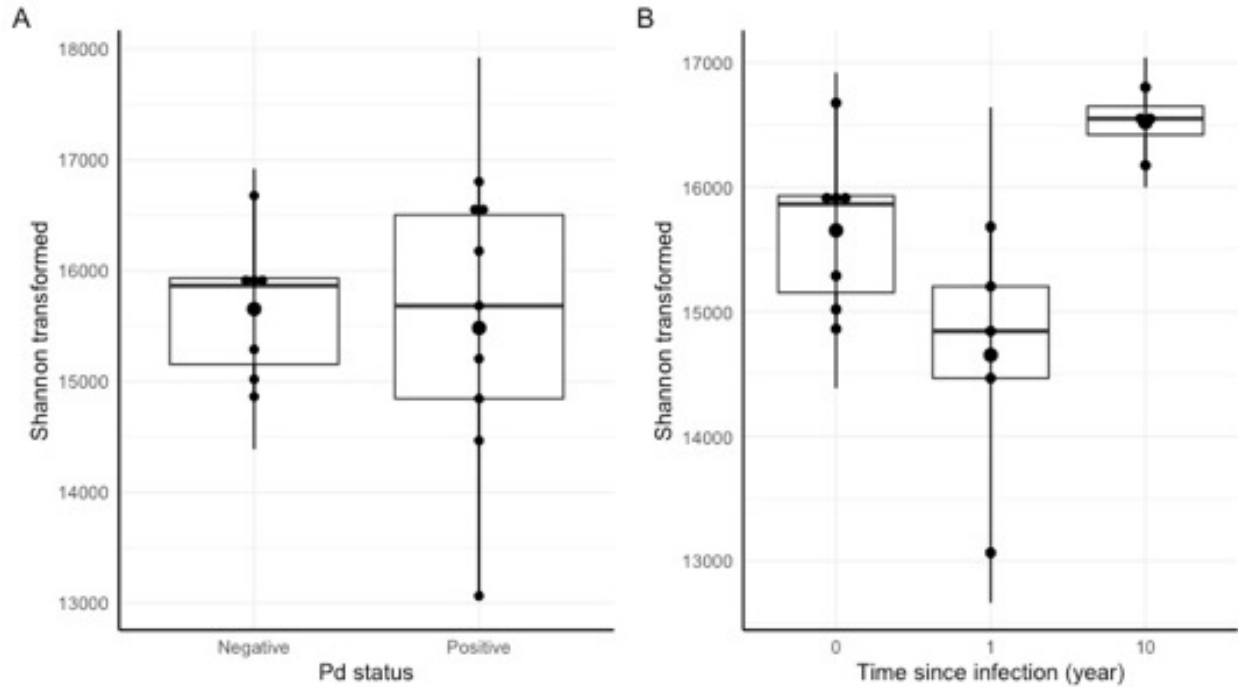
Fig. 3.1. Functional Shannon diversity of skin metagenome samples transformed at COG2 level according to (A) Pd status and (B) time since infection. All pairwise comparisons among years are significantly different in time since infection groups (Table 3.2).

Table 3.3. db-RDA model tests of Aitchison distance at COG2 level.

Model formula	F statistic	P-value	R^2 adjusted
~Pd status | collection years	1.25	0.30	NA
~time since infection | collection year	2.34	**0.03***	0.15
~Pd status + time since infection | collection years	2.34	**0.03***	0.15

Stars and bold indicate significant results. ***⩽0.001. **⩽0.01. *⩽0.05. COG2 total response matrix inertia = 3.5345.

Table 3.4. db-RDA model tests of Aitchison distance at COG3 level.

Model formula	F statistic	P-value	R^2 adjusted
∼Pd status | site, collection method, collection years	0	NA	NA
∼time since infection | site, collection method, collection years	0	NA	NA
∼Pd status + time since infection | site, collection method. collection years	0	NA	NA
∼site | collection method, collection years	1.54	**0.03***	0.09
∼Pd status | collection method, collection years	0	NA	NA
∼time since infection | collection method, collection years	2.11	**0.01****	0.07
∼Pd status + time since infection | collection method, collection years	2.11	**0.01****	0.07
∼time since infection + site | collection method, collection years	1.54	**0.03***	0.09

Stars and bold indicate significant results. ***⩽0.001. **⩽0.01. *⩽0.05. COG3 total response matrix inertia = 1641.0519.
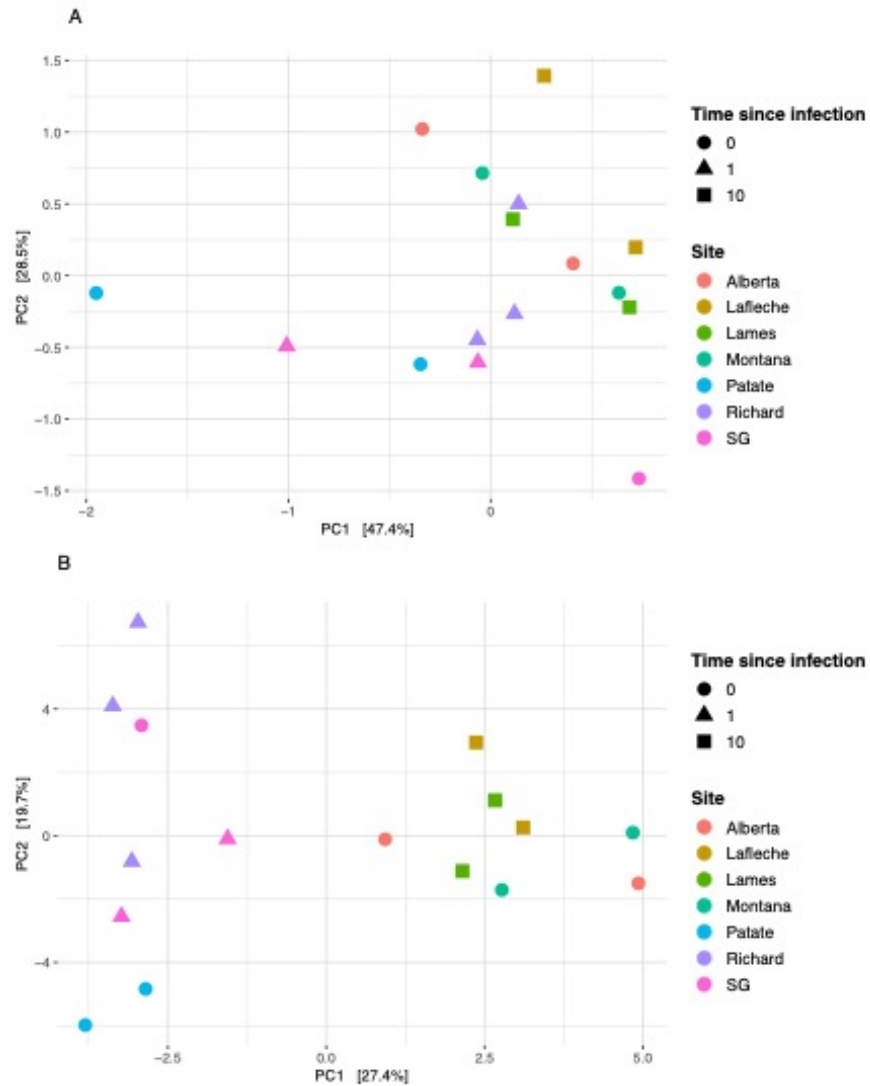
Fig. 3.2. Principal component analysis of Aitchison skin functional metagenome profile according to time since infection and sites for (A) COG2 level and (B) COG3 level. Each point represents a bat metagenome samples.

3.3.3. ANCOM on functional profile

We conducted the ANCOM analysis on the 332 more abundant COG3 functions representing more than 1% of total abundance on the 16 pooled samples. Eleven functions differed according to time since infection (Fig. 3.3 and Table S3.4). The 1-year since infection samples appeared to be the most distinct, with three functions differing from the not-infected group and ten functions differing from the 10-year group (Fig. 3.3). The 1-year group exhibited the lowest abundance for the *Outer membrane protein porin*, the *ABC type transport system involved in lipoprotein release permease component* and *Ribulose 5 phosphate 4 epimerase and related epimerases and aldolases*. The *Phospholipase C*, *Putative theorine efflux protein*, *High affinity Fe2 Pe2 permease*, *Mn2 and Fe2 transporter of the NRAMP family*, and *Transcriptional regulators* were significantly different between the 10-year group and one-year group for which abundance was the lowest. On the contrary, the functions *Asparagine synthase glutamine hydrolyzing* and *Type II restriction enzyme methylase subunits* had higher abundances in the 1-year group compared to the 10-year group (Fig. 3.3). The pre-infection group and 10-year group appeared to have similar function abundances, except for *A 4 amino 4 deoxy L arabinose transferase and related glycosyltransferases of PMT family* which exhibited larger functional abundances in the 10-year group (Fig. 3.3).
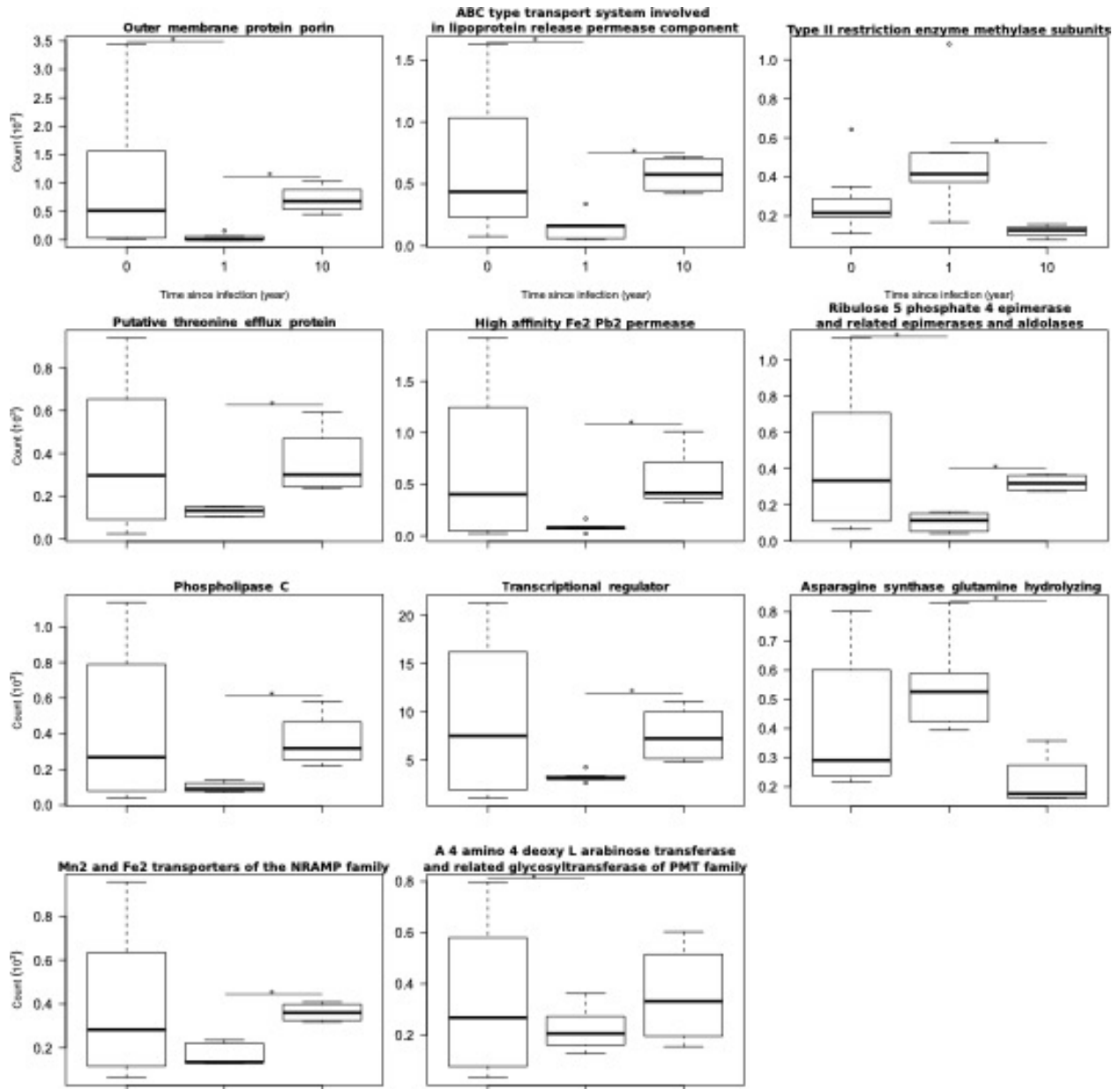
Fig. 3.3. Count abundance of functions detected as significantly divergent by ANCOM according to time since infection groups at 0.8 thresholds (Table S3.4 for W statistics). Stars indicate significant differences between corresponding groups.

3.3.4. Bipartite analysis

We explored the microbial functions without *a priori* group definition using a bipartite graph analysis on the metagenome samples pooled by sites and collection years at COG3 level. We performed the modules and species specificity index computation on the most abundant ($>1\%$) functions of the eight pooled samples (see Table S3.5 for modules and the ten functions with higher species specificity by module). Out of these 177 functions, the nine functions with higher species specificity index were considered as the most discriminant between modules (Fig. 3.4).

The first module clusters Pd-negative bats collected from Patate with the 1-year infected bats from SG19 (Fig. 3.4) and is characterized by 71 functions (see Table S3.5). Among the nine more discriminant functions, three belong to this module including *ATP dependent Lon protease bacterial type*, *Arylsulfatase A and related enzymes*, *Type I site specific restriction modification system R restriction subunit and related helicases* (Fig. 3.4). Pd-negative bats from site SG16 are part of a second module associated with 33 functions (Table S3.5) including two among the nine more discriminant functions: *Catalase Outer membrane receptor proteins mostly Fe transport* (Fig. 3.4). The 1-year infected bats from the Richard site are forming a third module characterized by 25 functions (Table S3.5 and Fig. 3.4). The last module clusters Pd-negative bats collected from sites Montana and Alberta with 10-year surviving colonies collected at sites Lames and Lafleche. These four sites together are characterized by 42 functions (Table S3.5), including four among the nine most discriminant functions: *High affinity Fe2 Pb2 permease*, *Transposase and inactivated derivatives TnpA family*, *Outer membrane protein porin* and *ABC type transport system involved in lipoprotein release permease component* (Fig 3.4).
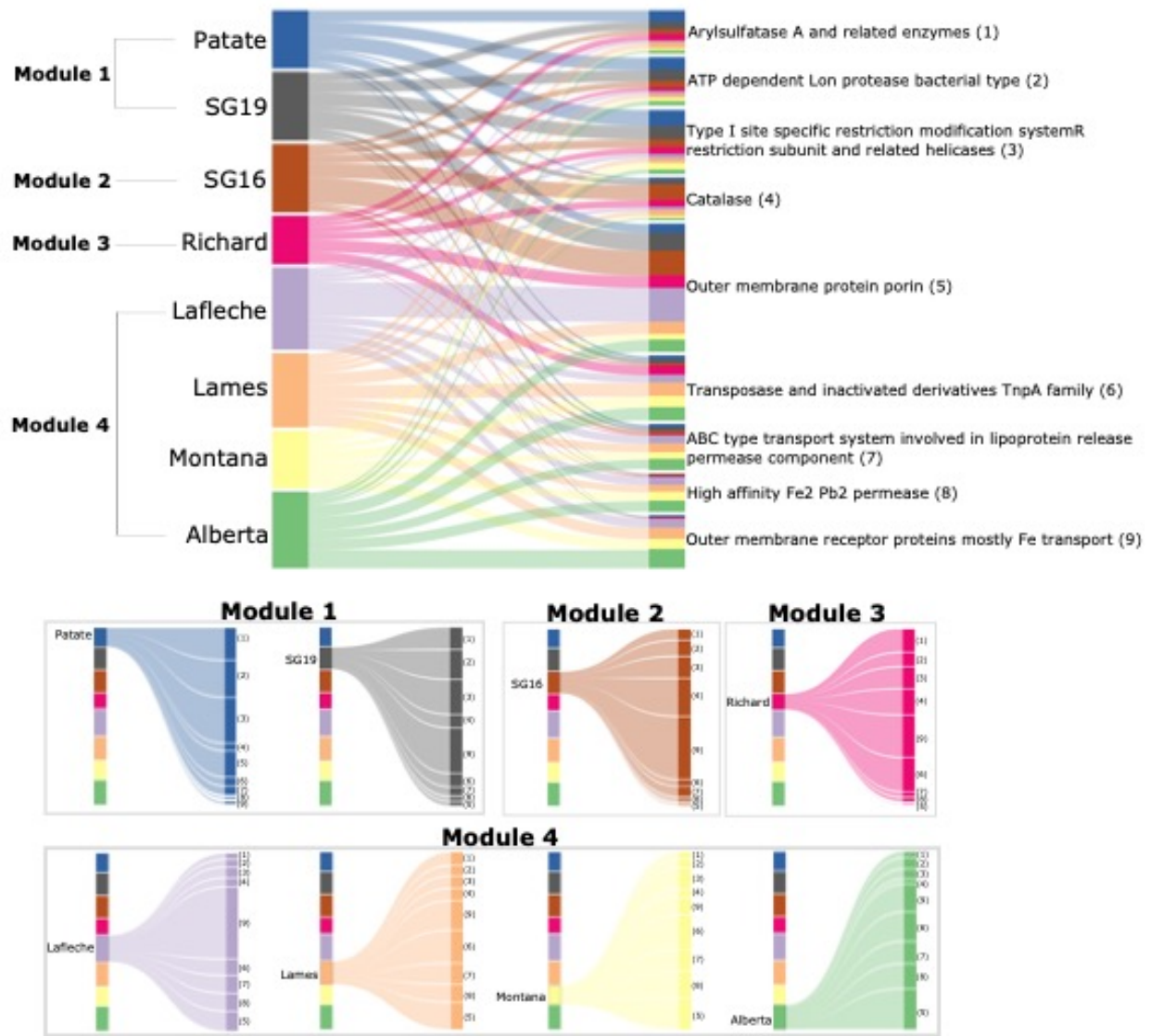
Fig. 3.4. Bipartite graph associating samples pooled by sites and collection years with the more abundant functions at COG3 level (>1%). Only the nine functions with the higher species specificity index are presented (see Table S3.5). The four different modules identified in the complete bipartite graph are highlighted to illustrate the relationships with the corresponding functions. Wider links are indicative of relatively more abundant functions in a sample.

3.4. Discussion

In this study, we revealed the functional potential of the skin microbiome of hibernating little brown bat colonies affected and not affected by Pd using shotgun metagenomics. Our objectives were to establish the effect of the infection and time since infection on the functional metagenome and detect discriminant functions in bat skin microbiome samples to decipher how the microbiome could potentially influence or be influenced by WNS.

We discovered that the functional metagenome structure of bat colonies was affected by the Pd infection in the first year of infection but largely recovers after 10 years. Indeed, we observed an effect of Pd on metagenome beta diversity after 1 year, but not after 10 years. Previous studies have shown a loss of alpha diversity in bats just infected by Pd (Ange-Stark et al., 2019; Grisnik et al., 2020), but ten years persisting Pd-positive bat colonies regained diversity at higher levels than pre-infected bats. This could indicate an enrichment in new functions allowing to face the disease. Yet, this trend was only observable at higher functional level (COG2) and will need further study to be elucidated in WNS context. Consistently, with respect to our first hypothesis, we found no support that Pd status influences the metagenome structure. As such, our results are in agreement with Grisnik et al. (2020) who revealed considerable functional redundancy among Pd-positive and Pd-negative specimens, although for a different species of bat (*P. subflavus*). Interestingly, a significant difference in functional profiles was observed by comparing the beta diversity of 10-year infected and 1-year infected bat colonies, and this structural pattern could be representative of selection for a particular functional profile allowing facing the disease or a return to a normal state. The functional evidence that skin microbiome appears to be mostly disturbed just after infection is consistent with overall mortality patterns that are peaking in the first years following Pd infection (Langwig et al., 2017).

Consistently with community structural results, we detected change in predominant function abundances following the first year of infection, but the 10-year group appeared to return to compositional abundance similar to that of uninfected bats. The predominant functions detected are part of various biological processes, such as molecular function or cellular component (UniProt, 2019). Interestingly, some functions detected are involved in iron (Fe2+) and manganese (Mn2+) acquisition and transport (*Mn2+ and Fe2+ transporter of the NRAMP family-like protein*, *High affinity Fe2 Pb2 permease* and *Outer membrane receptor proteins mostly Fe* (UniProt, 2019). Iron and manganese are essential metals that play a central role in infection processes because they serve as cofactors in a multitude of reactions, including many with direct and indirect roles in virulence (Gerwien et al., 2018). Hosts can also fight pathogens by deploying toxic levels of certain metals (Hood

& Skaar, 2012). Then, upregulation or downregulation of function influencing Fe2+ and Mn2+ bioavailability could influence Pd invasion (S. M. Reeder et al., 2017; Gerwien et al., 2018). Our results do not indicate a clear trend of upregulation or downregulation, but higher abundances of such functions were observed in bat colonies not infected as well as in persisting bat colonies. In the persisting group, these functions could help by competing for nutrients with the fungus (Gerwien et al., 2018), and this is consistent with our second hypothesis postulating that gene functions associated with antifungal properties or fungus competition will be more prevalent in bats surviving WNS. We also detected that *Phospholipases C* was more abundant in surviving bats compared with just infected bats. These phospholipases could be toxic can cause cell lysis in eukaryotes (Titball, 1993), and thus may potentially reduce fungal invasion. However, as these functions are in low abundance in just infected colonies, this is also consistent with the hypothesis of disruption by the fungus causing drop in these functions and potentially negatives effect on microbiome and bats health that must be further investigated.

This study provides evidence of important change in gene profile following disease infection, but these changes could be site-specific (colony-specific). Indeed, we observed that some Pd-negative sites were more similar to 1-year infected sites than to Pd-positive sites with surviving bats. As the skin microbiome varies between sites (Avena et al., 2016; Lemieux-Labonté et al., 2017; Ange-Stark et al., 2019), we could expect site-specific selection under such pathogen pressure. It is also expected that bats will resist or tolerate WNS by site-specific or colony-specific mechanisms (e.g. physiological, behavioural, etc.) (Langwig et al., 2017). Although our results do not directly support the protective role of the skin microbiome against WNS, there is a possibility that the metagenome may act synergistically with other mechanisms and help prevent Pd infection. Also, we must stress that shotgun metagenomics is only informing on the functional potential of putative COGs, and not on what is truly expressed by the corresponding genes (Jansson & Hofmockel, 2018).

We are aware that the sampling of hibernation colonies sites with and without WNS at different time points represent an important confounding factor, and that having longitudinal data for multiple sites would increase the explanatory power to unravel the microbiome influence and potential to fight this disease. Yet, we were able to control for confounding effects such as sites, collection years and collection method in our analysis and have shown a significant effect of Pd with time since infection. We believe that our study presents an important step to understand the role of the functional metagenome in wild bat colonies facing an emergent fungal pathogen. Overall, our results reveal that functional metagenome profiles vary greatly just after Pd invasion, and that such diversified response could impact individual fitness. Our analysis also suggests a return to a stable state in persisting bat

colonies infected for 10 years. It is still unclear whether the skin microbiome could offer protection against Pd, or simply be affected by the disease. Future studies using combined metaomics approaches and considering other resistance and tolerance mechanisms such as environmental selection and physiological adaptation will be key to untangle the microbiome role and influence in the WNS context.

3.5. Availability of data and materials

The datasets supporting the conclusions of this article will be available upon publication

3.6. Acknowledgements

3.7. Supplementary files

Table S3.1. Illumina NovaSeq 6000 S4 PE150 Sequencing Shotgun library information by sample.

SampleID	Number of Reads	Number of Bases	Number of Cycles	Average Quality
RL18pool1	26803053	8094522006	318	36
RL18pool2	22446671	6778894642	318	36
Albpool1	20252019	6116109738	318	36
Albpool3	15632117	4720899334	318	36
Lafpool2	22901019	6916107738	318	36
Lafpool3	22592508	6822937416	318	35
Lamespool2	21542918	6505961236	318	35
Lamespool3	16787323	5069771546	318	35
Mont1pool1	25210427	7613548954	318	36
Montpool3	17196312	5193286224	318	36
Patpool1	19772503	5971295906	318	36
Patpool3	7824715	2363063930	318	36
RL18pool3	19740865	5961741230	318	36
SG163pool	15407384	4653029968	318	36
SG192pool	23710558	7160588516	318	36
SG19pool1	22893338	6913788076	318	35

Table S3.2. Linear mixed model of bat skin functional alpha diversity at COG2 level and COG3 levels.

COG level	Model formula	Null model AIC	Model AIC	Likelihood ratio	*P*-value
COG2	~collection method | site, collection years	266.12	267.33	0.79	0.37
	~heated | site, collection years	266.12	268.04	0.08	0.78
COG3	~collection method | site, collection years	519.60	521.59	0.02	0.90
	~heated | site, collection years	519.60	520.26	1.34	0.25

Stars and bold indicate significant results. ***≤0.001. **≤0.01. *≤0.05.

Table S3.3. Db-RDA of bat skin functional Aitchison distance at COG2 and COG3 levels for potential controlled factor. Only the significant factors are added to models in Tables 3.3 and 3.4

Model formula	COG level	*F* statistic	*P*-value	R^2 adjusted
~collection method	COG2	0.89	0.46	NA
	COG3	2.20	**0.02***	0.074
~heated	COG2	0.39	0.81	NA
	COG3	1.62	0.07	NA
~site	COG2	1.62	0.09	NA
	COG3	2.35	**1e-04***	0.35
~collection years	COG2	2.22	**0.05***	0.20
	COG3	1.60	**0.02***	0.11

Stars and bold indicate significant results. ***≤0.001. **≤0.01. *≤0.05. COG2 total response matrix inertia = 3.5345. COG3 total response matrix inertia = 1641.0519.

Table S3.4. ANCOM W statistic results of abundant COG3 function while adjusting for sites, collection years, heated, and collection method, for times since infection group. Only significant differently abundant function at threshold 0.8 are presented.

Pairwise comparison	Functions COG3	W stat
1-year vs. 10-year	Outer membrane protein porin	332
	ABC type transport system involved in lipoprotein release permease component	323
	Ribulose 5 phosphate 4 epimerase and related epimerases and aldolases	312
	Phospholipase C	297
	Putative threonine efflux protein	293
	High affinity Fe2 Pb2 permease	287
	Asparagine synthase glutamine hydrolyzing	280
	Mn2 and Fe2 transporters of the NRAMP family	278
	Type II restriction enzyme methylase subunits	275
	Transcriptional regulator	269
0-year vs. 1-year	Outer membrane protein porin	332
	ABC type transport system involved in lipoprotein release permease component	322
	Ribulose 5 phosphate 4 epimerase and related epimerases and aldolases	315
0-year vs. 10-year	A 4 amino 4 deoxy L arabinose transferase and related glycosyltransferases of PMT family	278

Table S3.5. Module list and Species specificity index of COG3 functional genes on most abundant predicted genes (>1%). The ten functions with the highest Species specificity index are presented for each module.

Module	COG3 functions	Species specificity
Module 1	ATP dependent Lon protease bacterial type	0.23
	Arylsulfatase A and related enzymes	0.22
	Type I site specific restriction modification system R restriction subunit and related helicases	0.20
	Inorganic pyrophosphatase	0.18
	Response regulator containing CheY like receiver AAA type ATPase and DNA binding domains	0.16
	Transposase and inactivated derivatives	0.15
	Asparagine synthase glutamine hydrolyzing	0.15
	Mismatch repair ATPase MutS family	0.14
	Type I restriction modification system methyltransferase subunit	0.14
	DNA directed RNA polymerase sigma subunit sigma70 sigma32	0.13
Module 2	Catalase	0.29
	Outer membrane receptor proteins mostly Fe transport	0.21
	Subtilisin like serine proteases	0.18
	Large extracellular alpha helical protein	0.16
	A 1 4 alpha glucan branching enzyme	0.16
	Long chain acyl CoA synthetases AMP forming	0.16
	ABC type sugar transport systems permease components	0.15
	Predicted metal dependent hydrolase with the TIM barrel fold	0.15
	Lhr like helicases	0.14
	Predicted dehydrogenases and related proteins	0.13
Module 3	ABC type transport system involved in resistance to organic solvents periplasmic component	0.16
	ABC type sugar transport system permease component	0.15
	Site specific recombinases DNA invertase Pin homologs	0.14
	Cysteine synthase	0.11
	Acyl dehydratase	0.11
	DNA segregation ATPase FtsK SpoIIIE and related proteins	0.09
	HrpA like helicases	0.09
	Superfamily I DNA and RNA helicases	0.09
	ABC type sugar transport system periplasmic component	0.07
	Phosphomannomutase	0.07
Module 4	Outer membrane protein porin	0.37
	High affinity Fe2 Pb2 permease	0.31
	Transposase and inactivated derivatives TnpA family	0.20
	ABC type transport system involved in lipoprotein release permease component	0.20
	Arabinose efflux permease	0.19
	ABC type uncharacterized transport system permease component	0.18
	Transcriptional regulators	0.18
	RecB family exonuclease	0.16
	ABC type nitrate sulfonate bicarbonate transport systems periplasmic components	0.16
	Membrane fusion protein	0.16

Conclusion

4.0. Impacts du microbiome sur le syndrome du museau blanc

Cette thèse a permis l'acquisition de connaissances fondamentales sur le microbiome cutané des chiroptères, dans une optique de compréhension d'une maladie fongique de la faune. Nos résultats suggèrent que le microbiome peut agir comme protection, mais qu'il serait aussi probablement affecté par l'infection. La thèse met également de l'avant les différences entre les analyses basées sur la taxonomie et celles basées sur les fonctions du microbiome des chauves-souris.

Le **Chapitre 1** a permis de caractériser pour la première fois le microbiote cutané de la petite chauve-souris brune (*M. lucifugus*) en période d'hibernation. Nous avons découvert que ce microbiote cutané demeurait différent du microbiote de l'environnement en termes d'abondance et de diversité. De plus, nous avons détecté une influence importante du site d'échantillonnage sur la composition du microbiote. La comparaison des communautés microbiennes de chauves-souris survivantes et non affectées par le SMB a démontré une baisse de la diversité chez les survivantes (Fig. 0.5). En accord avec l'hypothèse de la sélection des microorganismes antifongiques, nous avons observé que ces taxons étaient plus abondants chez les chauves-souris survivantes (Fig. 0.5). L'enrichissement de ces microorganismes potentiellement bénéfiques dans le microbiote cutané prélevé dans des hibernacles infectés par le champignon Pd est une découverte encourageante pour le rétablissement des populations de chauves-souris affectées par le SMB. Ces résultats révèlent aussi le potentiel des mesures de gestion qui pourraient encourager la transmission, la croissance et l'établissement de taxons bactériens bénéfiques sur les chauves-souris et dans les hibernacles. Cependant, nos résultats mettent également en évidence les risques associés à certaines mesures de gestion. Notamment, les traitements chimiques qui perturbent le microbiote cutané ou atténuent la sélection d'une communauté de microbes bénéfiques pourraient causer plus de tort que de bien pour le rétablissement des populations de chauves-souris et la résistance à long terme au SMB. Ainsi, il faudrait confirmer le potentiel sélectif de tout

traitement potentiel et vérifier qu'il a des impacts minimes sur le microbiote des chauves-souris et des hibernacles avant de l'appliquer en nature. Afin de contrôler l'effet confondant de la localisation (site) et de mieux cerner l'effet du champignon sur le microbiote, il faudrait dans le futur analyser le microbiote à un même hibernacle avant et après infection ainsi que suivre l'évolution du microbiote sur plusieurs années, et ce pour plusieurs sites.

Le **Chapitre 2** a permis d'étudier la réponse du microbiote de la grande chauve-souris brune (*E. fuscus*) suite à l'infection au Pd en milieu contrôlé. Cette étude a permis d'établir que le microbiote reste globalement stable malgré l'infection et que des taxons antifongiques composent en majorité la communauté microbienne de cette espèce (Fig. 0.5). Ces conclusions sont cohérentes avec l'hypothèse de résistance via le microbiote. Cependant, nos résultats indiquent que l'inoculation par Pd a réduit la capacité de l'hôte (ou de son microbiote) à réguler le microbiote cutané, entraînant une plus grande variation dans le temps chez les individus infectés. Il faudrait dans le futur cibler l'effet de ce changement sur la valeur adaptative de l'espèce. De plus, il faudrait analyser le potentiel fonctionnel du microbiome afin de cibler les mécanismes qui peuvent contribuer à la résistance. Une étude en milieu naturel serait nécessaire afin de voir si le microbiote/microbiome de cette espèce répond à l'infection en hibernacle comme en milieu contrôlé. Étudier *E. fuscus*, une espèce peu affectée par le SMB, est essentiel afin de mieux comprendre les potentiels mécanismes de défense contre le champignon via le microbiome.

Le **Chapitre 3** a permis d'évaluer les fonctions du microbiome cutané (métagénome fonctionnel) de *M. lucifugus* en contexte de SMB à l'aide de la métagénomique, une approche à plus haute résolution que le séquençage d'amplicons pour observer le potentiel du microbiome. L'étude a permis d'établir l'effet du temps depuis l'infection sur le métagénome fonctionnel. Les chauves-souris dans leur première année d'infection ont un métagénome fonctionnel altéré, mais celui-ci revient à une structure et composition similaire à celle d'avant infection après 10 ans (Fig 0.5). Certaines fonctions détectées suite à l'infection sont associées à des gènes reliés au transport et à l'assimilation de métaux, des facteurs limitants pour la croissance du champignon. Ces gènes pourraient donc avoir un rôle à jouer dans la résistance à l'infection. Or, le métagénome fonctionnel indique plutôt une vulnérabilité au champignon et non une résistance qui se développe suite à la pression sélective du Pd, contrairement aux résultats du chapitre 1. La capacité fonctionnelle n'est toutefois qu'un indice des fonctions traduites dans le microbiome, ce qu'une approche métatranscriptomique permettrait de confirmer. Dans les premières années qui suivent l'infection, il serait utile d'assurer le suivi d'un site afin de voir l'évolution temporelle du métagénome fonctionnel. Un moyen efficace de tester les effets du champignon serait d'infecter des chauves-souris et de les faire hiberner en conditions contrôlées afin de récolter des échantillons longitudinaux

pour suivre la progression de la maladie et l'état de santé de l'hôte. Cette approche permettrait de cibler plus précisément les fonctions du métagénome qui pourraient intéragir avec la maladie.
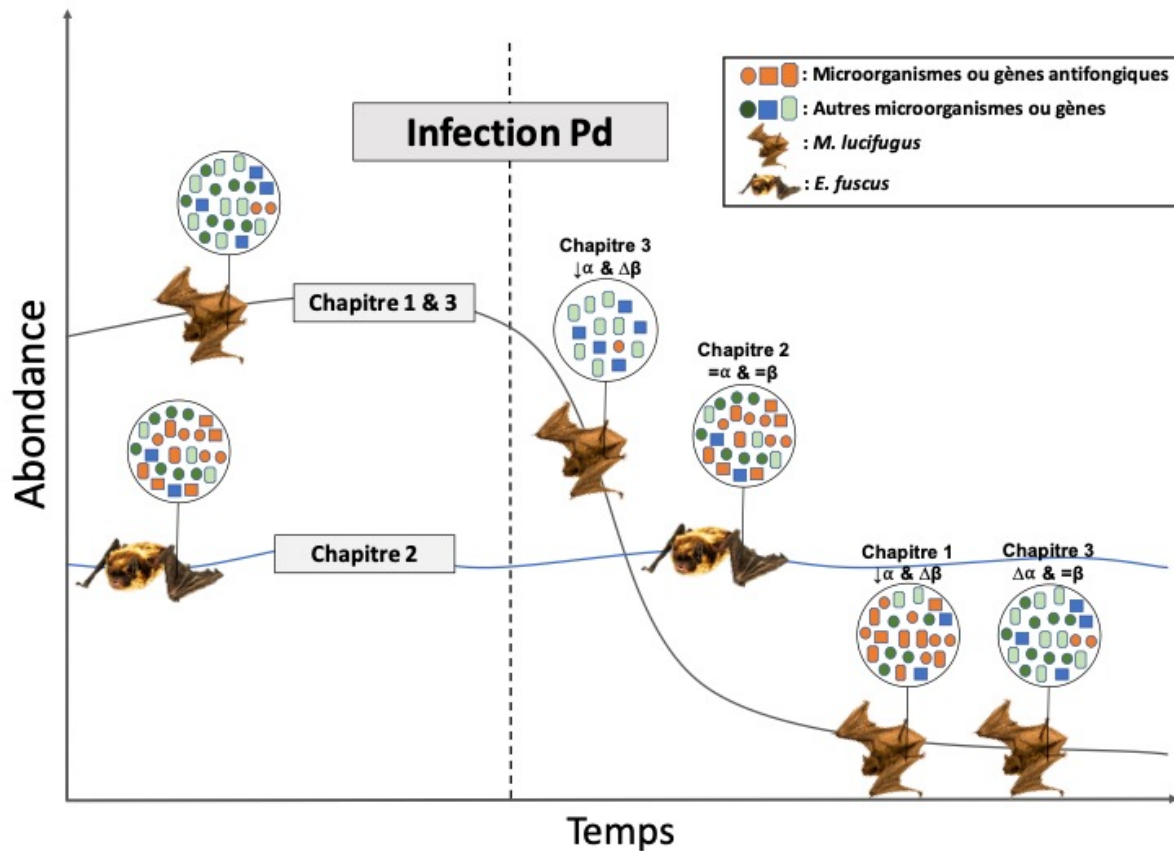
Fig. 4.1. Cadre conceptuel de la thèse et schématisation des résultats. Le chapitres 1 démontre une baisse de diversité et un enrichissement en taxon antifongique dans le microbiote de *M. lucifugus* survivantes au SMB. Le chapitre 2 démontre que le microbiote de *E. fuscus* demeure stable face à l'infection par Pd et que les taxons au potentiel antifongique sont abondants. Le chapitre 3 démontre un changement du métagénome fonctionnel suite à l'infection par Pd chez *M. lucifugus*, mais celui-ci revient à un état d'avant infection après plusieurs années.

4.1. Microbiome et conservation des chiroptères

Une des contributions majeures de cette thèse est d'avoir révélé le potentiel du microbiome pour lutter contre le champignon responsable du SMB. Cependant, comment appliquer les connaissances acquises afin de rechercher des solutions au SMB? Nous suggérons tout d'abord d'inclure le microbiome dans l'étude de traitements expérimentaux

afin d'établir les effets du champignon sur le microbiome et d'évaluer les conséquences pour la santé de l'hôte. De cette façon, il sera possible de minimiser les effets néfastes d'un traitement qui serait appliqué à grande échelle. Il est aussi important de considérer des approches site-spécifiques dans la lutte contre le SMB. Puisque le microbiome varie fortement d'un site à l'autre, les chauves-souris retrouvées dans différents hibernacles peuvent avoir développé différents mécanismes de résistance via le microbiome.

Cette thèse a permis d'établir les bases de l'étude du microbiome chez les chauves-souris nord-américaines, mais il reste encore beaucoup à découvrir. Grâce aux recherches des dernières années, nous savons que le microbiome est un vecteur de protection ou de vulnérabilité potentielle. Il est donc essentiel d'établir les conséquences de son débalancement pour son hôte, telles qu'une susceptibilité accrue à d'autres infections ou même une aggravation des lésions liées au Pd. Dans les applications futures en conservation, la construction d'indices de santé du microbiome pour les espèces menacées pourrait aider à identifier les changements de la communauté microbienne qui peuvent entraîner la vulnérabilité de l'hôte. Cibler des cas spécifiques de dysbiose qui exacerbent la maladie lors d'une infection par un pathogène pourrait également permettre l'identification de biomarqueurs de la maladie afin d'aider à la protection de certaines populations plus sensibles.

Bien entendu, l'utilisation de méthodes de pointe telles que la métatranscriptomique et la métabolomique pourrait faciliter l'étude simultanée des composés produits par le microbiome, l'hôte et le champignon. Il serait ainsi plus facile d'élucider les interactions microbiome-pathogène-hôte et cela contribuerait grandement à la compréhension de l'infection. Ce genre d'étude effectuée en nature repose néanmoins sur un suivi à long terme des populations infectées et non infectées ainsi que sur des expériences en laboratoire afin de cerner tous les facteurs impliqués dans la tolérance et la résistance à la maladie.

Il est essentiel d'adapter les façons dont nous abordons la protection des espèces et de leurs microbiomes (West et al., 2019). Nous souhaitons que les travaux de cette thèse permettent de sensibiliser les acteurs de la conservation à l'existence et à l'importance du microbiome pour son hôte. Nous souhaitons également que cette thèse serve de tremplin pour l'étude du microbiome chez les chauves-souris et tout autre organisme faisant face à une maladie émergente dans le futur. L'étude du microbiome de la faune en est à ces débuts et beaucoup de questions restent encore à élucider. Il faudra dans le futur investir des ressources additionnelles pour pouvoir utiliser cette technologie à son plein potentiel à des fins de conservation.

4.1. Les défis des études sur le microbiome

La baisse des coûts du séquençage de nouvelle génération depuis les dernières décennies a permis un accès universel au matériel génétique des communautés microbiennes et de ce fait, a favoriser l'étude des microorganismes non cultivables (van Dijk et al., 2014). Le séquençage à haut débit a permis d'accroitre notamment les connaissances sur le microbiome des chauves-souris. Cependant, cette méthode comporte des limites qui peuvent, dans certains cas, remettre en cause l'exactitude des résultats (Brooks et al., 2015).

La majorité des études sur le microbiome utilisent le séquençage d'amplicons qui consiste à extraire, amplifier et séquencer de courts fragments d'ADN en copie unique, qui se retrouvent entre des régions conservées du génome. Ces marqueurs génétiques se veulent universels, c'est-à-dire qu'ils doivent se retrouver dans une grande diversité de microorganismes tout en étant assez variables pour les discerner les uns des autres (Dahllöf et al., 2000; Soergel et al., 2012). En réalité, un marqueur totalement universel et discriminant n'existe pas, car on peut observer de la variation au sein d'un même marqueur dépendamment de la région sélectionnée (Yang et al., 2016). De même, des biais d'amplification peuvent être introduits par la PCR au moment de générer les amplicons. On sait que l'ADN de certains microorganismes est plus facile à extraire et à amplifier (lyse plus facile des cellules, meilleure efficacité des amorces, Gram négatif, contenu GC) (Feinstein et al., 2009; Pinto & Raskin, 2012; Gohl et al., 2016). Par conséquent, certains taxons seront sur- ou sous-représentés lors de la construction des librairies (Brooks et al., 2015). En dépit de ces limites, le séquençage d'amplicons demeure un outil accessible, efficace et abordable afin d'explorer les communautés du microbiome dans une grande variété de contexte.

D'autres approches de métaomique sont disponibles afin d'étudier les communautés microbiennes en profondeur. Alors que la métagenomique s'intéresse au séquençage des gènes (ADN), la métatranscriptomique détermine ce qui est transcrit (ARN), la métaprotéomique identifie les protéines et la métabolomique caractérise les métabolites présents (Wilmes & Bond, 2006; Turnbaugh & Gordon, 2008; Franzosa et al., 2015). Ces techniques permettent l'étude complète et simultanée de l'ensemble du microbiome (bactéries, archée, virus, et eucaryotes) (Norman et al., 2014), mais elles sont cependant très lourdes en termes de ressources techniques, financières et computationnelles. Notamment, la quantité d'ADN disponible dans nos frottis de peau était insuffisante et nous avons dû faire des « pools » d'échantillons afin d'effectuer le séquençage du métagénome. De plus, les ressources informatiques requises pour l'analyse de ces données métagénomiques ont exigé que nous utilisions des serveurs externes en temps partagé, ce qui limitait grandement l'effectif de notre étude. En raison de ces contraintes, le nombre d'échantillons des analyses

métagénomiques est souvent beaucoup plus faible que les études basées sur le séquençage d'amplicons.

Or, le séquençage d'amplicons, de même que la métagénomique, possèdent des limites communes. Les banques de données utilisées pour l'identification des taxons ou l'annotation fonctionnelle des gènes sont basées sur l'accumulation des connaissances actuelles qui ne sont pas toujours représentatives de la communauté étudiée. Ces bases de données sont souvent biaisées en faveur des microorganismes ou des environnements les plus étudiés (par exemple, les microbes d'intérêt médical ou les taxons du microbiome humain). Dès lors, il n'est pas rare d'obtenir des assignations taxonomiques et fonctionnelles erronées ou impossibles lorsqu'on s'intéresse au microbiome d'organismes rarement étudiés, tels que les chauves-souris. Le choix de la banque de données est tout aussi important, car celle-ci influence directement les assignations possibles (Balvočiūtė and Huson, 2017). Parce qu'une grande proportion de fonctions et de taxons demeure encore inconnue, il est important d'utiliser les banques de données les plus à jour, ce que nous avons fait dans le cadre de cette thèse.

Un autre enjeu à considérer lors de l'analyse du microbiome est la contamination potentielle des échantillons. En effet, il est pratiquement impossible d'assurer l'absence de contamination considérant que de l'ADN de plusieurs microorganismes contamine déjà les kits d'extraction (Salter et al., 2014). L'effet de cette contamination est encore plus important pour les échantillons ayant une faible biomasse, par exemple les frottis de peau (Salter et al., 2014). Nous avons pris soin de minimiser les effets de la contamination en ajoutant des contrôles négatifs et positifs lors de l'extraction et l'amplification de nos échantillons.

Bien qu'il existe encore plusieurs limites techniques et méthodologiques, l'étude du microbiome a fait des progrès importants au cours de la dernière décennie. Le nombre de nouveaux algorithmes développés par la communauté scientifique atteste de l'intérêt grandissant des recherches sur le microbiome et du désir profond d'interpréter les résultats à leur juste valeur. De nouvelles méthodes qui tiennent compte de la nature compositionnelle des communautés microbiennes ont été mises de l'avant récemment (Gloor et al., 2017). Afin de gagner en précision et répétabilité, les «Amplicon sequence variant» (ASV) ont été proposés pour remplacer les OTUs (Callahan et al., 2017). L'organisation de la thèse illustre l'évolution des approches méthodologiques de 2015 (Chapitre 1) à 2020 (Chapitre 3). Elle démontre que l'étude du microbiome évolue rapidement et qu'elle vise toujours à se perfectionner.

Références bibliographiques

Aitchison, J. (1982). The statistical analysis of compositional data. *Journal of the Royal Statistical Society: Series B (Methodological)*, *44*(2).

Aitchison, J., Barceló-Vidal, C., Martín-Fernández, J. A., & Pawlowsky-Glahn, V. (2000). Logratio analysis and compositional distance. *Mathematical Geology*, *32*(3).

Albesa, I., Barberis, L. I., Pàjaro, M. C., & Eraso, A. J. (1985). Pyoverdine production by *Pseudomonas fluorescens* in synthetic media with various sources of nitrogen. *Microbiology*, *131*(12), 3251–3254.

Allender, M. C., Dreslik, M., Wylie, S., Phillips, C., Wylie, D. B., Maddox, C., . . . Kinsel, M. J. (2011). *Chrysosporium* sp. infection in eastern massasauga rattlesnakes. *Emerging Infectious Diseases*, *17*(12), 2383.

Allender, M. C., Raudabaugh, D. B., Gleason, F. H., & Miller, A. N. (2015). The natural history, ecology, and epidemiology of *Ophidiomyces ophiodiicola* and its potential impact on free-ranging snake populations. *Fungal Ecology*, *17*, 187–196.

Almlab. (2015). Almlab/SmileTrain. *https://github.com/almlab/SmileTrain*.

Anderson, M. J. (2001, February). A new method for non-parametric multivariate analysis of variance: non-parametric manova for ecology. *Austral Ecology*, *26*(1), 32–46. Retrieved 2020-01-17, from `http://doi.wiley.com/10.1111/j.1442-9993.2001.01070.pp.x` doi: 10.1111/j.1442-9993.2001.01070.pp.x

Anderson, M. J. (2006, March). Distance-Based Tests for Homogeneity of Multivariate Dispersions. *Biometrics*, *62*(1), 245–253. Retrieved 2020-01-17, from `http://doi.wiley.com/10.1111/j.1541-0420.2005.00440.x` doi: 10.1111/j.1541-0420.2005.00440.x

Ange-Stark, M. A., Cheng, T. L., Hoyt, J. R., Langwig, K. E., Parise, K. L., Frick, W. F., . . . Foster, J. T. (2019). White-nose syndrome restructures bat skin microbiomes. *BioRxiv*, 614842.

Antony-Babu, S., Stien, D., Eparvier, V., Parrot, D., Tomasi, S., & Suzuki, M. T. (2017). Multiple Streptomyces species with distinct secondary metabolomes have identical 16S rRNA gene sequences. *Scientific Reports*, *7*(1), 1–8.

Auteri, G. G., & Knowles, L. L. (2020). Decimated little brown bats show potential for adaptive change. *Scientific Reports*, *10*(1), 1–10.

Avena, C. V., Parfrey, L. W., Leff, J. W., Archer, H. M., Frick, W. F., Langwig, K. E., . . . McKenzie, V. J. (2016, November). Deconstructing the bat skin microbiome: influences of the host and the environment. *Frontiers in Microbiology*, *7*. Retrieved 2020-01-24, from `http://journal.frontiersin.org/article/10.3389/fmicb.2016.01753/full`   doi: 10.3389/fmicb.2016.01753

Bahrndorff, S., Alemu, T., Alemneh, T., & Lund Nielsen, J. (2016). The microbiome of animals: implications for conservation biology. *International Journal of Genomics*, *2016*.

Ballmann, A. E., Torkelson, M. R., Bohuski, E. A., Russell, R. E., & Blehert, D. S. (2017). Dispersal hazards of *Pseudogymnoascus destructans* by bats and human activity at hibernacula in summer. *Journal of Wildlife Diseases*, *53*(4), 725–735.

Baron, S. S., & Rowe, J. J. (1981, December). Antibiotic action of pyocyanin. *Antimicrobial Agents and Chemotherapy*, *20*(6), 814–820. Retrieved 2020-01-17, from `http://aac.asm.org/cgi/doi/10.1128/AAC.20.6.814`   doi: 10.1128/AAC.20.6.814

Bataille, A., Lee-Cruz, L., Tripathi, B., Kim, H., & Waldman, B. (2016, January). Microbiome variation across amphibian skin regions: implications for chytridiomycosis mitigation efforts. *Microbial Ecology*, *71*(1), 221–232. Retrieved 2020-01-17, from `http://link.springer.com/10.1007/s00248-015-0653-0`   doi: 10.1007/s00248-015-0653-0

Belden, L. K., & Harris, R. N. (2007, December). Infectious diseases in wildlife: the community ecology context. *Frontiers in Ecology and the Environment*, *5*(10), 533–539. Retrieved 2020-01-17, from `http://doi.wiley.com/10.1890/060122`   doi: 10.1890/060122

Belkaid, Y., & Hand, T. W. (2014, March). Role of the microbiota in immunity and inflammation. *Cell*, *157*(1), 121–141. Retrieved 2020-09-21, from `https://www.cell.com/cell/abstract/S0092-8674(14)00345-6`   doi: 10.1016/j.cell.2014.03.011

Benjamini, Y., & Hochberg, Y. (1995). Controlling the False Discovery Rate: A Practical and Powerful Approach to Multiple Testing. *Journal of the Royal Statistical Society. Series B (Methodological)*, *57*(1), 289–300. Retrieved from `http://www.jstor.org/stable/2346101`

Berger, L., Speare, R., Daszak, P., Green, D. E., Cunningham, A. A., Goggin, C. L., . . . McDonald, K. R. (1998). Chytridiomycosis causes amphibian mortality associated with population declines in the rain forests of Australia and Central America. *Proceedings of the National Academy of Sciences*, *95*(15), 9031–9036.

Blehert, D. S., Hicks, A. C., Behr, M., Meteyer, C. U., Berlowski-Zier, B. M., Buckles, E. L., . . . Stone, W. B. (2009, January). Bat white-nose syndrome: an emerging fungal pathogen? *Science*, *323*(5911), 227–227. Retrieved 2020-01-20, from `http://www.sciencemag.org/cgi/doi/10.1126/science.1163874`   doi: 10.1126/science.1163874

Bletz, M. C., Kelly, M., Sabino-Pinto, J., Bales, E., Van Praet, S., Bert, W., . . . Martel, A.

(2018, August). Disruption of skin microbiota contributes to salamander disease. *Proceedings of the Royal Society B: Biological Sciences*, *285*(1885), 20180758. Retrieved 2020-09-21, from `https://royalsocietypublishing.org/doi/full/10.1098/rspb.2018.0758` doi: 10.1098/rspb.2018.0758

Bletz, M. C., Loudon, A. H., Becker, M. H., Bell, S. C., Woodhams, D. C., Minbiole, K. P. C., & Harris, R. N. (2013, June). Mitigating amphibian chytridiomycosis with bioaugmentation: characteristics of effective probiotics and strategies for their selection and use. *Ecology Letters*, *16*(6), 807–820. Retrieved 2020-01-17, from `http://doi.wiley.com/10.1111/ele.12099` doi: 10.1111/ele.12099

Bletz, M. C., Perl, R. G. B., Bobowski, B. T. C., Japke, L. M., Tebbe, C. C., Dohrmann, A. B., . . . Vences, M. (2017, July). Amphibian skin microbiota exhibits temporal variation in community structure but stability of predicted Bd-inhibitory function. *The ISME Journal*, *11*(7), 1521–1534. Retrieved 2020-01-17, from `http://www.nature.com/articles/ismej201741` doi: 10.1038/ismej.2017.41

Bouma, H. R., Carey, H. V., & Kroese, F. G. M. (2010, October). Hibernation: the immune system at rest? *Journal of Leukocyte Biology*, *88*(4), 619–624. Retrieved 2020-01-24, from `http://doi.wiley.com/10.1189/jlb.0310174` doi: 10.1189/jlb.0310174

Boyles, J. G., Cryan, P. M., McCracken, G. F., & Kunz, T. H. (2011, April). Economic importance of bats in agriculture. *Science*, *332*(6025), 41–42. Retrieved 2020-01-17, from `http://www.sciencemag.org/cgi/doi/10.1126/science.1201366` doi: 10.1126/science.1201366

Brook, C. E., & Dobson, A. P. (2015). Bats as special reservoirs for emerging zoonotic pathogens. *Trends in Microbiology*, *23*(3), 172–180.

Brooks, J. P., Edwards, D. J., Harwich, M. D., Rivera, M. C., Fettweis, J. M., Serrano, M. G., . . . Vaginal Microbiome Consortium (additional members) (2015, March). The truth about metagenomics: quantifying and counteracting bias in 16S rRNA studies. *BMC Microbiology*, *15*(1), 66. Retrieved 2020-09-20, from `https://doi.org/10.1186/s12866-015-0351-6` doi: 10.1186/s12866-015-0351-6

Brucker, R. M., Harris, R. N., Schwantes, C. R., Gallaher, T. N., Flaherty, D. C., Lam, B. A., & Minbiole, K. P. C. (2008, November). Amphibian chemical defense: antifungal metabolites of the microsymbiont *Janthinobacterium lividum* on the salamander *Plethodon cinereus*. *Journal of Chemical Ecology*, *34*(11), 1422–1429. Retrieved 2020-01-24, from `http://link.springer.com/10.1007/s10886-008-9555-7` doi: 10.1007/s10886-008-9555-7

Brumfield, K. D., Huq, A., Colwell, R. R., Olds, J. L., & Leddy, M. B. (2020, February). Microbial resolution of whole genome shotgun and 16S amplicon metagenomic sequencing using publicly available NEON data. *PLOS ONE*, *15*(2), e0228899. Retrieved 2020-11-16, from `https://journals.plos.org/plosone/article?id=10.1371/`

`journal.pone.0228899` (Publisher: Public Library of Science) doi: 10.1371/journal.pone .0228899

Brunet-Rossinni, A. K., & Austad, S. N. (2004). Ageing studies on bats: a review. *Bioge-rontology*, *5*(4), 211–222.

Brüssow, H. (2016). Biome engineering-2020. *Microbial Biotechnology*, *9*(5), 553–563. doi: 10.1111/1751-7915.12391

Buchfink, B., Xie, C., & Huson, D. H. (2015). Fast and sensitive protein alignment using DIAMOND. *Nature Methods*, *12*(1), 59–60.

Burke, C., Steinberg, P., Rusch, D., Kjelleberg, S., & Thomas, T. (2011, August). Bacterial community assembly based on functional genes rather than species. *Proceedings of the National Academy of Sciences*, *108*(34), 14288–14293. Retrieved 2020-12-02, from `https://www.pnas.org/content/108/34/14288` (Publisher: National Academy of Sciences Section: Biological Sciences) doi: 10.1073/pnas.1101591108

Callahan, B. J., McMurdie, P. J., & Holmes, S. P. (2017). Exact sequence variants should replace operational taxonomic units in marker-gene data analysis. *The ISME Journal*, *11*(12), 2639–2643.

Callahan, B. J., McMurdie, P. J., Rosen, M. J., Han, A. W., Johnson, A. J. A., & Holmes, S. P. (2016). DADA2: high-resolution sample inference from Illumina amplicon data. *Nature Methods*, *13*(7), 581.

Calle, M. L. (2019). Statistical analysis of metagenomics data. *Genomics & Informatics*, *17*(1).

Canadian Wildlife Service, & Committee on the Status of Endangered Wildlife in Canada. (2013). *COSEWIC assessment and status report on the Little Brown Myotis (Myotis lucifugus), Northern Myotis (Myotis septentrionalis), Tri-colored Bat (Perimyotis subflavus) in Canada.* Retrieved 2020-01-17, from `https://central.bac-lac.gc.ca/ .item?id=CW69-14-688-2014-eng&op=pdf&app=Library` (OCLC: 895341011)

Caporaso, J., Kuczynski, J., Stombaugh, J., Bittinger, K., Bushman, F. D., Costello, E. K., ... Knight, R. (2010, May). QIIME allows analysis of high-throughput community sequencing data. *Nature Methods*, *7*(5), 335–336. Retrieved 2020-01-17, from `http://www.nature.com/articles/nmeth.f.303` doi: 10.1038/nmeth.f.303

Caporaso, J., Lauber, C. L., Walters, W. A., Berg-Lyons, D., Lozupone, C. A., Turnbaugh, P. J., ... Knight, R. (2011, March). Global patterns of 16S rRNA diversity at a depth of millions of sequences per sample. *Proceedings of the National Academy of Sciences*, *108*(Supplement_1), 4516–4522. Retrieved 2020-01-17, from `http://www.pnas.org/cgi/ doi/10.1073/pnas.1000080107` doi: 10.1073/pnas.1000080107

Castelino, M., Eyre, S., Moat, J., Fox, G., Martin, P., Ho, P., ... Barton, A. (2017, December). Optimisation of methods for bacterial skin microbiome investigation: primer selection and comparison of the 454 versus MiSeq platform. *BMC Microbiology*, *17*(1),

23. Retrieved 2020-01-17, from `http://bmcmicrobiol.biomedcentral.com/articles/10.1186/s12866-017-0927-4` doi: 10.1186/s12866-017-0927-4

Cheng, T. L., Gerson, A., Moore, M. S., Reichard, J. D., DeSimone, J., Willis, C. K. R., ... Kilpatrick, A. M. (2019, April). Higher fat stores contribute to persistence of little brown bat populations with white-nose syndrome. *Journal of Animal Ecology*, *88*(4), 591–600. Retrieved 2020-01-17, from `https://onlinelibrary.wiley.com/doi/abs/10.1111/1365-2656.12954` doi: 10.1111/1365-2656.12954

Cheng, T. L., Mayberry, H., McGuire, L. P., Hoyt, J. R., Langwig, K. E., Nguyen, H., ... Frick, W. F. (2017, June). Efficacy of a probiotic bacterium to treat bats affected by the disease white-nose syndrome. *Journal of Applied Ecology*, *54*(3), 701–708. Retrieved 2020-01-17, from `http://doi.wiley.com/10.1111/1365-2664.12757` doi: 10.1111/1365-2664.12757

Chiba, H., Agematu, H., Kaneto, R., Terasawa, T., Sakai, K., Dobashi, K., & Yoshioka, T. (1999). Rhodopeptins (Mer-N1033), novel cyclic tetrapeptides with antifungal activity from *Rhodococcus* sp. *The Journal of Antibiotics*, *52*(8), 695–699.

Cho, I., & Blaser, M. J. (2012, March). The human microbiome: at the interface of health and disease. *Nature Reviews. Genetics*, *13*(4), 260–270. doi: 10.1038/nrg3182

Clark, R. W., Marchand, M. N., Clifford, B. J., Stechert, R., & Stephens, S. (2011). Decline of an isolated timber rattlesnake (*Crotalus horridus*) population: interactions between climate change, disease, and loss of genetic diversity. *Biological Conservation*, *144*(2), 886–891.

Coleman, J. T. H. (2012). North American bat death toll exceeds 5.5 million from white-nose syndrome. *https://www.fws.gov/news/ShowNews.cfm?ID=0DA47708-D93C-21F4-3AA3E6EEB217DAA0*.

Coleman, J. T. H., & Reichard, J. D. (2014). Bat white-nose syndrome in 2014: a brief assessment seven years after discovery of a virulent fungal pathogen in North America. *Outlooks on Pest Management*, *25*(6), 374–377.

Cornelison, C. T., Keel, M. K., Gabriel, K. T., Barlament, C. K., Tucker, T. A., Pierce, G. E., & Crow, S. A. (2014, December). A preliminary report on the contact-independent antagonism of *Pseudogymnoascus destructans* by *Rhodococcus rhodochrous* strain DAP96253. *BMC Microbiology*, *14*(1), 246. Retrieved 2020-01-17, from `http://bmcmicrobiol.biomedcentral.com/articles/10.1186/s12866-014-0246-y` doi: 10.1186/s12866-014-0246-y

Cortese, T. A., & Nicoll, P. A. (1970, January). In vivo observations of skin appendages in the bat wing. *Journal of Investigative Dermatology*, *54*(1), 1–10. Retrieved 2020-01-24, from `https://linkinghub.elsevier.com/retrieve/pii/S0022202X15477863` doi: 10.1111/1523-1747.ep12551469

Cox, M. P., Peterson, D. A., & Biggs, P. J. (2010). SolexaQA: At-a-glance quality assessment

of Illumina second-generation sequencing data. *BMC Bioinformatics*, *11*(1), 1–6.

Cryan, P. M., Meteyer, C., Boyles, J. G., & Blehert, D. S. (2010). Wing pathology of white-nose syndrome in bats suggests life-threatening disruption of physiology. *BMC Biology*, *8*(1), 135. Retrieved 2020-01-17, from `http://bmcbiol.biomedcentral.com/articles/10.1186/1741-7007-8-135` doi: 10.1186/1741-7007-8-135

Cryan, P. M., Meteyer, C. U., Blehert, D. S., Lorch, J. M., Reeder, D. M., Turner, G. G., . . . Russell, R. E. (2013). Electrolyte depletion in white-nose syndrome bats. *Journal of Wildlife Diseases*, *49*(2), 398–402.

Curtis, M. M., & Sperandio, V. (2011, March). A complex relationship: the interaction among symbiotic microbes, invading pathogens, and their mammalian host. *Mucosal Immunology*, *4*(2), 133–138. Retrieved 2020-01-17, from `http://www.nature.com/articles/mi201089` doi: 10.1038/mi.2010.89

Czenze, Z. J., Park, A. D., & Willis, C. K. R. (2013, August). Staying cold through dinner: cold-climate bats rewarm with conspecifics but not sunset during hibernation. *Journal of Comparative Physiology B*, *183*(6), 859–866. Retrieved 2020-01-17, from `http://link.springer.com/10.1007/s00360-013-0753-4` doi: 10.1007/s00360-013-0753-4

Czenze, Z. J., & Willis, C. K. R. (2015, July). Warming up and shipping out: arousal and emergence timing in hibernating little brown bats (*Myotis lucifugus*). *Journal of Comparative Physiology B*, *185*(5), 575–586. Retrieved 2020-01-17, from `http://link.springer.com/10.1007/s00360-015-0900-1` doi: 10.1007/s00360-015-0900-1

Dahllöf, I., Baillie, H., & Kjelleberg, S. (2000). rpoB-based microbial community analysis avoids limitations inherent in 16S rRNA gene intraspecies heterogeneity. *Applied and Environmental Microbiology*, *66*(8), 3376–3380.

Daszak, P. (2000, January). Emerging infectious diseases of wildlife– threats to biodiversity and human health. *Science*, *287*(5452), 443–449. Retrieved 2020-01-17, from `http://www.sciencemag.org/cgi/doi/10.1126/science.287.5452.443` doi: 10.1126/science.287.5452.443

Davies, P. T., & Tso, M. K.-S. (1982). Procedures for reduced-rank regression. *Applied Statistics*, *31*(3), 244. Retrieved 2020-01-17, from `https://www.jstor.org/stable/10.2307/2347998?origin=crossref` doi: 10.2307/2347998

Davis, W. H. (1970). Hibernation: ecology and physiological ecology. *Biology of Bats*, *1*, 265–300.

Davy, C. M., Donaldson, M. E., Bandouchova, H., Breit, A. M., Dorville, N. A. S., Dzal, Y. A., . . . Kyle, C. J. (2020, January). Transcriptional host–pathogen responses of *Pseudogymnoascus destructans* and three species of bats with white-nose syndrome. *Virulence*, *11*(1), 781–794. Retrieved 2020-06-23, from `https://doi.org/10.1080/21505594.2020.1768018` doi: 10.1080/21505594.2020.1768018

De Cáceres, M., & Legendre, P. (2009, December). Associations between species and groups

of sites: indices and statistical inference. *Ecology*, *90*(12), 3566–3574. Retrieved 2020-01-24, from `http://doi.wiley.com/10.1890/08-1823.1`   doi: 10.1890/08-1823.1

DeSantis, T. Z., Hugenholtz, P., Larsen, N., Rojas, M., Brodie, E. L., Keller, K., . . . Andersen, G. L. (2006, July). Greengenes, a chimera-checked 16S rRNA gene database and workbench compatible with ARB. *Applied and Environmental Microbiology*, *72*(7), 5069–5072. Retrieved 2020-01-24, from `http://aem.asm.org/cgi/doi/10.1128/AEM.03006-05`   doi: 10.1128/AEM.03006-05

Dobony, C. A., Hicks, A. C., Langwig, K. E., von Linden, R. I., Okoniewski, J. C., & Rainbolt, R. E. (2011, December). Little brown myotis persist despite exposure to white-nose syndrome. *Journal of Fish and Wildlife Management*, *2*(2), 190–195. Retrieved 2020-01-24, from `http://www.fwspubs.org/doi/abs/10.3996/022011-JFWM-014`   doi: 10.3996/022011-JFWM-014

Dormann, C. F., Gruber, B., & Fründ, J. (2008). Introducing the bipartite package: analysing ecological networks. *Interaction*, *1*(0.2413793).

Dray, S., & Dufour, A.-B. (2007). The ade4 package: implementing the duality diagram for ecologists. *Journal of Statistical Software*, *22*(4). Retrieved 2020-01-17, from `http://www.jstatsoft.org/v22/i04/`   doi: 10.18637/jss.v022.i04

Drees, K. P., Lorch, J. M., Puechmaille, S. J., Parise, K. L., Wibbelt, G., Hoyt, J. R., . . . Palmer, J. M. (2017). Phylogenetics of a fungal invasion: origins and widespread dispersal of white-nose syndrome. *MBio*, *8*(6), e01941–17.

Dufrene, M., & Legendre, P. (1997, August). Species assemblages and indicator species: the need for a flexible asymmetrical approach. *Ecological Monographs*, *67*(3), 345. Retrieved 2020-01-24, from `http://www.jstor.org/stable/2963459?origin=crossref`   doi: 10.2307/2963459

Edgar, R. C. (2010, October). Search and clustering orders of magnitude faster than BLAST. *Bioinformatics*, *26*(19), 2460–2461. Retrieved 2020-01-17, from `https://academic.oup.com/bioinformatics/article-lookup/doi/10.1093/bioinformatics/btq461`   doi: 10.1093/bioinformatics/btq461

Environnement et changement climatique Canada. (2018). *Programme de rétablissement de la petite chauve-souris brune (Myotis lucifugus), de la chauve-souris nordique (Myotis septentrionalis) et de la pipistrelle de l'Est (Perimyotis subflavus) au Canada.* Retrieved 2020-02-21, from `http://epe.lac-bac.gc.ca/100/201/301/weekly_acquisitions_list-ef/2018/18-52/publications.gc.ca/collections/collection_2018/eccc/En3-4-308-2018-fra.pdf` (OCLC: 1080940784)

Eskew, E. A., Worth, S. J., Foley, J. E., & Todd, B. D. (2015, September). American bullfrogs (*Lithobates catesbeianus*) resist infection by multiple isolates of *Batrachochytrium dendrobatidis*, including one implicated in wild mass mortality. *EcoHealth*, *12*(3), 513–518. Retrieved 2020-04-02, from `https://doi.org/10.1007/s10393-015-1035-2`   doi:

10.1007/s10393-015-1035-2

Ezekiel, M. (1930). *Methods of correlation analysis.* Oxford, England: Wiley.

Feinstein, L. M., Sul, W. J., & Blackwood, C. B. (2009). Assessment of bias associated with incomplete extraction of microbial DNA from soil. *Applied and Environmental Microbiology*, *75*(16), 5428–5433.

Fenton, M. B. (1970). A technique for monitoring bat activity with results obtained from different environments in southern Ontario. *Canadian Journal of Zoology*, *48*(4), 847–851.

Field, K. A., Johnson, J. S., Lilley, T. M., Reeder, S. M., Rogers, E. J., Behr, M. J., & Reeder, D. M. (2015, October). The white-nose syndrome transcriptome: activation of anti-fungal host responses in wing tissue of hibernating little brown myotis. *PLOS Pathogens*, *11*(10), e1005168. Retrieved 2020-09-16, from `https://journals.plos.org/plospathogens/article?id=10.1371/journal.ppat.1005168` doi: 10.1371/journal.ppat.1005168

Fischer, N. M., Dool, S. E., & Puechmaille, S. J. (2020, June). Seasonal patterns of *Pseudogymnoascus destructans* germination indicate host–pathogen coevolution. *Biology Letters*, *16*(6), 20200177. Retrieved 2020-06-23, from `https://royalsocietypublishing.org/doi/full/10.1098/rsbl.2020.0177` doi: 10.1098/rsbl.2020.0177

Fisher, M. C., Gurr, S. J., Cuomo, C. A., Blehert, D. S., Jin, H., Stukenbrock, E. H., . . . Cowen, L. E. (2020, June). Threats posed by the fungal kingdom to humans, wildlife, and agriculture. *mBio*, *11*(3), e00449–20. Retrieved from `http://mbio.asm.org/content/11/3/e00449-20.abstract` doi: 10.1128/mBio.00449-20

Fisher, M. C., Henk, D. A., Briggs, C. J., Brownstein, J. S., Madoff, L. C., McCraw, S. L., & Gurr, S. J. (2012, April). Emerging fungal threats to animal, plant and ecosystem health. *Nature*, *484*(7393), 186–194. Retrieved 2020-01-17, from `http://www.nature.com/articles/nature10947` doi: 10.1038/nature10947

Foley, J. E., Clifford, D., Castle, K., Cryan, P., & Ostfeld, R. S. (2011). Investigating and managing the rapid emergence of white-Nose syndrome, a novel, fatal, infectious disease of hibernating bats. *Conservation Biology*, *25*(2), 223–231. Retrieved 2020-02-20, from `https://conbio.onlinelibrary.wiley.com/doi/abs/10.1111/j.1523-1739.2010.01638.x` doi: 10.1111/j.1523-1739.2010.01638.x

Foley, N. M., Hughes, G. M., Huang, Z., Clarke, M., Jebb, D., Whelan, C. V., . . . Jones, G. (2018). Growing old, yet staying young: The role of telomeres in bats' exceptional longevity. *Science Advances*, *4*(2), eaao0926.

Fortunato, S. (2010). Community detection in graphs. *Physics Reports*, *486*(3-5), 75–174.

Frank, C. L., Ingala, M. R., Ravenelle, R. E., Dougherty-Howard, K., Wicks, S. O., Herzog, C., & Rudd, R. J. (2016). The effects of cutaneous fatty acids on the growth of *Pseudogymnoascus destructans*, the etiological agent of white-nose syndrome (WNS). *PLOS ONE*, *11*(4).

Frank, C. L., Michalski, A., McDonough, A. A., Rahimian, M., Rudd, R. J., & Herzog, C. (2014, December). The resistance of a north american bat species (*Eptesicus fuscus*) to white-nose syndrome (WNS). *PLOS ONE*, *9*(12), e113958. Retrieved 2020-01-17, from `https://dx.plos.org/10.1371/journal.pone.0113958` doi: 10.1371/journal.pone.0113958

Frank, C. L., Sitler-Elbel, K. G., Hudson, A. J., & Ingala, M. R. (2018). The antifungal properties of epidermal fatty acid esters: insights from white-nose syndrome (WNS) in bats. *Molecules*, *23*(8), 1986.

Franklinos, L. H. V., Lorch, J. M., Bohuski, E., Fernandez, J. R.-R., Wright, O. N., Fitzpatrick, L., . . . Baláž, V. (2017). Emerging fungal pathogen *Ophidiomyces ophiodiicola* in wild European snakes. *Scientific Reports*, *7*(1), 1–7.

Franzosa, E. A., Hsu, T., Sirota-Madi, A., Shafquat, A., Abu-Ali, G., Morgan, X. C., & Huttenhower, C. (2015, June). Sequencing and beyond: integrating molecular 'omics' for microbial community profiling. *Nature Reviews Microbiology*, *13*(6), 360–372. Retrieved 2020-09-20, from `https://www.nature.com/articles/nrmicro3451` doi: 10.1038/nrmicro3451

Frick, W. F., Cheng, T. L., Langwig, K. E., Hoyt, J. R., Janicki, A. F., Parise, K. L., . . . Kilpatrick, A. M. (2017, March). Pathogen dynamics during invasion and establishment of white-nose syndrome explain mechanisms of host persistence. *Ecology*, *98*(3), 624–631. Retrieved 2020-01-17, from `http://doi.wiley.com/10.1002/ecy.1706` doi: 10.1002/ecy.1706

Frick, W. F., Pollock, J. F., Hicks, A. C., Langwig, K. E., Reynolds, D. S., Turner, G. G., . . . Kunz, T. H. (2010, August). An emerging disease causes regional population collapse of a common North American bat species. *Science*, *329*(5992), 679–682. Retrieved 2020-01-17, from `http://www.sciencemag.org/cgi/doi/10.1126/science.1188594` doi: 10.1126/science.1188594

Frick, W. F., Puechmaille, S. J., Hoyt, J. R., Nickel, B. A., Langwig, K. E., Foster, J. T., . . . Kilpatrick, A. M. (2015, July). Disease alters macroecological patterns of North American bats: Disease alters macroecology of bats. *Global Ecology and Biogeography*, *24*(7), 741–749. Retrieved 2020-01-17, from `http://doi.wiley.com/10.1111/geb.12290` doi: 10.1111/geb.12290

Frick, W. F., Puechmaille, S. J., & Willis, C. K. R. (2016). White-nose syndrome in bats. In *Bats in the Anthropocene: Conservation of bats in a changing world* (pp. 245–262). Springer, Cham.

Frick, W. F., Reynolds, D. S., & Kunz, T. H. (2010). Influence of climate and reproductive timing on demography of little brown myotis *Myotis lucifugus. Journal of Animal Ecology*, *79*(1), 128–136.

Fritze, M., & Puechmaille, S. J. (2018). Identifying unusual mortality events in bats:

a baseline for bat hibernation monitoring and white-nose syndrome research. *Mammal Review*, *48*(3), 224–228. (ISBN: 0305-1838 Publisher: Wiley Online Library)

Fu, L., Niu, B., Zhu, Z., Wu, S., & Li, W. (2012). CD-HIT: accelerated for clustering the next-generation sequencing data. *Bioinformatics*, *28*(23), 3150–3152.

Fuller, N. W., McGuire, L. P., Pannkuk, E. L., Blute, T., Haase, C. G., Mayberry, H. W., ... Willis, C. K. R. (2020, March). Disease recovery in bats affected by white-nose syndrome. *Journal of Experimental Biology*, *223*(6). Retrieved 2020-11-24, from `https://jeb.biologists.org/content/223/6/jeb211912` (Publisher: The Company of Biologists Ltd Section: Research Article) doi: 10.1242/jeb.211912

Fuller, N. W., Reichard, J. D., Nabhan, M. L., Fellows, S. R., Pepin, L. C., & Kunz, T. H. (2011). Free-ranging little brown myotis (*Myotis lucifugus*) heal from wing damage associated with white-nose syndrome. *EcoHealth*, *8*(2), 154–162.

Gargas, A., Trest, M., Christensen, M., Volk, T., & Blehert, D. (2009, July). *Geomyces destructans* sp. nov. associated with bat white-nose syndrome. *Mycotaxon*, *108*(1), 147–154. Retrieved 2020-01-17, from `http://openurl.ingenta.com/content/xref?genre=article&issn=0093-4666&volume=108&issue=1&spage=147` doi: 10.5248/108.147

Geiser, F. (2004, March). Metabolic rate and body temperature reduction during hibernation and daily torpor. *Annual Review of Physiology*, *66*(1), 239–274. Retrieved 2020-01-24, from `http://www.annualreviews.org/doi/10.1146/annurev.physiol.66.032102.115105` doi: 10.1146/annurev.physiol.66.032102.115105

Gerwien, F., Skrahina, V., Kasper, L., Hube, B., & Brunke, S. (2018, January). Metals in fungal virulence. *FEMS Microbiology Reviews*, *42*(1). Retrieved 2020-09-14, from `https://academic.oup.com/femsre/article/42/1/fux050/4562650` doi: 10.1093/femsre/fux050

Gilbert, J. A., Quinn, R. A., Debelius, J., Xu, Z. Z., Morton, J., Garg, N., ... Knight, R. (2016, July). Microbiome-wide association studies link dynamic microbial consortia to disease. *Nature*, *535*(7610), 94–103. Retrieved 2020-09-21, from `https://www.nature.com/articles/nature18850` doi: 10.1038/nature18850

Glassing, A., Dowd, S. E., Galandiuk, S., Davis, B., & Chiodini, R. J. (2016, December). Inherent bacterial DNA contamination of extraction and sequencing reagents may affect interpretation of microbiota in low bacterial biomass samples. *Gut Pathogens*, *8*(1), 24. Retrieved 2020-01-17, from `http://gutpathogens.biomedcentral.com/articles/10.1186/s13099-016-0103-7` doi: 10.1186/s13099-016-0103-7

Gloor, G. B., Macklaim, J. M., Pawlowsky-Glahn, V., & Egozcue, J. J. (2017, November). Microbiome datasets are compositional: and this is not optional. *Frontiers in Microbiology*, *8*, 2224. Retrieved 2020-01-17, from `http://journal.frontiersin.org/article/10.3389/fmicb.2017.02224/full` doi: 10.3389/fmicb.2017.02224

Gohl, D. M., Vangay, P., Garbe, J., MacLean, A., Hauge, A., Becker, A., ... Beckman, K. B. (2016, September). Systematic improvement of amplicon marker gene methods for increased accuracy in microbiome studies. *Nature Biotechnology*, *34*(9), 942–949. Retrieved 2020-09-20, from `https://www.nature.com/articles/nbt.3601` doi: 10.1038/nbt.3601

Gower, J. C. (1966, December). Some distance properties of latent root and vector methods used in multivariate analysis. *Biometrika*, *53*(3/4), 325. Retrieved 2020-01-17, from `https://www.jstor.org/stable/2333639?origin=crossref` doi: 10.2307/2333639

Gower, J. C., & Legendre, P. (1986, March). Metric and Euclidean properties of dissimilarity coefficients. *Journal of Classification*, *3*(1), 5–48. Retrieved 2020-01-17, from `http://link.springer.com/10.1007/BF01896809` doi: 10.1007/BF01896809

Green, J. L., Bohannan, B. J. M., & Whitaker, R. J. (2008, May). Microbial Biogeography: From Taxonomy to Traits. *Science*, *320*(5879), 1039–1043. Retrieved 2020-12-02, from `https://science.sciencemag.org/content/320/5879/1039` (Publisher: American Association for the Advancement of Science Section: Special Reviews) doi: 10.1126/science.1153475

Grice, E. A., & Segre, J. A. (2011, April). The skin microbiome. *Nature Reviews Microbiology*, *9*(4), 244–253. Retrieved 2020-01-17, from `http://www.nature.com/articles/nrmicro2537` doi: 10.1038/nrmicro2537

Grisnik, M., Bowers, O., Moore, A. J., Jones, B. F., Campbell, J. R., & Walker, D. M. (2020, February). The cutaneous microbiota of bats has in vitro antifungal activity against the white nose pathogen. *FEMS Microbiology Ecology*, *96*(2), fiz193. Retrieved 2020-02-20, from `https://academic.oup.com/femsec/article/doi/10.1093/femsec/fiz193/5710932` doi: 10.1093/femsec/fiz193

Haegeman, B., Hamelin, J., Moriarty, J., Neal, P., Dushoff, J., & Weitz, J. S. (2013, June). Robust estimation of microbial diversity in theory and in practice. *The ISME Journal*, *7*(6), 1092–1101. Retrieved 2020-01-17, from `http://www.nature.com/articles/ismej201310` doi: 10.1038/ismej.2013.10

Hamm, P. S., Caimi, N. A., Northup, D. E., Valdez, E. W., Buecher, D. C., Dunlap, C. A., ... Porras-Alfaro, A. (2017, March). Western bats as a reservoir of novel streptomyces species with antifungal activity. *Applied and Environmental Microbiology*, *83*(5). Retrieved 2020-01-17, from `http://aem.asm.org/lookup/doi/10.1128/AEM.03057-16` doi: 10.1128/AEM.03057-16

Harazim, M., Horáček, I., Jakešová, L., Luermann, K., Moravec, J. C., Morgan, S., ... Martínková, N. (2018, August). Natural selection in bats with historical exposure to white-nose syndrome. *BMC Zoology*, *3*(1), 8. Retrieved 2020-09-16, from `https://doi.org/10.1186/s40850-018-0035-4` doi: 10.1186/s40850-018-0035-4

Harris, R. N., Brucker, R. M., Walke, J. B., Becker, M. H., Schwantes, C. R., Flaherty, D. C.,

. . . Minbiole, K. P. C. (2009, July). Skin microbes on frogs prevent morbidity and mortality caused by a lethal skin fungus. *The ISME Journal*, *3*(7), 818–824. Retrieved 2020-01-17, from `http://www.nature.com/articles/ismej200927` doi: 10.1038/ismej.2009.27

Hassan, H. M., & Fridovich, I. (1980, January). Mechanism of the antibiotic action pyocyanine. *Journal of Bacteriology*, *141*(1), 156–163.

Hess, G. (1996). Disease in metapopulation models: implications for conservation. *Ecology*, *77*(5), 1617–1632.

Hock, R. J. (1951, December). THE METABOLIC RATES AND BODY TEMPERATURES OF BATS. *The Biological Bulletin*, *101*(3), 289–299. Retrieved 2020-12-02, from `https://www.journals.uchicago.edu/doi/10.2307/1538547` doi: 10.2307/1538547

Holm, S. (1979). A simple sequentially rejective multiple test procedure. *Scandinavian Journal of Statistics*, *6*(2), 65–70. Retrieved 2020-01-24, from `https://www.jstor.org/stable/4615733`

Hood, M. I., & Skaar, E. P. (2012). Nutritional immunity: transition metals at the pathogen–host interface. *Nature Reviews Microbiology*, *10*(8), 525–537.

Hoyt, J. R., Cheng, T. L., Langwig, K. E., Hee, M. M., Frick, W. F., & Kilpatrick, A. M. (2015, April). Bacteria isolated from bats inhibit the growth of *Pseudogymnoascus destructans*, the causative agent of white-nose syndrome. *PLOS ONE*, *10*(4), e0121329. Retrieved 2020-01-17, from `https://dx.plos.org/10.1371/journal.pone.0121329` doi: 10.1371/journal.pone.0121329

Hoyt, J. R., Langwig, K. E., Okoniewski, J., Frick, W. F., Stone, W. B., & Kilpatrick, A. M. (2015). Long-term persistence of *Pseudogymnoascus destructans*, the causative agent of white-nose syndrome, in the absence of bats. *EcoHealth*, *12*(2), 330–333.

Hoyt, J. R., Langwig, K. E., White, J. P., Kaarakka, H. M., Redell, J. A., Parise, K. L., . . . Kilpatrick, A. M. (2019, December). Field trial of a probiotic bacteria to protect bats from white-nose syndrome. *Scientific Reports*, *9*(1), 9158. Retrieved 2020-01-17, from `http://www.nature.com/articles/s41598-019-45453-z` doi: 10.1038/s41598-019-45453-z

Hoyt, J. R., Sun, K., Parise, K. L., Lu, G., Langwig, K. E., Jiang, T., . . . Feng, J. (2016, January). Widespread bat white-nose syndrome fungus, Northeastern China. *Emerging Infectious Diseases*, *22*(1), 140–142. Retrieved 2020-01-17, from `http://wwwnc.cdc.gov/eid/article/22/1/15-1314_article.htm` doi: 10.3201/eid2201.151314

Jani, A. J., & Briggs, C. J. (2014, November). The pathogen *Batrachochytrium dendrobatidis* disturbs the frog skin microbiome during a natural epidemic and experimental infection. *Proceedings of the National Academy of Sciences*, *111*(47). Retrieved 2020-01-17, from `http://www.pnas.org/lookup/doi/10.1073/pnas.1412752111` doi: 10.1073/pnas.1412752111

Jansson, J. K., & Hofmockel, K. S. (2018). The soil microbiome—from metagenomics to metaphenomics. *Current Opinion in Microbiology*, *43*, 162–168.

Jonasson, K. A., & Willis, C. K. R. (2012, June). Hibernation energetics of free-ranging little brown bats. *The Journal of Experimental Biology*, *215*(12), 2141–2149. Retrieved 2020-01-17, from `http://jeb.biologists.org/lookup/doi/10.1242/jeb.066514` doi: 10.1242/jeb.066514

Jones, K. E., Patel, N. G., Levy, M. A., Storeygard, A., Balk, D., Gittleman, J. L., & Daszak, P. (2008, February). Global trends in emerging infectious diseases. *Nature*, *451*(7181), 990–993. Retrieved 2020-01-17, from `http://www.nature.com/articles/nature06536` doi: 10.1038/nature06536

Julliard, R., Clavel, J., Devictor, V., Jiguet, F., & Couvet, D. (2006). Spatial segregation of specialists and generalists in bird communities. *Ecology Letters*, *9*(11), 1237–1244.

Kacprzyk, J., Hughes, G. M., Palsson-McDermott, E. M., Quinn, S. R., Puechmaille, S. J., O'neill, L. A. J., & Teeling, E. C. (2017). A potent anti-inflammatory response in bat macrophages may be linked to extended longevity and viral tolerance. *Acta Chiropterologica*, *19*(2), 219–228.

Kim, D., Hahn, A. S., Wu, S.-J., Hanson, N. W., Konwar, K. M., & Hallam, S. J. (2015). FragGeneScan-Plus for scalable high-throughput short-read open reading frame prediction. In *2015 IEEE conference on computational intelligence in bioinformatics and computational biology (CIBCB)* (pp. 1–8). IEEE.

Klappenbach, J. A. (2001, January). rrndb: the ribosomal RNA operon copy number database. *Nucleic Acids Research*, *29*(1), 181–184. Retrieved 2020-01-17, from `https://academic.oup.com/nar/article-lookup/doi/10.1093/nar/29.1.181` doi: 10.1093/nar/29.1.181

Kolodny, O., Weinberg, M., Reshef, L., Harten, L., Hefetz, A., Gophna, U., . . . Yovel, Y. (2019, January). Coordinated change at the colony level in fruit bat fur microbiomes through time. *Nature Ecology & Evolution*, *3*(1), 116–124. Retrieved 2020-01-17, from `http://www.nature.com/articles/s41559-018-0731-z` doi: 10.1038/s41559-018-0731-z

Kooser, A., Kimble, J. C., Young, J. M., Buecher, D. C., Valdez, E. W., Porras-Alfaro, A., & Northup, D. E. (2015, March). External Microbiota of Western United States Bats: Does It Matter Where You Are From? *BioRxiv*. Retrieved 2020-01-24, from `http://biorxiv.org/lookup/doi/10.1101/017319` doi: 10.1101/017319

Kueneman, J. G., Woodhams, D. C., Harris, R., Archer, H. M., Knight, R., & McKenzie, V. J. (2016, September). Probiotic treatment restores protection against lethal fungal infection lost during amphibian captivity. *Proceedings of the Royal Society B: Biological Sciences*, *283*(1839), 20161553. Retrieved 2020-05-15, from `https://royalsocietypublishing.org/doi/10.1098/rspb.2016.1553` doi: 10.1098/rspb.2016.1553

Lahti, L., & Shetty, S. (2017). Tools for microbiome analysis in R. *http://microbiome.github.*

com/microbiome.

Lai, Y., Di Nardo, A., Nakatsuji, T., Leichtle, A., Yang, Y., Cogen, A. L., . . . Gallo, R. L. (2009, December). Commensal bacteria regulate Toll-like receptor 3–dependent inflammation after skin injury. *Nature Medicine*, *15*(12), 1377–1382. Retrieved 2020-01-17, from `http://www.nature.com/articles/nm.2062` doi: 10.1038/nm.2062

Langille, M. G. I. (2018, March). Exploring Linkages between Taxonomic and Functional Profiles of the Human Microbiome. *mSystems*, *3*(2), e00163–17. Retrieved 2020-11-16, from `https://msystems.asm.org/content/3/2/e00163-17` doi: 10.1128/mSystems.00163-17

Langwig, K. E., Frick, W. F., Bried, J. T., Hicks, A. C., Kunz, T. H., & Kilpatrick, A. M. (2012, September). Sociality, density-dependence and microclimates determine the persistence of populations suffering from a novel fungal disease, white-nose syndrome. *Ecology Letters*, *15*(9), 1050–1057. Retrieved 2020-01-17, from `http://doi.wiley.com/10.1111/j.1461-0248.2012.01829.x` doi: 10.1111/j.1461-0248.2012.01829.x

Langwig, K. E., Frick, W. F., Reynolds, R., Parise, K. L., Drees, K. P., Hoyt, J. R., . . . Kilpatrick, A. M. (2015, January). Host and pathogen ecology drive the seasonal dynamics of a fungal disease, white-nose syndrome. *Proceedings of the Royal Society B: Biological Sciences*, *282*(1799), 20142335. Retrieved 2020-01-17, from `https://royalsocietypublishing.org/doi/10.1098/rspb.2014.2335` doi: 10.1098/rspb.2014.2335

Langwig, K. E., Hoyt, J. R., Parise, K. L., Frick, W. F., Foster, J. T., & Kilpatrick, A. M. (2017, January). Resistance in persisting bat populations after white-nose syndrome invasion. *Philosophical Transactions of the Royal Society B: Biological Sciences*, *372*(1712), 20160044. Retrieved 2020-01-17, from `https://royalsocietypublishing.org/doi/10.1098/rstb.2016.0044` doi: 10.1098/rstb.2016.0044

Lauer, A., Simon, M. A., Banning, J. L., Lam, B. A., & Harris, R. N. (2008, February). Diversity of cutaneous bacteria with antifungal activity isolated from female four-toed salamanders. *The ISME Journal*, *2*(2), 145–157. Retrieved 2020-01-24, from `http://www.nature.com/articles/ismej2007110` doi: 10.1038/ismej.2007.110

Legendre, P., & Anderson, M. J. (1999, February). Distance-based redundancy analysis: testing multispecies responses in multifactorial ecological experiments. *Ecological Monographs*, *69*(1), 1–24. Retrieved 2020-01-17, from `http://doi.wiley.com/10.1890/0012-9615(1999)069[0001:DBRATM]2.0.CO;2` doi: 10.1890/0012-9615(1999)069[0001:DBRATM]2.0.CO;2

Lemieux-Labonté, V., Dorville, N. A. S.-Y., Willis, C. K. R., & Lapointe, F.-J. (2020). Antifungal potential of the skin microbiota of hibernating big brown bats (*Eptesicus fuscus*) infected with the causal agent of white-nose syndrome. *Frontiers in Microbiology*, *11*(1776). Retrieved 2020-09-29, from `https://www.frontiersin.org/articles/`

`10.3389/fmicb.2020.01776/full` doi: 10.3389/fmicb.2020.01776

Lemieux-Labonté, V., Simard, A., Willis, C. K. R., & Lapointe, F.-J. (2017, December). Enrichment of beneficial bacteria in the skin microbiota of bats persisting with white-nose syndrome. *Microbiome*, *5*(1), 115. Retrieved 2020-01-17, from `http://microbiomejournal.biomedcentral.com/articles/10.1186/s40168-017-0334-y` doi: 10.1186/s40168-017-0334-y

Lemieux-Labonté, V., Tromas, N., Shapiro, B. J., & Lapointe, F.-J. (2016, September). Environment and host species shape the skin microbiome of captive neotropical bats. *PeerJ*, *4*, e2430. Retrieved 2020-01-24, from `https://peerj.com/articles/2430` doi: 10.7717/peerj.2430

Leopardi, S., Blake, D., & Puechmaille, S. J. (2015, March). White-Nose Syndrome fungus introduced from Europe to North America. *Current Biology*, *25*(6), R217–R219. Retrieved 2020-11-24, from `http://www.sciencedirect.com/science/article/pii/S0960982215000792` doi: 10.1016/j.cub.2015.01.047

Lilley, T. M., Prokkola, J. M., Johnson, J. S., Rogers, E. J., Gronsky, S., Kurta, A., . . . Field, K. A. (2017, February). Immune responses in hibernating little brown myotis (*Myotis lucifugus*) with white-nose syndrome. *Proceedings of the Royal Society B: Biological Sciences*, *284*(1848), 20162232. Retrieved 2020-09-16, from `https://royalsocietypublishing.org/doi/full/10.1098/rspb.2016.2232` doi: 10.1098/rspb.2016.2232

Lilley, T. M., Wilson, I. W., Field, K. A., Reeder, D. M., Vodzak, M. E., Turner, G. G., . . . Paterson, S. (2020, April). Genome-wide changes in genetic diversity in a population of *Myotis lucifugus* affected by white-nose syndrome. *G3: Genes|Genomes|Genetics*, *10*(6), 2007–2020. Retrieved 2020-06-17, from `https://www.ncbi.nlm.nih.gov/pmc/articles/PMC7263666/` doi: 10.1534/g3.119.400966

Liu, C. H., Chen, X., Liu, T. T., Lian, B., Gu, Y., Caer, V., . . . Wang, B. T. (2007, July). Study of the antifungal activity of *Acinetobacter baumannii* LCH001 in vitro and identification of its antifungal components. *Applied Microbiology and Biotechnology*, *76*(2), 459–466. Retrieved 2020-01-24, from `http://link.springer.com/10.1007/s00253-007-1010-0` doi: 10.1007/s00253-007-1010-0

Longcore, J. E., Pessier, A. P., & Nichols, D. K. (1999, March). *Batrachochytrium dendrobatidis* gen. et sp. nov., a chytrid pathogenic to amphibians. *Mycologia*, *91*(2), 219–227. Retrieved 2020-01-17, from `https://www.tandfonline.com/doi/full/10.1080/00275514.1999.12061011` doi: 10.1080/00275514.1999.12061011

Lorch, J. M., Meteyer, C. U., Behr, M. J., Boyles, J. G., Cryan, P. M., Hicks, A. C., . . . Blehert, D. S. (2011, December). Experimental infection of bats with *Geomyces destructans* causes white-nose syndrome. *Nature*, *480*(7377), 376–378. Retrieved 2020-01-17, from `http://www.nature.com/articles/nature10590` doi: 10.1038/nature10590

Lorch, J. M., Muller, L. K., Russell, R. E., O'Connor, M., Lindner, D. L., & Blehert, D. S.

(2013). Distribution and environmental persistence of the causative agent of white-nose syndrome, *Geomyces destructans*, in bat hibernacula of the eastern United States. *Applied and Environmental Microbiology*, *79*(4), 1293–1301.

Louca, S., Parfrey, L. W., & Doebeli, M. (2016). Decoupling function and taxonomy in the global ocean microbiome. *Science*, *353*(6305), 1272–1277.

Loudon, A. H., Woodhams, D. C., Parfrey, L. W., Archer, H., Knight, R., McKenzie, V., & Harris, R. N. (2014, April). Microbial community dynamics and effect of environmental microbial reservoirs on red-backed salamanders (*Plethodon cinereus*). *The ISME Journal*, *8*(4), 830–840. Retrieved 2020-01-24, from `http://www.nature.com/articles/ismej2013200` doi: 10.1038/ismej.2013.200

Lozupone, C. A., Hamady, M., Kelley, S. T., & Knight, R. (2007, March). Quantitative and qualitative diversity measures lead to different insights into factors that structure microbial communities. *Applied and Environmental Microbiology*, *73*(5), 1576–1585. Retrieved 2020-01-17, from `http://aem.asm.org/cgi/doi/10.1128/AEM.01996-06` doi: 10.1128/AEM.01996-06

Lozupone, C. A., & Knight, R. (2005, December). UniFrac: a new phylogenetic method for comparing microbial communities. *Applied and Environmental Microbiology*, *71*(12), 8228–8235. Retrieved 2020-01-17, from `http://aem.asm.org/cgi/doi/10.1128/AEM.71.12.8228-8235.2005` doi: 10.1128/AEM.71.12.8228-8235.2005

Lozupone, C. A., Lladser, M. E., Knights, D., Stombaugh, J., & Knight, R. (2011, February). UniFrac: an effective distance metric for microbial community comparison. *The ISME Journal*, *5*(2), 169–172. Retrieved 2020-01-17, from `http://www.nature.com/articles/ismej2010133` doi: 10.1038/ismej.2010.133

Lueschow, S. R. (2015). *Effect of Pseudogymnoascus destructans on microbial community composition on bats* (Master's thesis, Ann Arbor, United States). Retrieved 2020-01-24, from `https://search.proquest.com/docview/1758623705/abstract/12CAFE27F6284316PQ/1`

Lutz, H. L., Jackson, E. W., Webala, P. W., Babyesiza, W. S., Peterhans, J. C. K., Demos, T. C., . . . Gilbert, J. A. (2019, December). Ecology and host identity outweigh evolutionary history in shaping the bat microbiome. *mSystems*, *4*(6). Retrieved 2020-09-19, from `https://msystems.asm.org/content/4/6/e00511-19` doi: 10.1128/mSystems.00511-19

Lyles, A. M., & Dobson, A. P. (1993). Infectious disease and intensive management: population dynamics, threatened hosts, and their parasites. *Journal of Zoo and Wildlife Medicine*, *24*(3), 315–326.

Ma, X., Zhang, Q., Zheng, M., Gao, Y., Yuan, T., Hale, L., . . . Yang, Y. (2019, May). Microbial functional traits are sensitive indicators of mild disturbance by lamb grazing. *The ISME Journal*, *13*(5), 1370–1373. Retrieved 2020-12-02, from `https://www.nature.com/`

articles/s41396-019-0354-7 (Number: 5 Publisher: Nature Publishing Group) doi: 10.1038/s41396-019-0354-7

Mackenzie, B. W., Waite, D. W., Hoggard, M., Douglas, R. G., Taylor, M. W., & Biswas, K. (2017). Bacterial community collapse: a meta-analysis of the sinonasal microbiota in chronic rhinosinusitis. *Environmental Microbiology*, *19*(1), 381–392. Retrieved 2020-09-21, from `https://sfamjournals.onlinelibrary.wiley.com/doi/abs/10.1111/1462-2920.13632` doi: 10.1111/1462-2920.13632

Maine, J. J., & Boyles, J. G. (2015, October). Bats initiate vital agroecological interactions in corn. *Proceedings of the National Academy of Sciences*, *112*(40), 12438–12443. Retrieved 2020-01-17, from `http://www.pnas.org/lookup/doi/10.1073/pnas.1505413112` doi: 10.1073/pnas.1505413112

Mainguy, J., Desrosiers, N., & Lelièvre, F. (2011). Cave-dwelling bats in the province of Québec: historical data about hibernacula population surveys: Unpublished report. *Ministère des Ressources naturelles et de la Faune*.

Makanya, A. N., & Mortola, J. P. (2007). The structural design of the bat wing web and its possible role in gas exchange. *Journal of Anatomy*, *211*(6), 687–697.

Mandal, S., Van Treuren, W., White, R. A., Eggesbø, M., Knight, R., & Peddada, S. D. (2015, May). Analysis of composition of microbiomes: a novel method for studying microbial composition. *Microbial Ecology in Health & Disease*, *26*(0). Retrieved 2020-01-17, from `http://www.microbecolhealthdis.net/index.php/mehd/article/view/27663` doi: 10.3402/mehd.v26.27663

Mandl, J. N., Schneider, C., Schneider, D. S., & Baker, M. L. (2018). Going to bat for studies of disease tolerance. *Frontiers in Immunology*, *9*, 2112.

Marchesi, J. R., & Ravel, J. (2015, December). The vocabulary of microbiome research: a proposal. *Microbiome*, *3*(1), 31, s40168–015–0094–5. Retrieved 2020-01-17, from `https://microbiomejournal.biomedcentral.com/articles/10.1186/s40168-015-0094-5` doi: 10.1186/s40168-015-0094-5

Martel, A., Spitzen-van der Sluijs, A., Blooi, M., Bert, W., Ducatelle, R., Fisher, M. C., . . . Pasmans, F. (2013, September). *Batrachochytrium salamandrivorans* sp. nov. causes lethal chytridiomycosis in amphibians. *Proceedings of the National Academy of Sciences*, *110*(38), 15325–15329. Retrieved 2020-01-17, from `http://www.pnas.org/cgi/doi/10.1073/pnas.1307356110` doi: 10.1073/pnas.1307356110

Mascuch, S. J., Moree, W. J., Hsu, C.-C., Turner, G. G., Cheng, T. L., Blehert, D. S., . . . Gerwick, L. (2015, March). Direct detection of fungal siderophores on bats with white-nose syndrome via fluorescence microscopy-guided ambient ionization mass spectrometry. *PLOS ONE*, *10*(3), e0119668. Retrieved 2020-01-17, from `https://dx.plos.org/10.1371/journal.pone.0119668` doi: 10.1371/journal.pone.0119668

Maslo, B., & Fefferman, N. H. (2015, August). A case study of bats and white-nose syndrome

demonstrating how to model population viability with evolutionary effects: Evolutionary Rescue and PVA. *Conservation Biology*, *29*(4), 1176–1185. Retrieved 2020-01-17, from `http://doi.wiley.com/10.1111/cobi.12485` doi: 10.1111/cobi.12485

Maslo, B., Valent, M., Gumbs, J. F., & Frick, W. F. (2015, October). Conservation implications of ameliorating survival of little brown bats with white-nose syndrome. *Ecological Applications*, *25*(7), 1832–1840. Retrieved 2020-01-24, from `http://doi.wiley.com/10.1890/14-2472.1` doi: 10.1890/14-2472.1

McGuire, L. P., Mayberry, H. W., & Willis, C. K. R. (2017, December). White-nose syndrome increases torpid metabolic rate and evaporative water loss in hibernating bats. *American Journal of Physiology-Regulatory, Integrative and Comparative Physiology*, *313*(6), R680–R686. Retrieved 2020-01-17, from `https://www.physiology.org/doi/10.1152/ajpregu.00058.2017` doi: 10.1152/ajpregu.00058.2017

McGuire, L. P., Turner, J. M., Warnecke, L., McGregor, G., Bollinger, T. K., Misra, V., . . . Willis, C. K. R. (2016, March). White-nose syndrome disease severity and a comparison of diagnostic methods. *EcoHealth*, *13*(1), 60–71. Retrieved 2020-01-17, from `http://link.springer.com/10.1007/s10393-016-1107-y` doi: 10.1007/s10393-016-1107-y

McLean, M. H., Dieguez, D., Miller, L. M., & Young, H. A. (2015, February). Does the microbiota play a role in the pathogenesis of autoimmune diseases? *Gut*, *64*(2), 332–341. Retrieved 2020-09-21, from `https://gut.bmj.com/content/64/2/332` doi: 10.1136/gutjnl-2014-308514

McMurdie, P. J., & Holmes, S. (2013, April). phyloseq: An R package for reproducible interactive analysis and graphics of microbiome census data. *PLOS ONE*, *8*(4), e61217. Retrieved 2020-01-17, from `https://dx.plos.org/10.1371/journal.pone.0061217` doi: 10.1371/journal.pone.0061217

Meteyer, C. U., Buckles, E. L., Blehert, D. S., Hicks, A. C., Green, D. E., Shearn-Bochsler, V., . . . Behr, M. J. (2009, July). Histopathologic criteria to confirm white-nose syndrome in bats. *Journal of Veterinary Diagnostic Investigation*, *21*(4), 411–414. Retrieved 2020-01-17, from `http://journals.sagepub.com/doi/10.1177/104063870902100401` doi: 10.1177/104063870902100401

Micalizzi, E. W., Mack, J. N., White, G. P., Avis, T. J., & Smith, M. L. (2017, June). Microbial inhibitors of the fungus *Pseudogymnoascus destructans*, the causal agent of white-nose syndrome in bats. *PLOS ONE*, *12*(6), e0179770. Retrieved 2020-01-17, from `http://dx.plos.org/10.1371/journal.pone.0179770` doi: 10.1371/journal.pone.0179770

Moore, M. S., Field, K. A., Behr, M. J., Turner, G. G., Furze, M. E., Stern, D. W. F., . . . Vodzak, M. E. (2018). Energy conserving thermoregulatory patterns and lower disease severity in a bat resistant to the impacts of white-nose syndrome. *Journal of Comparative Physiology B*, *188*(1), 163–176.

Moore, M. S., Reichard, J. D., Murtha, T. D., Nabhan, M. L., Pian, R. E., Ferreira, J. S.,

& Kunz, T. H. (2013, March). Hibernating little brown myotis (*Myotis lucifugus*) show variable immunological responses to white-nose syndrome. *PLOS ONE*, *8*(3), e58976. Retrieved 2020-09-16, from `https://journals.plos.org/plosone/article?id=10.1371/journal.pone.0058976` doi: 10.1371/journal.pone.0058976

Moore, M. S., Reichard, J. D., Murtha, T. D., Zahedi, B., Fallier, R. M., & Kunz, T. H. (2011, November). Specific alterations in complement protein activity of little brown myotis (*Myotis lucifugus*) hibernating in white-nose syndrome affected sites. *PLOS ONE*, *6*(11), e27430. Retrieved 2020-01-24, from `https://dx.plos.org/10.1371/journal.pone.0027430` doi: 10.1371/journal.pone.0027430

Mueller, U. G., & Sachs, J. L. (2015). Engineering microbiomes to improve plant and animal health. *Trends in Microbiology*, *23*(10), 606–617.

Mulec, J., Covington, E., & Walochnik, J. (2013, June). Is bat guano a reservoir of *Geomyces destructans*? *Open Journal of Veterinary Medicine*, *2013*(3), 161–167. Retrieved 2020-02-21, from `http://www.scirp.org/journal/PaperInformation.aspx?PaperID=32699` doi: 10.4236/ojvm.2013.32025

Naik, S., Bouladoux, N., Wilhelm, C., Molloy, M. J., Salcedo, R., Kastenmuller, W., ... Belkaid, Y. (2012, August). Compartmentalized control of skin immunity by resident commensals. *Science*, *337*(6098), 1115–1119. Retrieved 2020-01-17, from `http://www.sciencemag.org/cgi/doi/10.1126/science.1225152` doi: 10.1126/science.1225152

Nakayama, K., Kawato, H. C., Inagaki, H., Nakajima, R., Kitamura, A., Someya, K., & Ohta, T. (2000, April). Synthesis and antifungal activity of rhodopeptin analogues. 2. modification of the west amino acid moiety. *Organic Letters*, *2*(7), 977–980. Retrieved 2020-01-24, from `https://pubs.acs.org/doi/10.1021/ol005630k` doi: 10.1021/ol005630k

Newman, M. E. J. (2003). The structure and function of complex networks. *SIAM Review*, *45*(2), 167–256.

Newman, M. E. J., & Girvan, M. (2004). Finding and evaluating community structure in networks. *Physical Review E*, *69*(2), 026113.

Norman, J. M., Handley, S. A., & Virgin, H. W. (2014). Kingdom-agnostic metagenomics and the importance of complete characterization of enteric microbial communities. *Gastroenterology*, *146*(6), 1459–1469.

Oksanen, J., Blanchet, F. G., Friendly, M., Kindt, R., Legendre, P., McGlinn, D., ... Wagner, H. (2019, September). vegan: community ecology package. *https://CRAN.R-project.org/package=vegan*.

O'shea, T. J., Cryan, P. M., Cunningham, A. A., Fooks, A. R., Hayman, D. T., Luis, A. D., ... Wood, J. L. N. (2014). Bat flight and zoonotic viruses. *Emerging Infectious Diseases*, *20*(5), 741.

Pinheiro, J., Bates, D., DebRoy, S., & Sarkar, D. (2017). R Core Team (2017) nlme: linear and nonlinear mixed effects models. R package version 3.1-131. *https://CRAN. R-project.*

org/package= nlme.

Pinto, A. J., & Raskin, L. (2012). PCR biases distort bacterial and archaeal community structure in pyrosequencing datasets. *PLOS ONE*, *7*(8), e43093.

Podlutsky, A. J., Khritankov, A. M., Ovodov, N. D., & Austad, S. N. (2005, November). A New Field Record for Bat Longevity. *The Journals of Gerontology: Series A*, *60*(11), 1366–1368. Retrieved 2020-11-24, from `https://academic.oup.com/biomedgerontology/article/60/11/1366/623072` (Publisher: Oxford Academic) doi: 10.1093/gerona/60.11.1366

Poisot, T., Canard, E., Mouquet, N., & Hochberg, M. E. (2012). A comparative study of ecological specialization estimators. *Methods in Ecology and Evolution*, *3*(3), 537–544.

Poretsky, R., Rodriguez-R, L. M., Luo, C., Tsementzi, D., & Konstantinidis, K. T. (2014, April). Strengths and Limitations of 16S rRNA Gene Amplicon Sequencing in Revealing Temporal Microbial Community Dynamics. *PLOS ONE*, *9*(4), e93827. Retrieved 2020-11-16, from `https://journals.plos.org/plosone/article?id=10.1371/journal.pone.0093827` (Publisher: Public Library of Science) doi: 10.1371/journal.pone .0093827

Preheim, S. P., Perrotta, A. R., Friedman, J., Smilie, C., Brito, I., Smith, M. B., & Alm, E. (2013a, January). Chapter Eighteen - Computational Methods for High-Throughput Comparative Analyses of Natural Microbial Communities. In E. F. DeLong (Ed.), *Methods in Enzymology* (Vol. 531, pp. 353–370). Academic Press. Retrieved 2020-01-17, from `http://www.sciencedirect.com/science/article/pii/B9780124078635000186` doi: 10.1016/B978-0-12-407863-5.00018-6

Preheim, S. P., Perrotta, A. R., Friedman, J., Smilie, C., Brito, I., Smith, M. B., & Alm, E. (2013b). Computational methods for high-throughput comparative analyses of natural microbial communities. *Methods in Enzymology*, *531*, 353–370. doi: 10.1016/B978-0-12 -407863-5.00018-6

Preheim, S. P., Perrotta, A. R., Martin-Platero, A. M., Gupta, A., & Alm, E. J. (2013, November). Distribution-based clustering: using ecology to refine the operational taxonomic unit. *Applied and Environmental Microbiology*, *79*(21), 6593–6603. Retrieved 2020-01-17, from `http://aem.asm.org/lookup/doi/10.1128/AEM.00342-13` doi: 10.1128/AEM.00342-13

Price, M. N., Dehal, P. S., & Arkin, A. P. (2010, March). FastTree 2 – approximately maximum-likelihood trees for large alignments. *PLOS ONE*, *5*(3), e9490. Retrieved 2020-01-17, from `https://dx.plos.org/10.1371/journal.pone.0009490` doi: 10.1371/journal.pone.0009490

Price, P. B. (1938). The bacteriology of normal skin; a new quantitative test applied to a study of the bacterial flora and the disinfectant action of mechanical cleansing. *The Journal of Infectious Diseases*, *63*(3), 301–318. Retrieved 2020-01-24, from `https://`

www.jstor.org/stable/30088420

Puechmaille, S. J., Frick, W. F., Kunz, T. H., Racey, P. A., Voigt, C. C., Wibbelt, G., & Teeling, E. C. (2011, November). White-nose syndrome: is this emerging disease a threat to European bats? *Trends in Ecology & Evolution*, *26*(11), 570–576. Retrieved 2020-01-17, from `https://linkinghub.elsevier.com/retrieve/pii/S0169534711001923` doi: 10.1016/j.tree.2011.06.013

Quast, C., Pruesse, E., Yilmaz, P., Gerken, J., Schweer, T., Yarza, P., . . . Glöckner, F. O. (2012, November). The SILVA ribosomal RNA gene database project: improved data processing and web-based tools. *Nucleic Acids Research*, *41*(D1), D590–D596. Retrieved 2020-01-17, from `http://academic.oup.com/nar/article/41/D1/D590/1069277/The-SILVA-ribosomal-RNA-gene-database-project` doi: 10.1093/nar/gks1219

Quay, W. B. (1970). Integument and derivatives. *Biology of Bats*, *2*, 1–56.

Ranjan, R., Rani, A., Metwally, A., McGee, H. S., & Perkins, D. L. (2016, January). Analysis of the microbiome: Advantages of whole genome shotgun versus 16S amplicon sequencing. *Biochemical and Biophysical Research Communications*, *469*(4), 967–977. Retrieved 2020-11-16, from `http://www.sciencedirect.com/science/article/pii/S0006291X15310883` doi: 10.1016/j.bbrc.2015.12.083

Raudabaugh, D. B., & Miller, A. N. (2013). Nutritional capability of and substrate suitability for *Pseudogymnoascus destructans*, the causal agent of bat white-nose syndrome. *PLOS ONE*, *8*(10).

Raudabaugh, D. B., & Miller, A. N. (2015). Effect of trans, trans-farnesol on *Pseudogymnoascus destructans* and several closely related species. *Mycopathologia*, *180*(5-6), 325–332.

Real, L. A. (1996). Sustainability and the ecology of infectious disease. *Bioscience*, *46*(2), 88–97.

Rebollar, E. A., Antwis, R. E., Becker, M. H., Belden, L. K., Bletz, M. C., Brucker, R. M., . . . Harris, R. N. (2016). Using "omics" and integrated multi-omics approaches to guide probiotic selection to mitigate chytridiomycosis and other emerging infectious diseases. *Frontiers in Microbiology*, *7*. Retrieved 2020-09-21, from `https://www.frontiersin.org/articles/10.3389/fmicb.2016.00068/full` doi: 10.3389/fmicb.2016.00068

Rebollar, E. A., Bridges, T., Hughey, M. C., Medina, D., Belden, L. K., & Harris, R. N. (2019, July). Integrating the role of antifungal bacteria into skin symbiotic communities of three Neotropical frog species. *The ISME Journal*, *13*(7), 1763–1775. Retrieved 2020-01-17, from `http://www.nature.com/articles/s41396-019-0388-x` doi: 10.1038/s41396-019-0388-x

Rebollar, E. A., Martínez-Ugalde, E., & Orta, A. H. (2020, June). The amphibian skin microbiome and its protective role against Chytridiomycosis. *Herpetologica*, *76*(2), 167–177. Retrieved 2020-09-20, from `https://meridian.allenpress.com/herpetologica/`

article/76/2/167/441175/The-Amphibian-Skin-Microbiome-and-Its-Protective
doi: 10.1655/0018-0831-76.2.167

Reeder, D. M., Frank, C. L., Turner, G. G., Meteyer, C. U., Kurta, A., Britzke, E. R., . . . Blehert, D. S. (2012, June). Frequent arousal from hibernation linked to severity of infection and mortality in bats with white-nose syndrome. *PLOS ONE*, *7*(6), e38920. Retrieved 2020-01-17, from `https://dx.plos.org/10.1371/journal.pone.0038920` doi: 10.1371/journal.pone.0038920

Reeder, D. M., & Turner, G. R. (2008). Working together to combat white-nose syndrome: a report of a meeting on 9–11 June 2008. *Albany, New York. Bat Res. News*, *49*, 75–78.

Reeder, S. M., Palmer, J. M., Prokkola, J. M., Lilley, T. M., Reeder, D. M., & Field, K. A. (2017, November). *Pseudogymnoascus destructans* transcriptome changes during white-nose syndrome infections. *Virulence*, *8*(8), 1695–1707. Retrieved 2020-01-17, from `https://www.tandfonline.com/doi/full/10.1080/21505594.2017.1342910` doi: 10.1080/21505594.2017.1342910

Reichard, J. D., Fuller, N. W., Bennett, A. B., Darling, S. R., Moore, M. S., Langwig, K. E., . . . Reynolds, D. S. (2014). Interannual survival of *Myotis lucifugus* (Chiroptera: Vespertilionidae) near the epicenter of white-nose syndrome. *Northeastern Naturalist*, *21*(4), N56.

Reichard, J. D., & Kunz, T. H. (2009). White-nose syndrome inflicts lasting injuries to the wings of little brown myotis (*Myotis lucifugus*). *Acta Chiropterologica*, *11*(2), 457–464.

Reyes, E. A., Bale, M. J., Cannon, W. H., & Matsen, J. M. (1981, March). Identification of *Pseudomonas aeruginosa* by pyocyanin production on Tech agar. *Journal of Clinical Microbiology*, *13*(3), 456–458.

Reynolds, H. T., & Barton, H. A. (2014). Comparison of the white-nose syndrome agent *Pseudogymnoascus destructans* to cave-dwelling relatives suggests reduced saprotrophic enzyme activity. *PLOS ONE*, *9*(1).

Reynolds, H. T., Ingersoll, T., & Barton, H. A. (2015). Modeling the environmental growth of *Pseudogymnoascus destructans* and its impact on the white-nose syndrome epidemic. *Journal of Wildlife Diseases*, *51*(2), 318–331.

Rocke, T. E., Kingstad-Bakke, B., Wüthrich, M., Stading, B., Abbott, R. C., Isidoro-Ayza, M., . . . Lankton, J. S. (2019). Virally-vectored vaccine candidates against white-nose syndrome induce anti-fungal immune response in little brown bats (*Myotis lucifugus*). *Scientific Reports*, *9*(1), 1–12.

Romano-Bertrand, S., Licznar-Fajardo, P., Parer, S., & Jumas-Bilak, E. (2015, February). Impact de l'environnement sur les microbiotes : focus sur l'hospitalisation et les microbiotes cutanés et chirurgicaux. *Revue Francophone des Laboratoires*, *2015*(469), 75–82. Retrieved 2020-01-24, from `https://linkinghub.elsevier.com/retrieve/pii/S1773035X15728248` doi: 10.1016/S1773-035X(15)72824-8

Roth, R. R., & James, W. D. (1988, October). Microbial ecology of the skin. *Annual Review of Microbiology*, *42*(1), 441–464. Retrieved 2020-01-24, from `http://www.annualreviews.org/doi/10.1146/annurev.mi.42.100188.002301` doi: 10.1146/annurev.mi.42.100188.002301

Råberg, L., Graham, A. L., & Read, A. F. (2009, January). Decomposing health: tolerance and resistance to parasites in animals. *Philosophical Transactions of the Royal Society B: Biological Sciences*, *364*(1513), 37–49. Retrieved 2020-01-17, from `https://royalsocietypublishing.org/doi/10.1098/rstb.2008.0184` doi: 10.1098/rstb.2008.0184

Råberg, L., Sim, D., & Read, A. F. (2007, November). Disentangling genetic variation for resistance and tolerance to infectious diseases in animals. *Science*, *318*(5851), 812–814. Retrieved 2020-01-17, from `http://www.sciencemag.org/cgi/doi/10.1126/science.1148526` doi: 10.1126/science.1148526

Sabino-Pinto, J., Bletz, M. C., Islam, M. M., Shimizu, N., Bhuju, S., Geffers, R., . . . Vences, M. (2016, August). Composition of the cutaneous bacterial community in japanese amphibians: effects of captivity, host species, and body region. *Microbial Ecology*, *72*(2), 460–469. Retrieved 2020-05-15, from `http://link.springer.com/10.1007/s00248-016-0797-6` doi: 10.1007/s00248-016-0797-6

Salter, S. J., Cox, M. J., Turek, E. M., Calus, S. T., Cookson, W. O., Moffatt, M. F., . . . Walker, A. W. (2014, December). Reagent and laboratory contamination can critically impact sequence-based microbiome analyses. *BMC Biology*, *12*(1), 87. Retrieved 2020-01-17, from `https://bmcbiol.biomedcentral.com/articles/10.1186/s12915-014-0087-z` doi: 10.1186/s12915-014-0087-z

Sanders, M. E. (2008). Probiotics: definition, sources, selection, and uses. *Clinical Infectious Diseases*, *46*, S58–S61.

Sass, G., Nazik, H., Penner, J., Shah, H., Ansari, S. R., Clemons, K. V., . . . Stevens, D. A. (2017, October). Studies of *Pseudomonas aeruginosa* mutants indicate pyoverdine as the central factor in inhibition of *Aspergillus fumigatus* biofilm. *Journal of Bacteriology*, *200*(1), e00345–17. Retrieved 2020-01-17, from `https://jb.asm.org/lookup/doi/10.1128/JB.00345-17` doi: 10.1128/JB.00345-17

Scott, M. E. (1988). The impact of infection and disease on animal populations: implications for conservation biology. *Conservation Biology*, *2*(1), 40–56.

Sen, R., Ishak, H. D., Estrada, D., Dowd, S. E., Hong, E., & Mueller, U. G. (2009, October). Generalized antifungal activity and 454-screening of *Pseudonocardia* and *Amycolatopsis* bacteria in nests of fungus-growing ants. *Proceedings of the National Academy of Sciences*, *106*(42), 17805–17810. Retrieved 2020-01-17, from `http://www.pnas.org/cgi/doi/10.1073/pnas.0904827106` doi: 10.1073/pnas.0904827106

Shannon, C. E. (1948, July). A mathematical theory of communication. *Bell System*

Technical Journal, *27*(3), 379–423. Retrieved 2020-01-17, from `http://ieeexplore.ieee`
`.org/lpdocs/epic03/wrapper.htm?arnumber=6773024` doi: 10.1002/j.1538-7305.1948
.tb01338.x

Singh, J. S. (2002). The biodiversity crisis: a multifaceted review. *Current Science*, *82*(6),
638–647.

Sisk, M. O. (1957, November). A study of the sudoriparous glands of the little brown bat,
Myotis lucifugus. *Journal of Morphology*, *101*(3), 425–455. Retrieved 2020-01-24, from
`http://doi.wiley.com/10.1002/jmor.1051010303` doi: 10.1002/jmor.1051010303

Soergel, D. A. W., Dey, N., Knight, R., & Brenner, S. E. (2012). Selection of primers for
optimal taxonomic classification of environmental 16S rRNA gene sequences. *The ISME
Journal*, *6*(7), 1440–1444.

Sokolov, V. E. (1982). *Mammal skin*. Univ of California Press.

Song, S. J., Lauber, C., Costello, E. K., Lozupone, C. A., Humphrey, G., Berg-Lyons, D.,
. . . Knight, R. (2013, April). Cohabiting family members share microbiota with one
another and with their dogs. *eLife*, *2*, e00458. Retrieved 2020-01-24, from `https://`
`elifesciences.org/articles/00458` doi: 10.7554/eLife.00458

Sterbing-D'Angelo, S., Chadha, M., Chiu, C., Falk, B., Xian, W., Barcelo, J., . . . Moss, C. F.
(2011). Bat wing sensors support flight control. *Proceedings of the National Academy of
Sciences*, *108*(27), 11291–11296.

Stuart, S. N., Chanson, J. S., Cox, N. A., Young, B. E., Rodrigues, A. S. L., Fischman,
D. L., & Waller, R. W. (2004). Status and trends of amphibian declines and extinctions
worldwide. *Science*, *306*(5702), 1783–1786.

Svensson, E. I., & Råberg, L. (2010, May). Resistance and tolerance in animal enemy–victim
coevolution. *Trends in Ecology & Evolution*, *25*(5), 267–274. Retrieved 2020-01-17, from
`https://linkinghub.elsevier.com/retrieve/pii/S0169534709003711` doi: 10.1016/
j.tree.2009.12.005

Swartz, S. M., Freeman, P. W., & Stockwell, E. F. (2003). Ecomorphology of bats: com-
parative and experimental approaches relating structural design to ecology. *Bat Ecology*,
257, 300.

Tatusov, R. L., Galperin, M. Y., Natale, D. A., & Koonin, E. V. (2000, January). The COG
database: a tool for genome-scale analysis of protein functions and evolution. *Nucleic Acids
Research*, *28*(1), 33–36. Retrieved 2020-07-23, from `https://www.ncbi.nlm.nih.gov/`
`pmc/articles/PMC102395/`

Team, R. C. (2018). *R: A language and environment for statistical computing; 2015.*

Terry, C. (2018). bipartiteD3: Interactive bipartite graphs. R package version 0.1. 0.
https://CRAN. R-project. org/package= bipartiteD3.

Thomas, D. W. (1995). Hibernating bats are sensitive to nontactile human disturbance.
Journal of Mammalogy, *76*(3), 940–946.

Thomas, D. W., Dorais, M., & Bergeron, J.-M. (1990). Winter energy budgets and cost of arousals for hibernating little brown bats, *Myotis lucifugus*. *Journal of Mammalogy*, *71*(3), 475–479.

Thomas, S. P., & Suthers, R. A. (1972). The physiology and energetics of bat flight. *Journal of Experimental Biology*, *57*(2), 317–335.

Titball, R. W. (1993, June). Bacterial phospholipases C. *Microbiological Reviews*, *57*(2), 347–366. Retrieved 2020-09-15, from `https://www.ncbi.nlm.nih.gov/pmc/articles/PMC372913/`

Trivedi, J., Lachapelle, J., Vanderwolf, K. J., Misra, V., Willis, C. K. R., Ratcliffe, J. M., . . . Kohn, L. M. (2017). Fungus causing white-nose syndrome in bats accumulates genetic variability in North America with no sign of recombination. *msphere*, *2*(4), e00271–17.

Tukey, J. W. (1977). *Exploratory data analysis* (Vol. 2). Reading, MA.

Turnbaugh, P. J., & Gordon, J. I. (2008). An invitation to the marriage of metagenomics and metabolomics. *Cell*, *134*(5), 708–713.

Turner, G. G., Meteyer, C. U., Barton, H., Gumbs, J. F., Reeder, D. M., Overton, B., . . . Blehert, D. S. (2014, July). Nonlethal screening of bat-wing skin with the use of ultraviolet fluorescence to detect lesions indicative of white-nose syndrome. *Journal of Wildlife Diseases*, *50*(3), 566–573. Retrieved 2020-01-17, from `http://www.bioone.org/doi/10.7589/2014-03-058` doi: 10.7589/2014-03-058

Turner, G. G., & Reeder, D. M. (2009). Update of white-nose syndrome in bats, September 2009. *Bat Research News*, *50*(3), 47–53.

Turner, G. G., Reeder, D. M., & Coleman, J. T. H. (2011). A Five-year Assessment of Mortality and Geographic Spread of White-nose Syndrome in North American Bats and a Look to the Future. *Bat Research News*, *54*(2), 13–27. Retrieved 2020-01-24, from `https://reviverestore.org/httplongnow-orgrevivewp-contentuploadsuser-publicationsturner-et-al-2011-brn-wns-pdf/`

Tuttle, M. D., Darling, S. R., Youngbaer, P., & Kunz, T. H. (2009). White-nose syndrome: science strategy meeting II. *Austin, TX*.

UniProt. (2019). UniProt: a worldwide hub of protein knowledge. *Nucleic Acids Research*, *47*(D1), D506–D515.

Vanderwolf, K. J., McAlpine, D. F., Forbes, G. J., & Malloch, D. (2012). Bat populations and cave microclimate prior to and at the outbreak of white-nose syndrome in New Brunswick. *The Canadian Field-Naturalist*, *126*(2), 125–134.

van Dijk, E. L., Auger, H., Jaszczyszyn, Y., & Thermes, C. (2014, September). Ten years of next-generation sequencing technology. *Trends in Genetics*, *30*(9), 418–426. Retrieved 2020-09-20, from `http://www.sciencedirect.com/science/article/pii/S0168952514001127` doi: 10.1016/j.tig.2014.07.001

Verant, M. L., Meteyer, C. U., Speakman, J. R., Cryan, P. M., Lorch, J. M., & Blehert, D. S.

(2014, December). White-nose syndrome initiates a cascade of physiologic disturbances in the hibernating bat host. *BMC Physiology*, *14*(1), 10. Retrieved 2020-01-17, from `http://bmcphysiol.biomedcentral.com/articles/10.1186/s12899-014-0010-4` doi: 10.1186/s12899-014-0010-4

Voig, C. C., Caspers, B., & Speck, S. (2005). Bats, bacteria, and bat smell: sex-specific diversity of microbes in a sexually selected scent organ. *Journal of Mammalogy*, *86*(4), 745–749.

Walke, J. B., Becker, M. H., Loftus, S. C., House, L. L., Cormier, G., Jensen, R. V., & Belden, L. K. (2014, November). Amphibian skin may select for rare environmental microbes. *The ISME Journal*, *8*(11), 2207–2217. Retrieved 2020-01-24, from `http://www.nature.com/articles/ismej201477` doi: 10.1038/ismej.2014.77

Walke, J. B., Becker, M. H., Loftus, S. C., House, L. L., Teotonio, T. L., Minbiole, K. P. C., & Belden, L. K. (2015, October). Community structure and function of amphibian skin microbes: an experiment with bullfrogs exposed to a chytrid fungus. *PLOS ONE*, *10*(10). Retrieved 2020-04-02, from `https://www.ncbi.nlm.nih.gov/pmc/articles/PMC4596541/` doi: 10.1371/journal.pone.0139848

Walter, J., Maldonado-Gómez, M. X., & Martínez, I. (2018, February). To engraft or not to engraft: an ecological framework for gut microbiome modulation with live microbes. *Current Opinion in Biotechnology*, *49*, 129–139. Retrieved 2020-01-17, from `https://linkinghub.elsevier.com/retrieve/pii/S0958166917301118` doi: 10.1016/j.copbio.2017.08.008

Warnecke, L., Turner, J. M., Bollinger, T. K., Lorch, J. M., Misra, V., Cryan, P. M., . . . Willis, C. K. R. (2012, May). Inoculation of bats with European *Geomyces destructans* supports the novel pathogen hypothesis for the origin of white-nose syndrome. *Proceedings of the National Academy of Sciences*, *109*(18), 6999–7003. Retrieved 2020-01-17, from `http://www.pnas.org/cgi/doi/10.1073/pnas.1200374109` doi: 10.1073/pnas.1200374109

Warnecke, L., Turner, J. M., Bollinger, T. K., Misra, V., Cryan, P. M., Blehert, D. S., . . . Willis, C. K. R. (2013). Pathophysiology of white-nose syndrome in bats: a mechanistic model linking wing damage to mortality. *Biology Letters*, *9*(4), 20130177.

Weiss, S., Xu, Z. Z., Peddada, S., Amir, A., Bittinger, K., Gonzalez, A., . . . Knight, R. (2017, December). Normalization and microbial differential abundance strategies depend upon data characteristics. *Microbiome*, *5*(1), 27. Retrieved 2020-01-17, from `http://microbiomejournal.biomedcentral.com/articles/10.1186/s40168-017-0237-y` doi: 10.1186/s40168-017-0237-y

West, A. G., Waite, D. W., Deines, P., Bourne, D. G., Digby, A., McKenzie, V. J., & Taylor, M. W. (2019, January). The microbiome in threatened species conservation. *Biological Conservation*, *229*, 85–98. Retrieved 2020-01-17, from `https://linkinghub.elsevier`

.com/retrieve/pii/S0006320718311145 doi: 10.1016/j.biocon.2018.11.016

Western, D. (1992). The biodiversity crisis: a challenge for biology. *Oikos*, 29–38.

Whitaker, J. O., & Rissler, L. J. (1993). Do bats feed in winter? *American Midland Naturalist*, 200–203.

Wibbelt, G., Kurth, A., Hellmann, D., Weishaar, M., Barlow, A., Veith, M., ... Blehert, D. S. (2010, August). White-nose syndrome fungus (*Geomyces destructans*) in bats, Europe. *Emerging Infectious Diseases*, *16*(8), 1237–1243. Retrieved 2020-01-17, from http://wwwnc.cdc.gov/eid/article/16/8/10-0002_article.htm doi: 10.3201/eid1608.100002

Wilder, A. P., Frick, W. F., Langwig, K. E., & Kunz, T. H. (2011, December). Risk factors associated with mortality from white-nose syndrome among hibernating bat colonies. *Biology Letters*, *7*(6), 950–953. Retrieved 2020-09-20, from https://royalsocietypublishing.org/doi/10.1098/rsbl.2011.0355 doi: 10.1098/rsbl.2011.0355

Wilkinson, G. S., & South, J. M. (2002). Life history, ecology and longevity in bats. *Aging Cell*, *1*(2), 124–131.

Willis, C. K., & Wilcox, A. (2014, June). Hormones and hibernation: possible links between hormone systems, winter energy balance and white-nose syndrome in bats. *Hormones and Behavior*, *66*(1), 66–73. Retrieved 2020-01-17, from https://linkinghub.elsevier.com/retrieve/pii/S0018506X14000762 doi: 10.1016/j.yhbeh.2014.04.009

Wilmes, P., & Bond, P. L. (2006). Metaproteomics: studying functional gene expression in microbial ecosystems. *Trends in Microbiology*, *14*(2), 92–97.

Winter, A. S., Hathaway, J. J. M., Kimble, J. C., Buecher, D. C., Valdez, E. W., Porras-Alfaro, A., ... Northup, D. E. (2017, October). Skin and fur bacterial diversity and community structure on American southwestern bats: effects of habitat, geography and bat traits. *PeerJ*, *5*, e3944. Retrieved 2020-11-25, from https://peerj.com/articles/3944 (Publisher: PeerJ Inc.) doi: 10.7717/peerj.3944

Winter, A. S., Kimble, J. C., Young, J. M., Buecher, D. C., Valdez, E. W., Hathaway, J. J., ... Northup, D. E. (2016, October). *External bacterial diversity on bats in the southwestern United States: Changes in bacterial community structure above and below ground* (preprint). PeerJ Preprints. Retrieved 2020-01-24, from https://peerj.com/preprints/2493v1 doi: 10.7287/peerj.preprints.2493v1

Woo, V., Eshleman, E. M., Rice, T., Whitt, J., Vallance, B. A., & Alenghat, T. (2019, May). Microbiota inhibit epithelial pathogen adherence by epigenetically regulating C-type lectin expression. *Frontiers in Immunology*, *10*, 928. Retrieved 2020-01-17, from https://www.frontiersin.org/article/10.3389/fimmu.2019.00928/full doi: 10.3389/fimmu.2019.00928

Woodhams, D. C., Brandt, H., Baumgartner, S., Kielgast, J., Küpfer, E., Tobler, U., ... McKenzie, V. (2014, April). Interacting symbionts and immunity in the amphibian skin

mucosome predict disease risk and probiotic effectiveness. *PLOS ONE*, *9*(4), e96375. Retrieved 2020-01-17, from `https://dx.plos.org/10.1371/journal.pone.0096375` doi: 10.1371/journal.pone.0096375

Wray, A. K., Jusino, M. A., Banik, M. T., Palmer, J. M., Kaarakka, H., White, J. P., ... Peery, M. Z. (2018, June). Incidence and taxonomic richness of mosquitoes in the diets of little brown and big brown bats. *Journal of Mammalogy*, *99*(3), 668–674. Retrieved 2020-01-17, from `https://academic.oup.com/jmammal/article/99/3/668/4993282` doi: 10.1093/jmammal/gyy044

Xu, M., Pokrovskii, M., Ding, Y., Yi, R., Au, C., Harrison, O. J., ... Littman, D. R. (2018, February). c-MAF-dependent regulatory T cells mediate immunological tolerance to a gut pathobiont. *Nature*, *554*(7692), 373–377. Retrieved 2020-09-21, from `https://www.nature.com/articles/nature25500` doi: 10.1038/nature25500

Yang, B., Wang, Y., & Qian, P.-Y. (2016, March). Sensitivity and correlation of hypervariable regions in 16S rRNA genes in phylogenetic analysis. *BMC Bioinformatics*, *17*(1), 135. Retrieved 2020-09-20, from `https://doi.org/10.1186/s12859-016-0992-y` doi: 10.1186/s12859-016-0992-y

Zaneveld, J. R., McMinds, R., & Vega Thurber, R. (2017, September). Stress and stability: applying the Anna Karenina principle to animal microbiomes. *Nature Microbiology*, *2*(9), 17121. Retrieved 2020-01-17, from `http://www.nature.com/articles/nmicrobiol2017121` doi: 10.1038/nmicrobiol.2017.121

Zukal, J., Bandouchova, H., Brichta, J., Cmokova, A., Jaron, K. S., Kolarik, M., ... Martínková, N. (2016, April). White-nose syndrome without borders: *Pseudogymnoascus destructans* infection tolerated in Europe and Palearctic Asia but not in North America. *Scientific Reports*, *6*(1), 19829. Retrieved 2020-01-17, from `http://www.nature.com/articles/srep19829` doi: 10.1038/srep19829

Annexe A

Environment and host species shape the skin microbiome of captive neotropical bats

Virginie Lemieux-Labonté, Nicolas Tromas, Jesse B. Shapiro and François-Joseph Lapointe

Département de sciences biologiques, Université de Montréal, Montréal, Québec, Canada

Abstract. A wide range of microorganisms inhabit animal skin. This microbial community (microbiome) plays an important role in host defense against pathogens and disease. Bats (Chiroptera: Mammalia) are an ecologically and evolutionarily diversified group with a relatively unexplored skin microbiome. The bat skin microbiome could play a role in disease resistance, for example, to white nose syndrome (WNS), an infection which has been devastating North American bat populations. However, fundamental knowledge of the bat skin microbiome is needed before understanding its role in health and disease resistance. Captive neotropical frugivorous bats *Artibeus jamaicensis* and *Carollia perspicillata* provide a simple controlled system in which to characterize the factors shaping the bat microbiome. Here, we aimed to determine the relative importance of habitat and host species on the bat skin microbiome. We performed high-throughput 16S rRNA gene sequencing of the skin microbiome of two different bat species living in captivity in two different habitats. In the first habitat, *A. jamaicensis* and *C. perspicillata* lived together, while the second habitat contained only *A. jamaicensis*. We found that both habitat and host species shape

the composition and diversity of the skin microbiome, with habitat having the strongest influence. Cohabitating *A. jamaicensis* and *C. perspicillata* shared more similar skin microbiomes than members of the same species (*A. jamaicensis*) across two habitats. These results suggest that in captivity, the skin microbial community is homogenised by the shared environments and individual proximities of bats living together in the same habitat, at the expense of the innate host species factors. The predominant influence of habitat suggests that environmental microorganisms or pathogens might colonize bat skin. We also propose that bat populations could differ in pathogen susceptibility depending on their immediate environment and habitat.